# A COMPARATIVE STUDY OF UNLOADED TRANSMISSION LINE SWITCHING WITH DISCONNECTORS USING ATP/EMTP AND DIGSILENT POWERFACTORY SIMULATION TOOLS

by

Sharon Arigye-Mushabe


Supervised by:

Assoc. Prof. Komla A. Folly

A dissertation submitted in fulfilment of the academic requirements for the degree of

Master of Science in Engineering

In the Faculty of Engineering and The Built Environment

University of Cape Town

May 2010

# Declaration

I declare that all the work presented in this dissertation is my own work. All work that is not my own has been acknowledged and referenced accordingly herein. This dissertation is being submitted for the degree of Master of Science in Engineering in the University of Cape Town. It has not been submitted before for any degree or examination at any other university.

| | |
|---|---|
| Signature of Author: | …… |
| Author: | Sharon Arigye-Mushabe |
| Student Number: | ARGSHA001 |
| Date: | May 2010 |
| Place: | Cape Town |

# Acknowledgements

I would like to acknowledge the following people for making this dissertation possible:

- I would like to thank my supervisor, Assoc. Prof. Komla Folly, for his willingness to supervise this project. I am indebted to him for his constant guidance, his patience, and most importantly, never giving up on me. My sincere gratitude to him for pushing me to continuously question why, what and how – life lessons to keep.

- To Eskom Distribution Western Region for the funding for this degree and allowing me access to resources, material and information that have made this project possible.

- To my family, thank you for the fervent prayers that have gotten me to this point – the end of a journey. My heartfelt thanks to you all! Thank you for your love, support and belief in me at those times when I thought I just could not carry on.

- To all my dear friends for encouragement, support and advice throughout the duration of the dissertation.

- Lastly, I would like to thank God Almighty for getting me through this journey. He has been faithful and steadfast. As it is promised in Phil 1:6 "*being confident of this, that he who began a good work in you will carry it on to completion until the day of Christ Jesus."* It is only through His Grace that I have managed to get this far and complete.

# Abstract

Disconnectors exist in most sub-transmission networks where high voltage equipment is used. The primary function of disconnectors is to electrically isolate equipment from the power system, such as breakers, for maintenance or repair. They are also used to interrupt negligible currents such as capacitive currents associated with unload transmission lines.

The switching operation of a disconnector where negligible current is interrupted results in overvoltages and switching transients being introduced to the network. These overvoltages and transients could lead to the safety of personnel being compromised or damage to equipment. Researchers have studied the subject in order to provide guidelines by which to predict the behaviour of switching operations with disconnector. Thus, using some of the guidelines of the previous studies, this study endeavours to determine whether the use of computer simulation is an adequate method by which the behaviour of a disconnector switching operation can be predicted.

Two simulation tools are used in the study, namely: Alternative Transient Program (ATP) and DigSILENT PowerFactory. The ATP simulation tool is used specifically to simulate power system transient problems. DigSILENT PowerFactory is an integrated power system analysis tool that is used for load flow studies in radial and meshed networks (balanced and unbalanced), and performs electro-magnetic transient simulations. This study compares simulation results obtained from these simulation tools. The power system model used in this work is based on a simplified model of an existing network in the Western Region of South Africa. The simulations focus on the energisation and de-energisation of a “no-load” transmission line.

Owing to the switching transients and overvoltages caused by the switching operation of a disconnector, the model chosen for simulation in both software packages needed to be modelled for fast transient solutions, in particular the transmission line model. Previous research findings

showed that distributed parameter line models produced better results for switching studies than lumped parameter line models. These were confirmed in this work by the simulations run in both ATP and PowerFactory.

For this study, a switching operation was deemed unlikely to succeed if overvoltages observed at the point of the switching were greater than 2.0p.u. Using the simulated model in both ATP and PowerFactory, the results showed that overvoltages were less than 2.0p.u., at the point of switching, during a disconnector switching operation. However, overvoltages greater than 2.0p.u. were observed at the receiving-end of the line, which could be problematic for equipment at the end of the line.

In both simulation tools, re-energising the line or "switching on" operation produced higher overvoltages than de-energising of the transmission line or "switching off" operation. This is due to a combination of reflected travelling waves as well as trapped charge on the line that contribute to the higher stresses experienced during the re-energising of the line.

Furthermore, two mitigation techniques were also investigated in this thesis. These techniques were to increase the source-side capacitance ($C_S$) of the disconnector or to switch the disconnector at the zero-crossing of the sinusoidally waveform across all phase currents. The technique of increasing the source-side capacitance ($C_S$) did reduce the overvoltages experienced by the network, although the reduction in overvoltages was not as significant as the reduction seen when the current was interrupted at the zero-crossing. Using ATP, the results from the zero-crossing current method showed a 27.5% reduction in overvoltages at the point of switching, while the introduction of source-side capacitance ($C_S$) yielded a reduction of 2.25%. Using PowerFactory, the zero-crossing current method resulted in a 11.9% reduction in overvoltages at the point of switching, whereas a reduction of 3.59% was only seen when the other technique was used. Owing to the substantial reduction in overvoltages provided by the zero-crossing current method, this technique is recommended for the reduction of overvoltages.

It was also recommended that field tests were necessary to verify the results obtained from both software packages. The field tests would also provide confirmation as to whether or not a de-energising operation produced higher overvoltages than the energising switching operation.

This study focussed only on the switching of capacitive currents by disconnects. However, it is recommended that the study be extended to simulate the behaviour of the disconnector while switching magnetising currents and bus-transfer currents.

# Table of Contents

# List of Figures

# List of Tables

# Glossary

| | |
|---|---|
| De-energise | The isolation of a line segment from the system with the other end open by interrupting the charging (capacitive) current |
| Disconnector | "*A mechanical switching device which provides, in an open position, an isolating distance in accordance with specified requirements"* [1]. |
| Isolating distance | "*The clearance between open contacts meeting the safety requirements specified for disconnectors*" [2]. |
| Open position | "*The position in which the predetermined clearance between open contacts in the main circuit of the mechanical switching device is secured*" [2]. |
| Closed position | "*The position in which the predetermined continuity of the main circuit of the mechanical switching device is secured*" [2]. |
| Opening operation | "*An operation by which the mechanical switching device is brought from the closed position to the open position*" [2]. |
| Closing operation | "*An operation by which the mechanical switching device is brought from the open position to the closed position*" [2]. |
| Arcing horns | "*One of a pair of diverging electrodes on which an arc is extended to the point of extinctions after the main contacts of the switching device have parted*" [3]. |
| Horn-gap switch | "*A switch provided with arcing horns*" [3]. |
| Re-ignition | "*A resumption of current between the contacts of a mechanical switching device during a breaking operation with an interval of zero current less than a quarter cycle of power frequency*" [2]. |
| Re-strike | "*A resumption of current between the contacts of a mechanical switching device during a breaking operation with an interval of zero current a quarter cycle of power frequency or longer*" [2]. |

# Abbreviations

| | |
|---|---|
| ATP | Alternative Transient Program |
| CIGRE | International Council on Large Electric Systems |
| EMTP | Electro-Magnetic Transient Program |
| IEC | International Electro-technical Commission |
| IEEE | Institute of Electrical and Electronics Engineers |
| LCC | Line/cable component of ATPDraw |
| PF | PowerFactory (simulation program from DigSILENT) |
| TRV | Transient Recovery Voltage |

# Chapter 1 Introduction

## 1.1 Background to the study

The primary function of disconnectors is to electrically isolate equipment from the power system for maintenance or repair. The isolation of equipment within a substation or from a substation itself is a recurrent and inescapable practice that is given consideration right from design stage. There are two main reasons for isolation. The first reason is to ensure efficient operation of the power system in cases where, for instance, shunt reactors are switched out of the power system network during peak load periods using circuit breakers and then isolated using disconnectors [4]. The second reason is for safe repair and/or maintenance on power system equipment for planned or remedial work due to unforeseen faults.

Disconnectors are known by various names around the world. The International Electro-technical Committee (IEC) [1] refers to these switches as disconnectors. In North America, these switches are known as air switches [5], disconnecting switches or disconnect switches [6]. In South Africa, they are interchangeably referred to as disconnectors or isolators or colloquially as "links". This thesis will refer to them as disconnectors.

The IEC 60050:441 standard, International Electrotechnical Vocabulary for Switchgear, controlgear and fuses [1], defines a disconnector as "*a mechanical switching device which provides, in the open position, an isolating distance in accordance with specified requirements*." It is further noted in the standard that a disconnector is "*capable of opening and closing a circuit when either negligible current is broken or made, or when no significant change in the voltage across the terminals of each of the poles of the disconnector occurs*". It is also stated that the disconnector is "*capable of carrying currents under normal circuit*

*conditions and carrying for specified time currents under abnormal conditions such as those of short circuits.*"

The IEC 62271-102 standard for High-Voltage switchgear and controlgear [7] further explains the definition provided in [1]. It states that 'negligible current' implies currents such as "*the capacitive currents of bushings, bus bars, connectors, very short lengths of cables, currents of permanently connected grading impedances of circuit-breakers and currents of voltage transformers and dividers*" [7]. The IEC 62271-102 also mentions that for the purpose of the explanation given for negligible current at rated voltages of 420kV and below, a capacitive current that is not more than 0.5A is a negligible current [7], whereas, 'no significant change in voltage' refers to "*such applications as the by-passing of induction voltage regulators or circuit breakers*" [7].

In other words, based on IEC 62271-102 [7], disconnectors are not designed to interrupt load currents associated with normal circuit conditions. The main purpose of a disconnector is to provide an 'isolating distance'. IEC 60050:441 [1] provides a definition for isolating distance as '*the clearance between open contacts meeting the safety requirements specified for disconnectors.*'

Moreover, the IEC standard [7] states that for "*a disconnector rated 52kV and above, a rated ability of bus-transfer current switching may be assigned*". Bus-transfer current is defined as the "*current which a disconnector is capable of switching when it transfers load from one bus system to another*" [7]. Later in IEC 62271-102, it is noted that the maximum bus-transfer current that the disconnector is capable of switching at a specified open circuit voltage will not normally exceed 1600A [7]. The specified open circuit voltage is discussed in Annex *B* in the standard [7].

By implication the IEC 62271-102 [7] suggests that disconnectors are capable of switching negligible currents and bus transfer current. Studies that have been carried out regarding the switching capability of disconnectors have classified the currents a disconnector is capable of switching into three types, namely: magnetising current, capacitive current and bus-transfer currents or loop switching current [8] [9]. These types of currents, however, depend on circuit configuration of the network where the disconnector is operated.

This thesis explores the switching capability of disconnectors. The study focuses on capacitive current switching of disconnectors by using two simulation tools: ATP and PowerFactory.

## 1.2 Problem Statement

The disconnectors exist in most sub-transmission networks where high voltage equipment is used. They are used regularly in normal day-to-day operation, including interruption of small currents. They are designed to carry a specific continuous rated current at a particular voltage level. They are designed for isolation, not to make or break currents. However, they are used to interrupt certain types of current such as magnetising current, bus-transfer current and capacitive current. Sometimes the current is interrupted successfully. That is to say the current was interrupted without posing a risk to personnel, or damaging the contacts of the disconnectors, or causing undesirable faults on the system due to overvoltages or short circuits. Other times, the operation is unsuccessful.

The practice of using disconnectors to switch negligible currents and bus-transfer (loop) currents has been used, mainly in North America, from as early as 1950 [8]. The practice was also evidenced from an earlier survey that was performed in 1966 by members of the Working group on Air Switches of the IEEE Switch, Fuse and Insulator Subcommittee [10], where it was found that utilities used disconnectors to interrupt magnetising currents, line charging current and loop currents on a trial and error basis [10]. However, it would be up to the individual user to decide whether the switching operation was successful as there were no clear guidelines to assess this.

Later, the IEEE Guide to Current Interruption with Horn-Gap Air Switches, IEEE C37.36b-1990 [5], was published and briefly highlighted some of the problems that are experienced due to a lack of rating and standard guidelines where disconnectors are concerned, namely [5]:

- Inconsistent user practices regarding the utilisation of air switches to interrupt currents;
- Improper use of disconnectors that has led to switch failures, system faults and outages;
- Excessive surge arrester operations during current interruption of small currents.

The IEEE C37.36b-1990 [5] then provided the user with suggested values for current interruption based on the work by Andrews *et al.* [8] and Peelo [11].

More recently in 2004, a study completed by Peelo [4] referred to the fact that the use of disconnectors to switch small currents was still common practice in North America. In the study, Peelo highlighted the switching capability and limits of disconnectors for the different types of currents that were switched, as well as the variables that affect the different current types that could be switched and those that could not be switched [4].

When a switch is opened, an arc is drawn between the contacts of the switch so as to 'recover' the voltages. However, in an opening operation, the insulation gap ("break gap") of the switch is increased as the contacts move away from each other. Should the insulation gap not be wide enough, a current re-strike will occur because the dielectric strength of the break-gap is not strong enough to withstand the voltage stresses across the contacts. If an adequate dielectric strength can be obtained across the contacts after the current zero, then the development of restrikes is eliminated. Moreover, if the current interrupting operation occurs when an arc current is at its current zero, that is to say when the current crosses through the zero-point of its sinusoidal waveform, the current will be interrupted. At which point the arc that is drawn during the switching operation is finally interrupted.

A transient can be described as a short-lived oscillation in a system caused by a sudden change of voltage or current. The primary cause of such a disturbance in a system is the closing or opening of a breaker or other switching equipment, a short circuit or earth fault or a lightning strike. As a result, current transient waves or travelling waves are generated on the lines, cables or bus-bar sections that are linked by the switch [12].

However, as mentioned before, the primary function of a disconnector is to electrically isolate equipment. During a switching operation, if the interrupted current is not fully broken by the time the disconnector is in the "open" position, the operation could result in flashovers to adjacent equipment, damage to the disconnector contacts due to the thermal effects of the arc that is drawn and physical harm to the operator. In order to minimise the occurrence of such an operation, the IEEE guide, IEEE C37.36b-1990, [5] suggests that the switching operator reclose the disconnector.

Furthermore, as an additional isolation requirement, disconnectors are required to have a greater voltage withstand capability across the open gap than to ground. The purpose of this is to ensure that any surge voltages in the power system cause a flashover to ground than across the open gap [4]. By so doing, the safety of operating personnel is maintained. Operating personnel are encouraged to always ensure, by visual inspection that the disconnector has interrupted the circuit before working on equipment.

The risk posed to operators is only applicable if the disconnector being switched is manually operated. Motor-operated disconnectors, which can be operated remotely by the switching operator, are available. However, they are more expensive than the manually operated disconnectors. At sub-transmission voltages of 66kV and 132kV, according to prices obtained from suppliers, the price range for a hand operated disconnector is between R30 000 and R45 000 [13]. A motorised disconnector is priced between R50 000 and R80 000 [13]. If one was to be used at a typical 132kV substation layout with two sources and two transformers, the substations could have up to 8 disconnectors installed. If the disconnectors were all hand-operated, the total amount for the disconnectors could be R360 000. If all eight disconnectors were motor operated, the total amount for the disconnectors alone would be up to R640 000. As a consequence, motor-operated disconnectors are rarely installed on sub-transmission networks. In addition, more manually operated disconnectors are installed on the sub-transmission networks, over and above the ones that are already in operation. In this thesis, the focus will be on manually operated disconnectors and reference to ‘disconnectors’ will refer to manually operated disconnectors.

Moreover, the operating regulations of the South African utility company, Eskom, require an insulating distance with visible break and a disconnector mechanically locked in the open position when personnel are working on any part of the power systems [14]. As alluded to earlier, many of the disconnectors in operation on the Eskom sub-transmission network are manually operated. During a switching operation of such disconnectors, the arc that is drawn is a concern to the operators that operate these switches. As mentioned before, if the arc continues to burn even when the disconnector is in a fully open position, the result could be equipment damage and hazard to personnel.

The results presented in this thesis are closely related to a study that was initiated by the Eskom Distribution Division in the Western Region. The study sets out to investigate how accurately one can predict the switching capability of a disconnector using simulation tools, and as a result, guide the switching operators, who operate the disconnectors, on whether or not the switching operation will be successful. Furthermore, the study will explore the extent to which the limited current interrupting capability of a disconnector can be utilised. The focus is on switching operations of capacitive currents as associated with unloaded overhead transmission lines.

## 1.3 Motivations and Objectives for the study

There is value in being able to predict within a stated margin of error the magnitude of the negligible current that can be switched by a disconnector, yet still not risk the safety of personnel or damage the contacts of the disconnector. Since disconnectors exist on the networks already, being able to use them to make or break current gives system planners and designers an opportunity to harness their current breaking capabilities. This is important in tough economic times; instead of using expensive breakers, load switches or motor-operated disconnectors, manually operated disconnectors can be used as an alternative.

The motivations behind this study are to investigate:

- Whether disconnectors can be used to optimise outage procedures by transferring current from one circuit to another without affecting customers.
- If a switching operation using a disconnector will be successful and safe depending on the type and magnitude of current being interrupted. This will be highly beneficial to the power utility.
- Whether both ATP and DigSILENT PowerFactory are appropriate tools that can be used to simulate the behaviour of disconnectors in power systems.

For transient simulations, like those associated with switching operations, an Electromagnetic Transient Program (EMTP) based tool is recommended by various researchers. ATP is a royalty

free version EMTP. It is widely used for digital simulations of transient phenomena of electromagnetic as well as electromechanical nature [15].

PowerFactory is a power system simulation software tool developed by DigSILENT. This software is capable of performing load flow studies in radial and meshed networks (balanced and unbalanced), short circuit analysis and electromagnetic transient simulation studies, to name but a few [16]. Eskom acquired a corporate licence for PowerFactory. The tool is used mainly for steady state simulations and rarely for transient studies.

The specific objectives to achieve in this study are:

- To develop a model for capacitive current switching associated with an unloaded transmission line using a disconnector.
- To simulate the developed model in ATP and PowerFactory to predict the capability of disconnectors to switch capacitive currents.

Thereafter, the simulation results produced in ATP and PowerFactory will be compared. To the best of the author's knowledge, this study is the first time that simulation results from ATP and PowerFactory software packages are compared for the modelling of switching operations using disconnectors.

## 1.4 Methodology

There are several elements involved when studying switching operations using disconnectors; for instance, the type of disconnector, the medium in which the disconnector operates, the circuit in which the disconnector operates and the type of current that is interrupted. One of the more important elements is the type of current being switched.

In an attempt to narrow the scope of the study, it was decided to choose one type of current to study. Capacitive currents became the focus of the study, in particular capacitive currents associated with unloaded transmission lines. Research suggested that switching of capacitive currents generated the more severe overvoltages up to 2p.u. on power systems [4]. Furthermore, at distribution voltage levels of 132kV, 66kV or lower, it is common practice to switch

unloaded transmission lines with disconnectors as the line lengths are shorter and thus have smaller capacitive currents.

In an effort to achieve one of the major objectives of this research, which is to predict whether or not a switching operation will be successful, computer simulations of the switching operation and network are used. To determine if the method is an adequate one, two simulation software tools are used to model the network components and the switching operations. Thereafter, the results of the simulations are compared. If the simulation results show overvoltages that are 2.0p.u. or greater at the point of switching, then the overvoltages are considered severe. And as a result, the switching operation is deemed unlikely to succeed.

A major portion of the study considers how the network is modelled in the simulation packages. The configuration of the network as seen from the terminals of the switch as well as the elements in the network will determine the amplitude, frequency and shape of the current and voltage oscillations [17].

Two types of time domain models have been developed for overhead lines:

- Lumped model.
- Distributed parameter model.

The distributed parameter model can be divided into two categories: the constant parameter and the frequency dependent parameter model [18]. The appropriate selection of a model depends on the line length and the highest frequency to be simulated.

Part of the simulation studies performed in ATP and PowerFactory examine the behaviour the different lines modelling techniques have on the overall switching operations. Based on results and expectations from the literature review, the results from ATP and PowerFactory are used to determine the most appropriate transmission line modelling technique for switching operations.

Mitigation techniques are identified to reduce overvoltages caused due to disconnector switching. These techniques are also simulated in ATP and PowerFactory and the results are presented.

The method in which the simulations were based during this study can be summarised as follows:

- A suitable network where a disconnector was used to switch capacitive current was identified. A network that forms part of the Eskom Distribution system was used.
- Information about the network elements were gathered to facilitate the modelling of the network in both simulation software tools.
- The power system model was simulated in ATPDraw and in PowerFactory. Load flow studies were performed on the models in both simulation packages and results were compared.
- Thereafter, the model was setup to run the switching studies. First, switching operations were made to unload the transmission line being switched to ensure no-load switching of the transmission line. Furthermore, the disconnectors were modelled as ideal switches, where current was interrupted immediately.
- Afterwards, in ATPDraw, an ATP simulation was run, while in PowerFactory, an electro-magnetic transient (EMT) simulation was run.
- Once the simulations were run, the voltages and currents at the source side and load side of the disconnector were measured. The highest overvoltage as well as current was recorded.

The next section discusses how the study and its results are structured and presented.

## 1.5 Outline of Thesis

The structure of this thesis is as follows:

Chapter 1 gives the background to the study, states the problem of the study and puts forward the objectives.

Chapter 2 presents literature related to disconnectors, switching operations, capacitive currents, and transmission line modelling techniques.

Chapter 3 introduces an electric circuit identified for the simulation tests. The simulation tools used in the study are briefly discussed. The modelling of the test circuits used in both simulation tools are discussed as well.

Chapter 4 explores the modelling considerations for switching operations, in particular the modelling of overhead transmission lines.

Chapter 5 shows the power system model used for the study and discusses the various other components used in the simulations.

Chapter 6 presents modelling considerations in the ATP software package.

Chapter 7 presents the modelling considerations using the DigSILENT PowerFactory software package.

Chapter 8 presents and discusses the results obtained from both simulation tools

Chapter 9 draws conclusions from the presented results and makes recommendations.

# Chapter 2 Literature Review

## 2.1 Introduction

In this chapter, a literature review of the contributions made by several authors on the subject of disconnector switching operations is provided, beginning with some of the earliest studies performed on disconnect switching operations in the early 1950s, up to one of the more recent studies published in 2004. The theories, findings and practices as observed by the researchers are examined and reviewed. First, a review of the international standards regarding disconnect switches is considered.

## 2.2 Definitions from Standards for Disconnectors

The National Committee of Standards South Africa, adopted the IEC standard, IEC 62271-102 for High Voltage switchgear and controlgear as a South African National Standard (SANS) in 2008. IEC 62271-102 replaced the third edition of IEC 60129. The IEC 60129 standard was published in 1984, with amendments added in 1992 and 1996. IEC 62271-102 is, thus, the most recent edition of the standard currently in use in South Africa.

The IEC 62271-102 standard [7], which makes reference to IEC 60050-441 [1], defines a disconnector as "*A mechanical switching device which provides, in the open position, an isolating distance in accordance with specific requirements*."

A definition for a mechanical switching device is provided by the IEC 60050-441 as: "*A switching device designed to close and open one or more electric circuits by means of separable contacts"* [1]. The definition for a mechanical switching device also notes that any

device "*may be designated according to the medium in which its contacts open and close, e.g. air, $SF_6$, oil*" [1]. Also, a switching device is defined as a device "*designed to make or break the current in one or more electric circuits*" [1].

Moreover, in defining a disconnector, the IEC 62271-102 notes that: "*A disconnector is capable of opening and closing a circuit when either negligible current is broken or made, or when no significant change in the voltage across the terminals of each of the poles of the disconnector occurs*" [7]. Further the standard states that a disconnector is "*capable of carrying currents under normal circuit conditions and carrying for a specified time currents under abnormal conditions such as short-circuit*" [7].

Additionally, IEC 62271-102 explains that 'negligible current' implies "*currents such as the capacitive currents of bushings, busbars, connections, very short lengths of cable, currents of permanently connected grading impedances of circuit-breakers and currents of voltage transformers and dividers*" [7]. The IEC 62271-102 standard advises that a current not exceeding 0.5 A is a negligible current for the purpose of the definition, for rated voltages of 420 kV and below; for rated voltage above 420 kV and currents exceeding 0.5 A, the manufacturer should be consulted. "*No significant change in the voltage*" refers to such applications as the by-passing of induction voltage regulators or circuit-breakers [7].

The IEC 62271-102 standard further notes that for a disconnector having a "*rated voltage of 52 kV and above, a rated ability of bus-transfer -current switching may be assigned*" [7]. 'Bus-transfer current switching' refers to the "*opening and closing of disconnectors under load when this load is not interrupted, but transferred from one bus to another*" [7]. In most North American publications, bus-transfer current switching is referred to as 'loop-current switching' [5], [6].

The Institute of Electrical and Electronic Engineers (IEEE) defines a disconnector as "*a mechanical switching device used for changing the connections in a circuit, or for isolating a circuit or equipment from the source of power*" [6]. The IEEE C37.30-1997 standard remarks that the disconnector is required to "*carry normal load current continuously and also abnormal or short-circuit currents for intervals as specified*" [6]. It says that the disconnector is "*also required to open or close circuits when negligible current is broken or made, or when no*

*significant change in the voltage across the terminals of each of the switch poles occurs*" [6]. Moreover, an earlier publication, the IEEE C37.36b-1990 [5], provided a guideline to use for disconnector switching of unloaded transformer currents and short-bus, overhead line and cable currents.

Both the IEC and IEEE standards agree that disconnectors are not designed to make or break large currents. However, the same standards recognise that disconnectors can be used to switch negligible currents and loop currents. These types of current mentioned in the notes of the IEEE and IEC standards are discussed briefly below.

### 2.2.1 Magnetising current

The one of currents identified in the standards is the magnetising current or unloaded transformer current. This is the current that typically flows when a transformer winding is energised. When a sinusoidal or alternating current is applied to a transformer winding, an alternating magnetic flux is induced in the core. The current, however, is non-sinusoidal and has a strong 3$^{rd}$ harmonic component. Heat is generated in the core, resulting in what is known as 'no-load' loss. The no-load loss is independent of the transformer loading. That is to say, the core is heated regardless of the amount of load on the transformer. Typically, transformers are designed such that the magnetising current is a small fraction of the rated current of the winding (less than 2A [4]) that is being energised.

### 2.2.2 Bus-transfer current switching or Loop switching

The next type of current that could be switched by a disconnector is a loop switching current. Loop switching is defined as the transfer of current from one circuit to a parallel circuit, for instance parallel transmission lines. This is the type of current referred to in the IEC standard, IEC 62271-102, as bus-transfer current switching. IEEE C37.30-1997 [6] refers to it as loop switching. Loop switching performed between busbars within a substation is known as bus-transfer. In other words, loop switching can be defined as the opening or closing to disconnectors under load but the load is not interrupted, instead it is transferred from one circuit to another [7]. Depending on what type of parallel circuit that is switched, the range of current varies from a few hundred amperes between transmission lines or up to 1600A between busbars

[9]. IEC 62271-102 [7] suggested a maximum bus-transfer current of 1600A, irrespective of the value of the rated normal current of the disconnector. The level of current transfer is determined by the arc voltage.

### 2.2.3 Capacitive current

The other type of current that can be interrupted by a disconnector is a capacitive current. The capacitive current referred to here is not the capacitive load current that is associated with capacitor banks. Instead, it is the capacitive current associated with a busbar, bushing, capacitive voltage transformer, an unloaded transmission line or an unloaded underground cable [5], [6], [7]. It is this type of no-load capacitive current that is considered as negligible. It is this type of capacitive current that forms the main focus of this study.

## 2.3 Types of Disconnectors

Various types of disconnectors are found in a sub-transmission network. Two of the major considerations to take into account when determining which type of disconnector should be used are: the spacing between the different phases of the switches as well as the clearance to other objects in the substation.

Phase spacing is a concern because when a switch is opened, the circuit will try to 'oppose' the action. The current will continue to flow as the insulating medium breaks down and an arc is drawn. As the arc is drawn, it extends in the direction that the opening contacts move. If the phase spacing is not adequate, the arc could come into contact with the phases or ground and form a short circuit. With this in mind, the types of disconnectors commonly used are listed below.

### 2.3.1 Horizontal break type

The horizontal break type of disconnector, shown in Figure 2.1, consists of only one movable blade and is mounted horizontally. When the disconnector is closed, the blade is in a horizontal position. As the disconnector opens, the blade moves in the horizontal plane to the right or left, depending on the blade orientation. This disconnector opens in a horizontal motion. This

motion necessitates an increase in phase spacing above standard values, so that in the open position the distance from blade to grounded object (or adjacent phase) is not compromised.

Figure 2.1 Horizontal break type disconnector [*Courtesy of Eskom*]

### 2.3.2 Vertical break type

The vertical break type of disconnector, shown in Figure 2.2, is similar to the horizontal break type in the sense that it consists of only one movable blade. It can be mounted horizontally or on its side. However, unlike the horizontal break type, this disconnector opens in a vertical motion, i.e. the blade moves in an upward direction. Standard phase spacing is used for this type of disconnector, but overhead clearances must be confirmed in order to cater for a fully open disconnector blade.

### 2.3.3 Centre side break type

The centre side break disconnector, shown in Figure 2.3, consists of two blades that are movable and engage at a point midway between their supports. When the disconnector is closed, the blades are in a horizontal position. The blades of this type of disconnector split open in the horizontal plane from their point of contact. As a consequence, phase spacing must be increased to achieve adequate clearance with adjacent structures.

Figure 2.2 Vertical Break type disconnector [4]

Figure 2.3 Centre side break type disconnector [*Courtesy of Eskom*]

### 2.3.4 Double side break type

The double side break disconnector is similar to the centre side break type, except that the blade of this type pivots at the centre. The blade opens out in the horizontal plane and is open at both its ends, refer to Figure 2.4.

Figure 2.4 Double break type disconnector [*Courtesy of Eskom*]

### 2.3.5 Pantograph type

This type, shown in Figure 2.5, has a 'scissor-like' type blade with a stirrup arrangement attached to the busbar at the top. Standard phase spacing is required for this type of disconnector.

Figure 2.5 Pantograph type of disconnector [*Courtesy of Eskom*]

### 2.3.6 Horn-gap disconnectors

In order to circumvent short circuits or damage to disconnector contacts caused by arcing during switching operations, arcing should be limited or avoided as much as possible. For this reason, one would find disconnectors fitted with arcing horns. The arcing horns do not contribute to current interruption but instead, provide a location for the arc to act. These types of disconnectors are referred to as horn-gap disconnectors. Different methods have been employed to try and reduce the arcing time during switching operations. In attempts to increase the switching capabilities of the disconnect switches, switches have been retrofitted with whip-type devices, air-blast devices or pres-insertion resistors. In other cases, the medium in which the contacts break or make current is altered, for instance vacuum switches or gas switches. These mitigating techniques have been used to numerous levels of success and documented in [8], [11] and [19].

## 2.4 Review of Previous Works

There is a wide range of contributions from authors that have influenced and shaped the current switching capabilities of disconnectors. However, only publications that have helped mould the direction and the focus of this thesis are reviewed in this section.

### 2.4.1 Contributions from Andrews, Janes and Andersson [8]

One of the earliest studies done on air break switches, and for many years quoted as an authoritative source was the work of Andrews, Janes and Andersson [8]. The study was published in 1950 and investigated the interrupting ability of horn–gap switches. The authors had three objectives, namely [8]:

- To study arc behaviour on horn gap switches under various system conditions;
- To determine the magnitude of currents that can be interrupted on existing switches under prevailing system conditions, and

- To determine basic switch design factors for successful operation under specified conditions.

At the time when the authors carried out their research, two basic concepts of the arc behaviour were generally recognised. One was that the arc length was proportional to the voltage and the second was that an unconfined arc would always extinguish itself if clearance permitted the arc to grow to the required critical length and the gap was wide enough to prevent re-striking [8].

Andrews *et al*. defined arc length as the actual complete length of the irregular circuitous arc path [8]. They introduced a term known as "reach". Arc reach was defined as the distance from a point midway between the arc extremities to the most remote point of the arc at the time of its maximum length [8]. Reach was devised as the measure of spread to provide a criterion for comparison with switch clearances.

There was lack of consensus between researchers on the relation of current and arc length at the time. Andrews *et al*. set out on a series of tests to determine any relation between switching operation using disconnectors as well as arc length, arc current, open-switch voltage and/or arc reach. In order to establish the true relationship between arc length and current, the authors decided to take direct physical measurement of current interrupted by a disconnector and the voltage across the disconnector terminals soon after interruption. They used a series of photos taken of the arcs with two cameras at right angles to provide arc dimensions and used oscillograms to obtain arc currents and voltages.

Measurements for transformer exciting current and loop current were performed, from which Andrew *et al*. [8] derived an equation for the limit for probable arc reach $L_{pr}$ . This equation (2.1) was used for magnetising and loop currents based on a series of test results from switching disconnectors at 33kV.

$$L_{pr} = 5.03EI \tag{2.1}$$

where:

5.03 is a constant with units in mm/kVA.

$L_{pr}$ is the probable arc reach in mm.

$E$ is the phase voltage in $kV_{rms}$ across the switch after interruption.

$I$ is the interrupted current in amperes.

Using statistical measures, the authors deduced that the equation would be valid for currents in the range 0 – 100A.

Tests were performed on 132kV horn-gap switches to determine the lengths of line that could be safely de-energised [8]. A line, measuring over 50 km, was divided up into sections of varying lengths. Measurements were taken at the spots where the authors thought the lines could be safely de-energised. Current values in most cases were calculated from the line characteristics and the prevailing voltage. The currents ranged from 2.2A to 20A [8]. From their report, Andrews *et al*. had little difficulty in interrupting currents of up to 7A within safe reaches for horizontal spacing of 4.88m. Above 7A they had to depend on wind to succeed in their operation [8].

The authors went further and also made the following generalised pronouncements [8]:

- An open arc formed on adequately separated electrodes would extinguish if it is free to expand to its critical length.
- A horn gap switch will successfully interrupt a current if its dimensions are adequate to permit the arc to grow to its critical length. An exception might be with the wind blowing in line with the arcing horns.
- With conventional horn-gap switches, arc length and reach are independent of the type of switch and the speed of operation.
- Two arcs in series have about the same total length as a single arc produced under the same condition. The pair may be of different lengths.

- Arcs are longer when interrupting line charging current than when interrupting a corresponding amount of resistive or inductive current with similar voltage across the switch gap.

In concluding their paper [8], Andrews *et al*. recommended that the most adequate and practical criterion required to determine the success of a switching operation was the arc reach. Furthermore, that for line charging current, the 132 kV test demonstrated that approximately 7 amperes, equivalent to the charging current of a 17 km of line may be safely interrupted. The test team also concluded that "*under favourable wind direction*", current as high as 20A could be interrupted [8]. However, the meaning of "*favourable wind*" direction was not discussed in the paper.

### 2.4.2 Contributions from other authors in early 1960s

Other authors also studied the de-energisation of transmission lines using air break switches. Foti and Lakas [20] ran tests on disconnectors fitted with and without resistors, with and without gas blast as well as tests on disconnectors fitted with gas blast-resistor combinations. For extra high voltages of 400kV, they recommended the use of gas blast devices on the disconnect switches when interrupting capacitive currents [20].

Rankin [21] performed line dropping tests where the air break switch opened approximately 28.7 miles (≈ 46.2km) of charging current. The switch sustained extensive arcing when operating at the 138kV voltage level. Approximately 20.3 miles (≈ 32.7km) or 8 amps of charging current was switched with what Rankin termed as "controlled arcing". This led Rankin to recommend a 20 mile switching limit for line charging current using a disconnect switch with no additions [21].

### 2.4.3 Results from a survey on interrupting ability of air break switches [10]

In the early 1960's the IEEE commissioned a survey to determine the operating practice of electric utility companies regarding the interruption of small magnitudes of magnetising, charging and loop currents using air-break switches [10]. The questionnaire was issued to 104

utility companies selected according to size and location in the United States. Of the 104 questionnaires that were sent out, 71 responded.

Among the questions asked in the survey was one that asked respondents to indicate if they used air break switches for de-energising radial lines. Sixty five percent indicated that they did, while 20 percent did not answer the question and 15 indicated that they did not use air break switches to de-energising radial lines. Another question asked the respondents to indicate if they used other devices in conjunction with air break switches, such as quick-breaks, puffers to aid in successful interruption. The majority of the respondents indicated that they did make use of other devices, the most popular being quick break devices and gas interrupters [10].

It was noted by the authors of the survey that, unfortunately, the questions in the survey were posed in such away that the answers depended on how the respondent interpreted the questions. Various concepts were not clearly defined in the questionnaire. For instance, a description of the type of disconnector used for the tests was not provided; that is to say whether or not they used vertical break, horizontal break or centre break switches. Definitions were not given for what constituted the type of system operated on: grounded system, or ungrounded system. Nevertheless, the data received from the respondents indicated the disconnectors are widely used for the interruption of negligible currents, at least in North America. Still, what was brought to the forefront by the survey was the extensive use of various types of interrupting devices by utilities to improve the switching capability of the disconnectors.

One of the responses to the survey that is worth a mention was from the Detroit Edison Company in Detroit, Michigan in the United States. The company indicated that it used air break switches to de-energise radial lines at voltages up to 40kV with no problems experienced as the lines were relatively short. However, on the 120kV systems, some lines had to have disconnectors fitted with resistors [10].

What is also mentioned by the Detroit Edison company is the “general 600kVA rule” used to interrupt capacitive currents. It is stated that as a general rule, the company limits the use of air break switches to interrupt an equivalent power threshold of 600kVA [10]. This rule was applied using equation (2.2):

$$3 \times \text{Current} \times \text{Voltage across the open switch} \quad (2.2)$$

In the survey, the Detroit Edison company further stated that at 1000kVA, or more, air break switches failed to interrupt the circuit unless wind direction and all other factors are favourable. In the absence of proper guidelines, the theory or general rule was then practised by various utilities with varying results. It was once practised sparingly by the South African utility, Eskom, as an indication to whether or not switching operations would be successful. However, the rule was later refuted in a study by another researcher, Peelo, as coincidental rather than factual and had no merit for application during switching operations with disconnectors [4].

### 2.4.4 First contribution by Peelo [11]

One of Peelo's earliest contributions in the assessment of the capability of disconnectors in interrupting current was through a paper he presented to the IEEE Transactions on Power Delivery in 1986.

In his 1986 paper, Peelo also recognised the problem that although disconnectors were widely used in de-energising sections of power systems, they were not designed to interrupt current. Yet they were invariably being used, without intention, to interrupt negligible current associated with no-load switching operations [11].

Peelo had two objectives for his study when it was initiated. The first was to determine the maximum magnetising, capacitive, and loop current that could be safely interrupted using air break disconnectors given particular phase spacings. The second was to develop rules for the application of disconnect switches with or without auxiliary interrupting devices [11].

In his paper, Peelo asserted that for capacitive current interruption the maximum arc reach was up to 2.75 times the limit of probable reach for a magnetising current. He stated that overvoltages experienced during capacitive current switching were high fast front overvoltages. High fast front overvoltages refer to the shape of the voltage waveform during the switching operation. The CIGRE Working Group 05 [22] explains high fast front overvoltages using an example of a transmission line being energised. If a transmission line is connected to a feeding bus, the transient voltage on the energised line starts with a step amplitude. This step amplitude experienced on the transmission line can include steep fronts and in some cases unfavourable

voltage peaks or spikes due to the different propagation velocities on the network [22]. Peelo [11] states that overvoltages as high as 2p.u. were measured at B.C. Hydro. And for his calculations, which are discussed next, he made assumptions that for switches rated 230kV and below, an overvoltage factor $k_0$ = 2.4p.u. is used. And for switches rated 500kV, the factor is 1.6p.u..

Peelo used the equation (2.1) that Andrews *et al*. developed to determine probable arc reach, to calculate the maximum allowable arc reach for a given phase spacing. Peelo made a few other assumptions, like the type of disconnector one used and the maximum overvoltage one could expect and derived equations (2.3) - (2.5) [11].

From equation (2.1), Peelo derived the following equations [11]:

$$\begin{aligned} P_{mr} &= 2.75\left(5.03\frac{U_{l\max}}{\sqrt{3}}\right)I_C \\ &= 1000d_r \end{aligned} \tag{2.3}$$

and

$$d_r = d_\varphi - \frac{k_0 U_{l\max}}{418.7} \tag{2.4}$$

where:

- $P_{mr}$ is the probable maximum reach.
- $U_{lmax}$ is the maximum system line-to-line voltage.
- $I_C$ is the maximum allowable capacitive current to be interrupted.
- $d_r$ is the maximum allowable arc reach.
- $d_\varphi$ is the minimum metal-to-metal phase-to-phase clearance.

From equations (2.3) and (2.4), $I_C$ could be calculated as follows:

$$I_C = \frac{126}{U_{l\max}}\left(d_\varphi - \frac{k_0 U_{l\max}}{418.7}\right) \tag{2.5}$$

For a network with a maximum system voltage of 72.5kV and a minimum metal-to-metal phase-to-phase clearance of 1m, the maximum allowable capacitive current using equation (2.5) was 1.02A.

Once the maximum capacitive current was calculated, Peelo translated that current into a line length in kilometres that could be dropped or de-energised by the disconnect switch. At a maximum system voltage of 72.5kV, the maximum line length that could be de-energised was 3.6km [11]. In the paper, Peelo suggested high speed whip type interrupting devices in order to de-energise longer line lengths. In addition, he recommended that all disconnectors rated 230kV and below be equipped with arcing horns [11].

### 2.4.5 Contributions by Knobloch on capacitive current switching [23]

In 1987, Knobloch presented results from an experimental circuit used to assess the transient phenomena that occurs during switching operations of outdoor disconnects. Up until 1987, most authors assumed there was a correlation between the current being interrupted and the success of the switching operation [8] [11]. However, that assumption was challenged by Knobloch [23]. What was proposed and discussed in his paper instead was a possible correlation between the arcing time associated with the discharge length of the isolating distance and the capacitive current being switched.

The experimental circuit used for the test presented in the Knobloch paper [23] involved extensive tests upon which capacitors of various sizes were operated on. The type of switch used was a pantograph disconnect switch and the experimental circuit categorised the capacitors into source-side capacitors ($C_s$) and load-side capacitors ($C_l$).

During the current interruption tests, Knobloch classified the transient phenomena that he observed into high frequency phenomena and low frequency phenomena. High frequency phenomena were typical for switching-on operations where $C_s > C_l$. Frequencies of up to 750kHz were observed for the experimental circuit used in the test. High frequency phenomena were described as frequencies that were generated when one capacitor discharged into another.

In contrast, the low frequency phenomena were determined by the inductance of the supply and the capacitors of the supply, $C_s$. Knobloch noted that under the low frequency conditions, for $C_s > C_l$, only when the voltage on the supply-side changed polarity, the potential difference between the supply side and load side of the disconnect switch was large enough to initiate a reignition or restrike. When $C_s \ll C_l$, a "severe overshoot of voltage occurred after the arc is extinguished" [23]. The arc is said to occur more frequently with the absence of an additional supply side capacitance. The author concluded that the load on a disconnector was generally greater during switching operation without a supply side capacitor than with a supply side capacitor.

During his tests, Knobloch noted that overvoltages of up to 1.6 times the peak value of the voltage were present on the supply side during a "switching-on" or energising operation. In contrast, twice the peak value of the voltage on the supply side is observed during de-energising operations. These extreme values were measured for cases where $C_s \ll C_l$ [23].

Knobloch concludes that [23]:

- Higher overvoltages are registered on the supply side of the disconnector than on the load side.
- Higher overvoltages happened when $C_s \ll C_l$.
- Higher values of overvoltages are measured during a "switching-off" or de-energising operation rather than during a "switching-on" operation or energising operation.
- Overvoltages are not more than double the peak value of alternating test voltage applied.

Unlike Peelo and Andrews *et al.*, Knobloch notes that there is no correlation between the overvoltage factors and the test voltage when switching capacitive currents. Furthermore, with the tests that he performed on outdoor disconnectors, he states that disconnectors are capable of switching off a capacitive current of at least 1A reliably irrespective of the voltage level.

### 2.4.6 IEEE Guide to Current Interruption [5]

By the late 1980s, it was well known that the practice of using disconnectors to interrupt negligible currents as those defined earlier in the chapter was widespread. In 1990, the IEEE published a guide intended "to provide air switch users with a means for determining the magnitude of excitation as well as resistive and capacitive currents that may be successfully interrupted with horn-gap, vertical break air switches in outdoor locations" [5].

The guide was put in place because of the lack of an interrupting rating on the disconnect switches which led to several problems, including [5]:

- Various and inconsistent user policies (practices) regarding the utilisation of air switches to interrupt currents.
- Improper use of air switches, which results in switch failures, system faults and outages.
- Excessive surge arrester operations during interruption of small currents with air switches.
- Installation of complex switching arrangements that could be replaced by simpler schemes that utilise the interruption capabilities of air switches.
- Extensive switching operations to avoid opening air switches in the energised mode wherein they might be required to interrupt small currents.

The document provides guiding principles to follow when switching transformer excitation currents as well as bus, line or cable capacitive currents. However, these guidelines are based primarily on the findings of Andrews *et al*. [8] and Peelo [11]. Suggested currents that may be switched with air switches equipped with arcing horns and have minimum phase clearances to grounded objects are listed too. These are calculated using equations (2.1) from Andrews *et al*. and equation (2.5) from Peelo.

### 2.4.7 Contribution by Patel, Holcombe and Parr [19]

In 1989, Patel, Holcombe and Parr published the results performed at the Georgia Power Company. The authors acknowledged the early contributions of Andrews *et al*. [8] and Peelo [11] as studies pertaining to air-break switches with or without a horn-gap device. However, Patel *et al.* wished to extend the evaluation for the application of air-break switches to include devices that increased the speed of interruption. The tests presented in their paper focused on air-break switches equipped with fast interrupting mechanical devices. In addition, Patel *et al*. set out to determine what influence parallel lines and line or conductor configuration had on charging current of 115kV lines [19].

The results of the tests performed at the Georgia Power company showed that [19]:

- Parallel lines on the same right-of-way, line configuration and conductor diameter did not significantly affect the line charging current.
- Conductor configuration significantly affected line charging current. Bundled conductor was found to increase charging current by up to 35% above single conductor.
- Six-wire configuration increased the charging current by 94% above a single conductor.

Another part of the study performed by Patel *et al*. was to test the interrupting capability of various quick-break switches to de-energise various length of transmission line. It was found, as expected, that high tip speed and minimum bounce of quick-break devices increased the charging current interruption capability. A 69.2 km line with a charging current of 15A at 115kV was de-energised with minor arcing when operated using a spring-operated high-speed-break device and a hydraulic push-pull operator [19].

### 2.4.8 Second contribution by Peelo [4]

In the early 2000s, Peelo embarked on an in-depth study of current interruption using high voltage air-break disconnectors. His study was based on utility practices by B.C. Hydro in Canada as well as laboratory tests at Eindhoven University of Technology and KEMA in the Netherlands. The objectives were [4]:

- To investigate and interpret free burning arc behaviour.
- To advance the basis for the use of air-break disconnectors.

Peelo studied current interruption using high voltage air-break disconnector for the interruption of transformer magnetising currents, capacitive currents and loop current switching. But, because this thesis focuses on the capacitive current interruption, only the results presented by Peelo on the matter of capacitive current interruption are discussed.

Peelo conducted a series of tests in 2003 at the KEMA High Power Lab to investigate the dependence of successful capacitive current switching on source and load side capacitance. This dependence had been noted in an earlier study by Knobloch [23]. Currents within a range of 0.23A to 2.3A were interrupted in the series of tests using a 300kV centre-break type disconnector [4]. The results from the tests that Peelo conducted agreed with the results from Knobloch, which stated that the highest overvoltages occurred when source-side capacitance was less than load side capacitance, i.e. $C_s < C_l$ or the ratio $C_s/C_l < 1$. Peelo determined that arc duration showed a dependency on the source-side capacitance. Again, the worst cases occurred for the lowest $C_s$ values. The arc was distinguished between two distinct modes, namely: the erratic mode and the stiff mode. Erratic mode is associated with higher overvoltages and longer arc durations, while the stiff mode is associated with lower values of capacitive current and $C_s/C_l > 1$ [4]. Figure 2.6 and Figure 2.7 taken from Peelo's work show the different modes exhibited by the arc. Figure 2.6 is of the erratic mode. Figure 2.7 shows the stiff mode [4].

However, the overvoltages obtained with the tests at KEMA had much higher overvoltages than those measured by Knobloch. Furthermore, it was observed that the overvoltages had no dependence on the current magnitude.

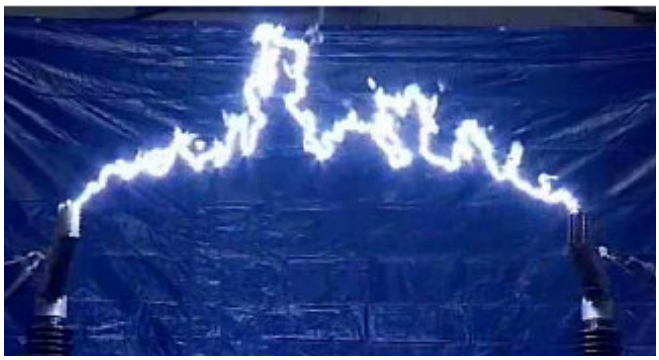

Figure 2.6 Capacitive current arc just before extinction: Erratic arc 2A, $C_s/C_l$=0.04 [4]

Figure 2.7 Capacitive current arc just before extinction: Stiff arc 1A, $C_s/C_l$ = 3.1 [4]

Peelo stated that a capacitive current switching arc is a succession of interruptions and re-strike (in contrast to loop current switching arc, which burns continuously) [9]. When $C_s/C_l$ is low, the transient arcing currents are higher and make interruption more difficult. Peelo concluded that high arcing currents were conducive to the occurrence of re-strikes and thus longer arcing durations. Peelo found that capacitive currents that were greater than 1A in magnitude produced arc channels that were thermally conducive to re-strikes. And so for currents greater than 1A, arc duration was not only dependent on $C_s$ and $C_l$ but also depended on achieving the minimum disconnector gap spacing required to withstand the recovery voltage before a re-strike took place [4]. In as much as overvoltages did not depend on current, Peelo concluded that arc duration depended on current being interrupted.

Another finding by Peelo was that the frequency of the overvoltage transient following voltage equalisation was determined by the source voltage and $C_s$ and $C_l$ in parallel. Frequencies between 500Hz and 3kHz were observed in the tests [9].

Among other objectives in his research, Peelo set out to verify the results from the tests conducted by Andrew *et al*. in the mid-1940's. The results of these tests published in a paper in 1950 [8] were discussed earlier in this chapter. Andrews' results have been the basis of several

studies, standards and guides relating to disconnect switches, including the IEEE guide to current interruption with horn-gap air switches [5].

With the tests that Peelo reproduced, nearly 50 years after Andrews *et al*. [8], Peelo found that the results between the two set of tests were not consistent. The tests were performed at the Powertech Laboratories in Canada and were specifically testing loop current switching. Loop current switching is significant here because the guides that were developed from the findings of Andrews *et al*. have their foundation in equation (2.1). Equation (2.1) was based on the tests performed on magnetising and loop current switching, which was later extended by Peelo [11] to include capacitive current switching.

The results presented by Peelo [4] showed arcing times in excess of 1s in contrast to arcing times of 0.5s or less presented by Andrews *et al*. The arc lengths of the Andrews *et al*. tests were longer than those recorded by Peelo. In addition, the arc reaches calculated using equation (2.1) were much greater than those recorded by the tests by Peelo. These arc reach variances were especially greater for loop currents at 69A and 103A.

The differences in the results between Peelo's test and those of Andrews *et al*. led Peelo to question the validity of the results presented by Andrews *et al*. and the use of equation (2.1) to estimate arc reaches. Another argument posed by Peelo was that Andrews *et al*. did not relate current interruption to arcing time [4]; and that they viewed the persistence of the arc as acceptable – even after the test disconnector was fully open – provided that the arc reach was not excessive [4]. Peelo felt that allowing the persistence of the arc defied the prudent notion that the current should be interrupted while the moving contact is still in motion, and that manually operating such disconnector with the arc still burning even with the contacts fully open would be unacceptable and unsafe.

Peelo then derived an equation to determine the peak overvoltage value to ground, $U_{ov}$, across the disconnector during capacitive current switching. The voltages on the source side $(U_s)$ and load side $(U_L)$ capacitances are used to determine the voltage across the disconnector [4], $(U_d)$.

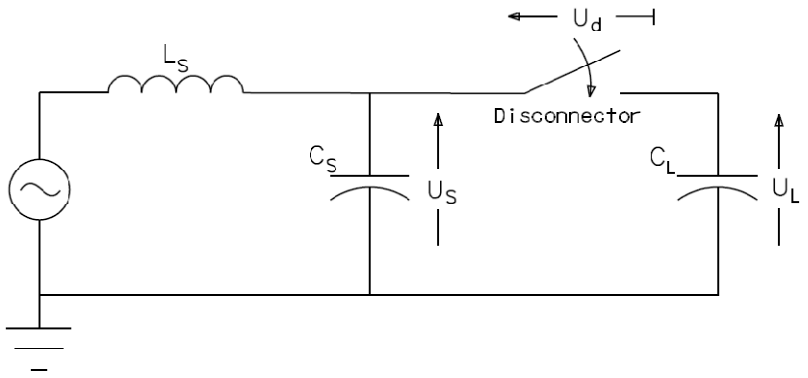


Figure 2.8 Simple circuit representation: capacitive current switching [4]

$$U_d = U_s + U_l \tag{2.6}$$

$$U_{ov} = U_s + \beta\left(\frac{U_d}{1+\frac{C_s}{C_l}}\right) \tag{2.7}$$

where:

$U_d$ is the voltage across the disconnector.

$\beta$ is the damping factor of the circuit.

From equation (2.7) when $C_s > C_l$, $U_{ov}$ will be low. When $C_s < C_l$, $U_{ov}$ will be high. Note the dependence of $U_{ov}$ on the ratio $C_s/C_l$.

## 2.5 Limitations of Disconnectors

The limitations for switching of disconnectors can be listed as follows:

1. Disconnectors are designed only to switch negligible currents. They cannot be made to make or break load currents.

2. The space allowed between the different phases when the disconnector is mounted is a limitation. If there is not enough space between adjacent phases to provide for the arc to

spread then the chances of flashovers between phases or phase to ground developing are increased.

3. The influence of weather, especially wind, poses a safety hazard for operators in particular. Field tests as documented by [8,10,4] show wind plays a favourable role in current interruption. However, it could promote movement of the arc and in so doing increase the risk for contact with adjacent phases or grounded structures.

4. If the current following a switching action exceeds its critical value, the maximum current value at interruption, the switching operation could fail entirely and/or result in thermal effects that would lead to burning out of the contacts as well as the undesirable prolonging of the arc.

It is important to note that in this study disconnectors are assumed to operate in air. The switches are also assumed to provide the electrical isolation from the power system in an open position and are not fitted with any auxiliary interrupting devices.

## 2.6 Common Research Methods used to Test Disconnector Switching Operations

Several approaches have been used by authors who have studied the switching capability of disconnectors. The most popular approach is the experimental one using field test results. This involves the setting up of high speed cameras positioned at various angles to the disconnector switches. Images of the arcs drawn during the switching operation are captured and from there the images are analysed and studied. This approach was used by Andrews *et al*. in the 1950s [8] and the method was still favoured by Peelo in 2004 [4].

Solving transient problems using hand calculations is cumbersome. Still, one can calculate solutions if simple circuits containing a small number of elements are used. Model reduction techniques would be required to get from large complex networks to user-friendly simple circuits. Model reduction of this kind generally leads to the over simplification of the transient

calculations. As a consequence of the circuit reduction, the user is left with steady state techniques being used to solve transient problems.

Computer simulation tools provide the accuracy and the speed needed to perform the complex calculations necessary to solve transient problems. However, one of the disadvantages of computer simulation tools is its user-friendliness. In other words, the ease with which the user can understand and learn how to use the computer simulation tools.

Over the years there have been several computational tools that have been used to solve transient problems. First, there was an analogue device called a Transient Network Analyser (TNA) [12], [24]. The TNA comprised of circuit elements, inductors and resistors, or analogue building blocks that were used to represent various components of the power system being analysed. They were used to investigate load flow, determine fault currents and perform stability studies on ac systems. The main drawback in using TNA was time: time to set up the model and time to organise and analyse the output [12], [17]. Later, conventional digital computer programs were developed. Over the years the ability of a digital computer to process large amounts of data in a systematic way and do in extremely short time has greatly improved.

There are several simulation software tools on the market. The Electro-magnetic transient program (EMTP) is one of the most widely spread and well-known computer programs used for electrical transient analyses. A royalty free version of EMTP, the Alternative Transient Program (ATP) is also available for use.

EMTP and in some cases ATP-EMTP have been used by several authors and work groups to analyse transient problems, related to switching overvoltages [18], [24], [25], [26], [27]. For instance, in [26], the aim of the authors was to compare the results from computer simulations and field tests when switching high voltage transmission lines. The computer simulations were performed using EMTP and a program developed by the authors based on Fourier transform methods. No name is given for the program the authors developed, although it is stated that it was developed for the purpose of comparison of the different line simulation techniques. The transmission lines were modelled using constant distributed parameter models calculated at 50Hz and at the natural frequency of the line as well as a frequency dependent model. The

results from these transmission line models were compared to field tests and found to be comparable. The constant parameter model calculated at the natural frequency of the line showed good agreement between the simulation results and the measured field results [26]. Moreover, the frequency dependent line model gave even better results [26].

An IEEE Working Group for system transients published modelling guidelines to use during digital computer simulations of fast front transients, such as those associated with switching operations [28]. The working group used the EMTP program as the choice simulation program with which to outline their guidelines. They did, however, state that the guidelines were broad enough to be used on other simulation programs.

Another simulation tool, even though it is relatively new, is PowerFactory. It was developed by DigSILENT and is a power system analysis tool that covers a number of applications, including electro-magnetic transient studies. ATPDraw, a graphical mouse-driven pre-processor of ATP, and PowerFactory are the simulation tools that are used for this thesis.

Although there have been investigations performed to observe and simulate switching overvoltages on transmission line as well as studies on the current interrupting capability of disconnectors, most of them, as indicated, have been performed using field tests and/or versions of EMTP. To the best of the author's knowledge, no studies have been performed where ATP simulation results have been compared to PowerFactory simulation results in modelling of switching transients where disconnectors are concerned.

## 2.7 Summary

The significant findings from studies carried out by other researchers can be summarised as follows:

- The 600kVA rule that was often used to determine whether or not capacitive currents could be interrupted was refuted. The rule was found to be coincidental and not factual.

- During capacitive current switching, the highest overvoltages occurred when the source-side capacitance was less than load side capacitance, i.e. $C_s < C_l$ or the ratio $C_s/C_l < 1$.

- Most studies of switching transients caused by disconnector switching operations have been based on field tests. Moreover, computer simulations that have been performed on this subject were carried out using EMTP based programs. The results from the computer simulations were found to be comparable to the results achieved during field tests.

Furthermore, disconnector switching is a widespread practice among utilities. However, understanding, measuring and predicting when and how best to carry out these switching operations has not been conclusively agreed to by researchers.

# Chapter 3 Switching Capacitive Currents

## 3.1 Introduction

The previous chapter presented findings from literature regarding disconnector switching operations. In this chapter, analyses of electrical transients associated with switching operations are discussed. Simplified circuits relevant to the study of the behaviour and response of the network to switching operations, namely the LC and RLC circuits, are presented. These circuits help to derive network characteristics needed to observe network responses, such as the characteristic impedance and frequency of the network.

## 3.2 The LC circuit

Electrical transients are introduced in the system when there are sudden changes in circuit conditions, for instance when a switch opens or closes or a fault occurs in a system. The time period over which transient voltage and current oscillations occur is in the range of microseconds to milliseconds, the analysis of which can get very complicated.

In order to gain a better understanding of the physical process which plays key roles in the transient time period of a power system, thorough analysis of the process is required. Analysis of a steady state circuits at power frequencies of 50 or 60Hz can be achieved successfully by means of calculus and phasors to represent voltages and currents. The power system transient frequencies, which are of concern in this study, go as high as kilohertz and megahertz. To

accurately represent the behaviour of a circuit which experiences transient phenomena, a circuit model would involve several differential and integro-differential equations, and these equations have to be solved to evaluate the circuit's transient response. The Laplace Transform method is used for this purpose.

The Laplace transform will only be used as a tool to assist in the transient circuit analysis. Only theory and transforms relevant to the study are presented here.

To assist in the understanding of transient analysis, a simple single phase representation of an overhead transmission line that is being switched is used by connecting an inductance and capacitance in series with each other. In Figure 3.1, two energy storage components are involved, an inductance storing the magnetic energy and the capacitance storing the electric energy.

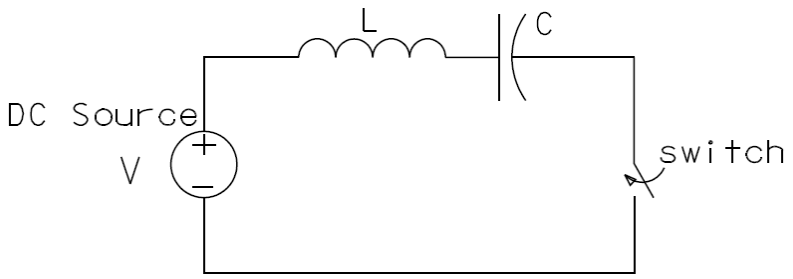


Figure 3.1 A DC source switched on an LC series network

In analysing the circuit shown in Figure 3.1, a DC source and an ideal switch is used in the analysis for simplicity. In the closed position, the switch behaves like an ideal conductor with zero resistance. In the open position, it behaves like an ideal isolator with an infinite resistance. The ideal switch changes from closed to open position instantaneously and the sinusoidal current is interrupted at the current zero.

Applying Kirchhoff's law to the circuit in Figure 3.1 gives:

$$L\frac{dI}{dt}+\frac{1}{C}\int Idt = V \tag{3.1}$$

Transforming the equation using the Laplace transform gives:

$$\frac{V}{s} = sLi(s) - LI(0) + \frac{i(s)}{sC} + \frac{V_C(0)}{s} \tag{3.2}$$

where:

$s$ is the Laplace variable.

$i(s)$ is the circuit current in the Laplace domain.

$I(0)$ is the initial current in the circuit.

$V_C(0)$ is the initial voltage across the capacitor.

Rearranging equation (3.2) results in

$$V - V_C(0) = s^2 Li(s) - sLI(0) + \frac{i(s)}{C} \tag{3.3}$$

$$V - V_C(0) = i(s)\left(s^2 L + \frac{1}{C}\right) - sLI(0) \tag{3.4}$$

By dividing (3.4) by$L$, and one gets:

$$\frac{V - V_C(0)}{L} = i(s)\left(s^2 + \frac{1}{LC}\right) - sI(0) \tag{3.5}$$

Due to the nature of the circuit shown in Figure 3.1, the current in the network is zero before the switch closes. Thus, the initial current $I(0) = 0$. Rearranging the equation results in the following:

$$i(s) = \frac{V - V_C(0)}{L} \frac{1}{s^2 + 1/LC} \tag{3.6}$$

Using the Laplace transform where $\mathcal{L}\left\{\frac{1}{s^2+\alpha^2}\right\} = \frac{1}{\alpha}\sin\alpha t$ , equation (3.6) transforms into:

$$I(t) = \frac{V - V_C(0)}{L} \frac{1}{1/\sqrt{LC}} \sin\left(1/\sqrt{LC}\right)t \tag{3.7}$$

If we let $1/LC = \omega_0^2$, then

$$I(t) = \left(V - V_C(0)\right)\sqrt{\frac{C}{L}} \sin(\omega_0 t) \tag{3.8}$$

Assuming that there is no charge on the capacitor initially when the switch closes, then $V_C(0) = 0$. Equation (3.8) simplifies to:

$$I(t) = V\sqrt{\frac{C}{L}} \sin(\omega_0 t) \tag{3.9}$$

From equation (3.9) one observes that the current in the circuit oscillates sinusoidally at a frequency of $\omega_0$. Furthermore, the ratio of the voltage to the current is given by $\sqrt{L/C}$. This ratio is called the surge impedance of the circuit [12]. Thus from equation (3.9), two important characteristics of any LC circuits have been determined, namely:

The frequency of the circuit:

$$\omega_0 = \frac{1}{\sqrt{LC}}, \tag{3.10}$$

and the surge impedance:

$$Z_0 = \sqrt{\frac{L}{C}}, \tag{3.11}$$

In practice, there is always damping in the series circuit and that can be represented by adding a resistance in series with $C$ and $L$ as shown in the next section [17].

## 3.3 The RLC circuit

All practical circuits have losses arising primarily from circuit resistance and iron losses in equipment. In transient analyses, losses are usually neglected to reduce the complication of the calculations. However, by neglecting the losses, the solutions given have severe high overvoltages. The introduction of a resistor always has the effect of damping out the natural oscillations of a circuit. How quickly the damping occurs depends on the value of $R$ relative to $L$ or $C$ [12].

Figure 3.2 illustrates two circuits: the parallel and series RLC circuit. First, a solution for the current in the inductor in the parallel circuit is considered. When the switch is closed $C$ discharges through $R$ and $L$. If $V_C$ is the capacitor voltage, then

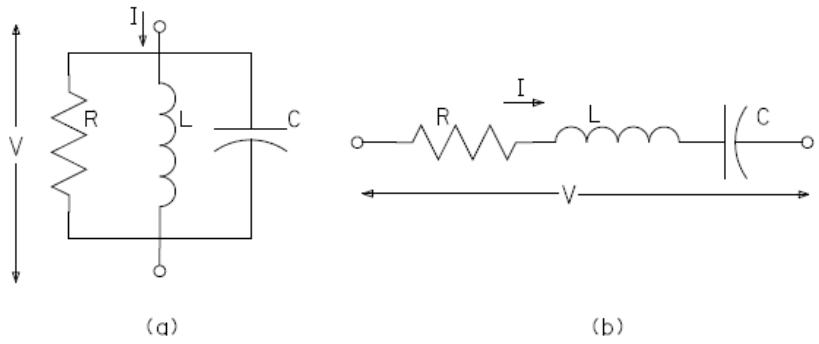


Figure 3.2 Parallel and series RLC circuits

$$-C\frac{dV_C}{dt} = I_L + \frac{V_C}{R}, \tag{3.12}$$

Where: $I_L$ is the current in the inductor.

Because we are considering a parallel circuit, then

$$V_C = L\frac{dI_L}{dt}, \tag{3.13}$$

Substituting $V_C$ in equation (3.12) and rearranging the equations results in:

$$\frac{d^2 I_L}{dt^2} + \frac{1}{RC}\frac{dI_L}{dt} + \frac{I_L}{LC} = 0 \tag{3.14}$$

In evaluating a series RLC circuit, shown in Figure 3.2 (b), Kirchhoff's voltage law leads to:

$$IR + L\frac{dI}{dt} + \frac{1}{C}\int I dt = V \tag{3.15}$$

To determine the current flowing in the circuit, differentiate equation (3.15) and this leads to:

$$\frac{d^2 I}{dt} + \frac{dI}{dt}\frac{R}{L} + \frac{1}{LC} I = 0, \tag{3.16}$$

From equations (3.14) and (3.16), it is noted that the differential equations describing the two RLC circuits in their transient state are similar. $I_L$ in the parallel circuit is the current through the inductor, similarly $I$ is the current through the inductor for the series circuit. The only difference is in the coefficients of their second terms. Further analysis of these equations shows that the coefficients of the second terms indicate the time constants of the circuits. $T_P$ is the time constant in the parallel circuit and $T_S$ is the time constant of the series circuit. That is to say:

$$\begin{aligned} RC &= T_P \\ \frac{L}{R} &= T_s \end{aligned} \tag{3.17}$$

The inverse of the coefficient of the third term of equation (3.16) is the square of the angular period of the undamped circuit.

$$LC = T^2 \tag{3.18}$$

Rewriting equations (3.15) and (3.16) using $T_P$, $T_S$ and $T^2$ gives:

For the parallel circuit,

$$\frac{d^2 I_L}{dt} + \frac{dI_L}{dt}\frac{1}{T_P} + I_L\frac{1}{T^2} = 0 \tag{3.19}$$

And for the series circuit,

$$\frac{d^2I}{dt}+\frac{dI}{dt}\frac{1}{T_S}+I\frac{1}{T^2}=0 \tag{3.20}$$

Working with the parallel circuit, and using the Laplace transform, equation (3.19) can be written as

$$\left(s^2+\frac{s}{T_P}+\frac{1}{T^2}\right)i_L(s)=\left(s+\frac{1}{T_P}\right)I_L(0)+I_L'(0) \tag{3.21}$$

where based on equation (3.13):

$$I_L'(0)=\frac{V_C(0)}{L}$$

If we assume $I_L(0)=0$ then equation (3.21) reduces to:

$$i_L(s)=\frac{V_C(0)}{L}\frac{1}{s^2+(s/T_P)+(1/T^2)} \tag{3.22}$$

Equation (3.22) shows the basic transform for a parallel RLC circuit. Simplifying the basic transform reveals the roots $s_1$ and $s_2$.

$$\begin{aligned}\frac{1}{s^2+(s/T_P)+(1/T^2)}&=\frac{1}{(s-s_1)(s-s_2)}\\&=\frac{1}{(s_1-s_2)}\left(\frac{1}{s-s_1}-\frac{1}{s-s_2}\right)\end{aligned} \tag{3.23}$$

When solving for $s_1$ and $s_2$ from equation (3.23) the roots are:

$$s_{1,2}=-\frac{1}{2T_P}\pm\frac{1}{2}\left(\frac{1}{T_P{}^2}-\frac{4}{T^2}\right)^{\frac{1}{2}} \tag{3.24}$$

And so,

$$i_L(s) = \frac{V_C(0)}{L\left[\left(1/T_P{}^2\right) - \left(4/T^2\right)\right]^{\frac{1}{2}}}\left(\frac{1}{s-s_1} - \frac{1}{s-s_2}\right) \tag{3.25}$$

The inverse transform of equation (3.25) is

$$I_L(t) = \frac{V_C(0)}{L\left[\left(1/T_P{}^2\right) - \left(4/T^2\right)\right]^{\frac{1}{2}}}\left(e^{s_1 t} - e^{s_2 t}\right) \tag{3.26}$$

The form of the solution of equation (3.26) will depend on the values of $s_1$ and $s_2$. $s_1$ and $s_2$ are real if $1/T_P^2 > 4/T^2$ and complex if $1/T_P^2 < 4/T^2$. We introduce a parameter, $\eta$ using equations (3.17) and (3.18) to assist in solving for the current in equation (3.26).

$$\begin{aligned} \frac{T_P{}^2}{T^2} &= (RC)^2\left(\frac{1}{LC}\right) \\ &= R^2\sqrt{\left(\frac{C}{L}\right)^2} \\ \eta^2 &= \frac{R^2}{Z_0{}^2}, \\ \eta &= \frac{R}{Z_0} \end{aligned} \tag{3.27}$$

And so, if $1/T_P^2 > 4/T^2$, then $\eta < \frac{1}{2}$; conversely if $1/T_P^2 < 4/T^2$, then $\eta < \frac{1}{2}$ Rewriting equation (3.24) in terms of $\eta$ yields [12], [17],

$$\begin{aligned} s_{1,2} &= -\frac{1}{2T_P}\left[1 \pm j\sqrt{4\eta^2 - 1}\right], \quad if\ \eta > \frac{1}{2} \\ s_{1,2} &= -\frac{1}{2T_P}\left[1 \mp \sqrt{1 - 4\eta^2}\right], \quad if\ \eta < \frac{1}{2} \end{aligned} \tag{3.28}$$

For $\eta = \frac{1}{2}$ in a parallel RLC circuit, the transform in equation (3.23) reduces to

$$\frac{1}{\left(s + 1/2T_P\right)^2} \tag{3.29}$$

Three solutions are determined for the current in the inductor of a parallel RLC circuit when a capacitor is discharged through the other branches, depending on the value of $\eta$. The solutions are:

$$
\begin{aligned}
I_L(t) &= \frac{V_C(0)}{L}\frac{2T_P e^{-t/2T_P}}{\left(4\eta^2-1\right)^{1/2}}\sin\left(4\eta^2-1\right)^{\frac{1}{2}}\frac{t}{2T_P}, \quad && n>\frac{1}{2} \\
I_L(t) &= \frac{V_C(0)}{L}te^{-t/2T_P}, && n=\frac{1}{2} \\
I_L(t) &= \frac{V_C(0)}{L}\frac{2T_P e^{-t/2T_P}}{\left(1-4\eta^2\right)^{1/2}}\sinh\left(1-4\eta^2\right)^{\frac{1}{2}}\frac{t}{2T_P}, && n<\frac{1}{2}
\end{aligned}
\tag{3.30}
$$

Note from equation (3.30) when $\eta = \frac{1}{2}$, the parallel RLC circuit is critically damped. When, $\eta > \frac{1}{2}$, the circuit is oscillatory or underdamped. And, finally when $\eta < \frac{1}{2}$, the circuit is overdamped.

In the expressions given above, the current contains sinusoidal functions with an angular frequency that depends on $\eta$. This is what contributes to the irregular shape of the current. The $e^{1/2T_P}$term determines the rate of decay of the current at a time constant of $1/2T_P$ [12].

The solution for the series RLC circuit is similar to the parallel RLC circuit. The exception is the time constant used is $T_S$ instead of $T_P$. Furthermore, the parameter $\lambda$ is used in the series circuit instead of $\eta$ where, $\lambda$ is the reciprocal of $\eta$ [12].

The circuits that have been studied thus far have lumped constants *R*, *L* and *C*. In steady state analysis, lumped element representation of the circuits would be sufficient. However, the approximations made with lumped circuit analysis are inadequate in some circuit analyses, including transient analyses.

The circuits that have been discussed thus far have been single phase circuits. Power systems are generally three phase systems, but they can be treated as single phases when the loads, voltages and currents are balanced. In instances where the system is balanced, then the single phase approach can be extended to analyse transients in the system. In cases where there is an unbalance, symmetrical components are used.

Three phase systems can be solidly grounded at their neutrals. They can be completely isolated from ground, or they can be grounded through a neutral impedance. Transient voltages created by switching operations often depend on which type of neutral is present [12].

## 3.4 Transient Recovery Voltages

A transient can be described as a short-lived oscillation in a system caused by a sudden change of voltage or current or load. When a switch is opened, an arc is drawn. Current transient waves are then generated [12]. The waves travel away from the switch in both directions.

When considering an opening operation of a disconnect switch, the insulation gap ("break gap") of the switch is increased as the contacts move away from each other. In the case of an air-break disconnect switch, the insulation gap is air. If the insulation gap is not wide enough such that the dielectric strength of the break-gap can withstand the voltage stresses across the contacts, a current re-strike will occur.

In 1994, CIGRE SC13 published a paper [29] where the principle of switching mechanisms pertaining to capacitive current switching are explained. The relevant findings are referred to in this chapter.

### 3.4.1 De-energising transmission lines

With the switching device closed, the peak values $U_0$ at the source and $U_C$ at the switching device are different by $\Delta U = U_0 - U_C$. After current interruption at current zero, the voltage $U_1$ adjusts to $U_0$ by a transient recovery voltage (TRV) wave called the initial jump, the reader should refer to Figure 3.3 for clarity. Essentially, the voltage across the terminals of the switching device is the difference between the TRV generated by the network elements at the supply side and the TRV generated at the load side [30]. The frequency and amplitude of the transient are given by the inherent features of the source network, namely $L_s$ and $C_s$ [29]. The highest overvoltages are known to occur when unloaded high-voltage transmission lines are energised and re-energised [30].

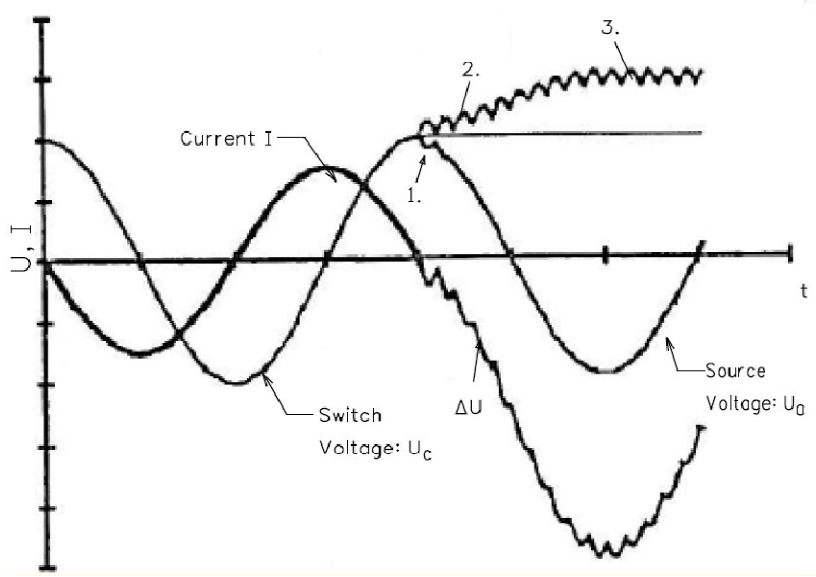


Figure 3.3 Voltage and current waveform at line deenergising: 1- initial jump of source side, 2 – transient caused by Ferranti effect, 3 – increase by intercoupling from second and third phase [29]

The switching device is stressed with a maximum voltage $U_0 + U_C$, i.e. approximately 2p.u. where 1p.u. refers to the source voltage, $U_0$. [29].

When overstressed by the recovery voltage a dielectric breakdown occurs and a flashover arc bridges the contacts of the switching device. If the dielectric breakdown is caused by the initial jumps and occurs within the first quarter cycle of the power frequency, the phenomenon is known as a reignition. The arcing is prolonged by another loop of the power frequency current, which is better for the switching device as the recovery voltage is then applied to a larger gap. If arcing took place after ¼ wavelength of the power frequency, the phenomenon is known as a re-strike [29], [30].

When the arc that is drawn is finally interrupted, a high-frequency oscillation is superimposed on the power frequency and appears across the contacts. Therefore, two components exist on the recovery voltage: the high-frequency damped oscillation and the power frequency recovery voltage [12], [30].

If the frequency of the recovery voltage is high, the voltage across the switch contacts rises very quickly. And if the rate of rise of the recovery voltage (RRRV) exceeds the rate at which the dielectric strength of the air builds up, the switch will not be able to hold off the voltage and a

're-ignition' will occur. The crux of the switching operation then becomes ensuring that adequate dielectric strength is generated across the switching contacts after the current zero to guarantee the elimination of re-ignitions and re-strikes.

During a re-ignition or a re-strike, the line voltage will conform to the momentary value of the source side voltage following a voltage and current oscillation. Frequency and amplitude of the oscillations of the recovery voltage depend upon line characteristics and impedance conditions at the source side of the disconnect switch.

A transmission line can be approximated by a lumped capacitance ($C$) and inductance ($L$). However, due to the distributed nature of the inductance and capacitance of the line and the Ferranti effect, the higher peak value of the power frequency occurs at the remote (receiving end of the line) than at the switching (sending) end of the line.

According to line theory at resonance wave length, 1500 km for 50Hz voltage signal, the voltage increase along the line would, theoretically, be infinite if the line was undamped. In reality, however, the voltage increase would be approximately 4% on a 500km line and 1% for a 200km line [29]. Therefore for line lengths below 200km, like those associated with transmission lines below 145kV, the Ferranti effect is considered to be negligible [12].

Another aspect one has to consider when switching overhead lines is the capacitive intercoupling that takes places between the conductors of the three phases. After interruption in the first phase the other two phases are still connected to the source side and intercoupling of power frequency voltage occurs from these other two phases. The voltage $U_i$ is coupled unto adjacent lines which are otherwise de-energised due to the stray capacitances to the phases that are energised. This is illustrated in Figure 3.4. The ratio of coupled voltage $U_i$ to the system voltage $U_1$ gives the coupling factor which depends on the ratio of capacitances but not on the line length. The value of the coupling factor $k$, depends on the line design. For a double circuit line, when two circuits are constructed on the same tower, the coupling factor can be higher when the neighbouring circuit is in operation [17], [29], [30]. The consequence due to capacitive coupling is peak values superimposed on the power frequency voltage, thus increasing the recovery voltage across the switching device by 0.2 to 0.4p.u. [29].

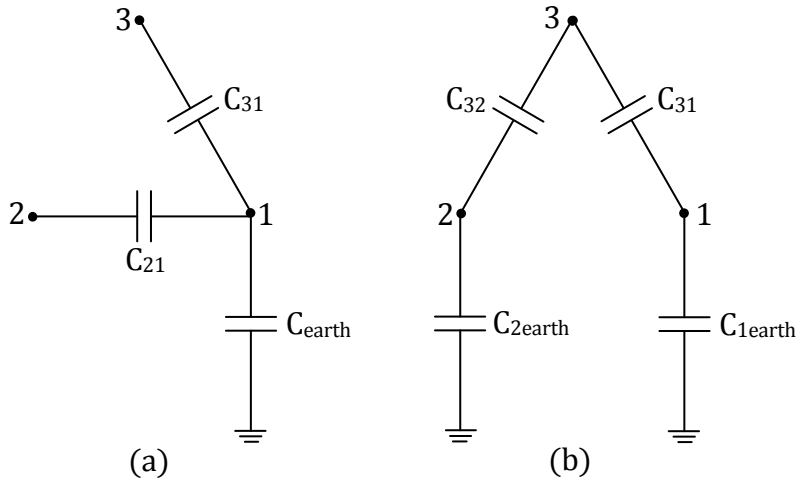


Figure 3.4 The coupling effect of the line capacitance when switching unloaded high-voltage transmission lines (a) phases 2 and 3 are still energised when phase 1 is switched. (b) phase 3 is still energised when phases 2 and 1 are switched off [17]

A combination of the voltage jump at the supply side, the transient voltage oscillation at the supply side, the voltage oscillation at the line side, and the capacitive coupling with neighbouring phases can result in a recovery voltage for the first phase to clear higher than 2.0 per unit, when a transmission line is switched off [17].

### 3.4.2 Energising transmission lines

During a line energisation operation, pre-ignition of the contact gap may occur if the line is charged to 1p.u. and the momentary voltage value on the source side is -1p.u.. The inrush current is given by the voltage across the switching device before pre-ignition and the effective surge impedance of the line. The frequency is given by the line length and the line parameters.

The inrush current is limited by the surge impedance. Energising short lines is not considered to be a severe stress on the switching device. However, when energising lines with trapped charge, overvoltages occur due to travelling wave effects. The switching device may not be critically stressed, but the line insulation and connected equipment will be severely stressed, particularly at higher rated voltages.

At the instant of current interruption, the contribution to the TRV is mainly from oscillating lumped elements. After the first few microseconds, reflected travelling waves arrive at the terminals of the switch and these travelling waves contribute to the transient recovery

waveform. The shape of the TRV waveform depends on the current that was interrupted, the line and cable lengths, the propagation velocity of the electromagnetic waves and the reflection rates at the discontinuities [30].

The details of wave propagation and travelling waves are beyond the scope of this thesis, although the fundamental principles are briefly explored. For this study, the switching operations are based on the use of disconnectors.

It should be mentioned, however, that operating procedures [14] where an operator is required to earth de-energised equipment for safety purposes reduces the likelihood of overvoltages due to trapped charges.

## 3.5 Travelling Waves on Transmission Lines

On an overhead transmission line, each unit of length possesses a certain inductance, capacitance and resistance. And these quantities are distributed over the entire length of the transmission line. The distributing feature allows the transmission line the ability to support the travelling waves of current and voltage waves. The properties of the electric field are represented by a capacitance and the inductance represents the magnetic field. It should be noted that with distributed elements, currents and voltages do not necessarily have the same value over the entire length of the line at the same instant of time [12], [17], [31].

If we consider an ideal, two-wire transmission line, the velocity at which a charge travels along the ideal line, i.e. a lossless line, is given by the wave velocity $v$ [12], [17]:

$$v = \frac{1}{\sqrt{LC}}, \tag{3.31}$$

The wave velocity depends on the geometry of the line and on the permittivity and permeability of the surrounding mediums. These factors determine the inductance $L$ and capacitance $C$ of the line being analysed [31]. On an ideal line, the wave velocity is constant.

The ratio between the voltage and current wave for an ideal line also depends on $L$ and $C$. This ratio is called the characteristic impedance of a transmission line and is given in equation (3.11). The symbol $Z_0$ is often used to denote the characteristic impedance of a lossless line.

## 3.6 Attenuation of Travelling Waves

A true representation of a transmission line includes losses. Losses are represented by a series resistance of the line $R$, and a parallel conductance $G$. These parameters are evenly distributed along the line, as are $L$ the inductance and $C$ the capacitance. This is illustrated in Figure 3.5.

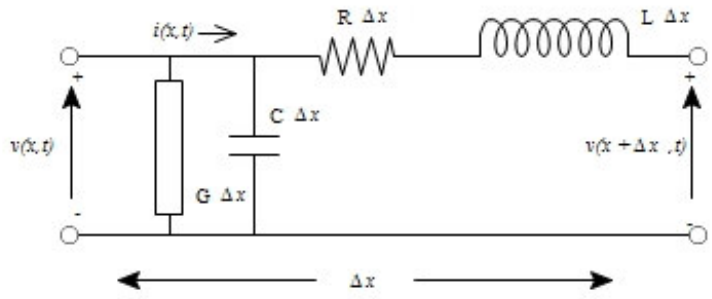


Figure 3.5 Small line segment of a lossy transmission line

The losses in the line segment $\Delta x$ at time $t_0$ are:

$$P_{loss} = i(x_0,t_0)^2 R\Delta x + v(x_0,t_0)^2 G\Delta x \tag{3.32}$$

Electromagnetic waves contain energy. In the absence of losses, the energy is stored in the electromagnetic field. The energy in the electric field is as a result of the capacitance $C$, while the magnetic field energy is as a consequence of the line inductance $L$ [12], [17], [31].

When the voltage and current waves travel along a transmission line with losses, the amplitude of the waves is exponentially decreased. The wave equations for the voltage and current can be represented by equation (3.33) [17]. This is called attenuation. Attenuation is small for a line with a low resistance and/or large characteristic impedance.

$$i(x,t) = i(x_0,t_0)e^{-0.5[(R/Z+ZG)]x}$$
$$v(x,t) = v(x_0,t_0)e^{-0.5[(R/Z+ZG)]x} \quad (3.33)$$

If $R/L = G/C$, the transmission line is distortionless. This translates to: losses in the electric field equalling the losses of the magnetic field. It means that the current and voltage waves keep their original shape and are only attenuated in amplitude. When this happens the wave velocity and characteristic impedance remain constant [31]. This is explained further in section 4.2.

When the transmission line is not distortionless, that is to say: $R/L \neq G/C$, the steepness of the wave front will decrease and the general shape of the waves will be more elongated when they travel along the line [17]. In practice, at frequencies below 1MHz on a typical transmission overhead power line, $R/L$ is much greater than $G/C$ by a factor of 1000 or so [32]. This is due to the high-frequency effects that the resistance undergoes [12]. Resistive losses are always higher than the losses due to leakage. The influence of shunt conductance $G$ is negligible on overhead lines, except at very low frequencies approaching DC [33]. In this study the value of $G$ for the transmission lines has been set to zero.

## 3.7 Behaviour of Travelling Waves at the Line Terminations

When a wave arrives at a discontinuity in a line, a point where the characteristic impedance of the line changes, like a short circuit or an open circuit, an adjustment of the travelling voltage or current wave occurs. This takes the form of the launch of two new wave pairs, the reflected wave and the refracted wave. The reflected wave travels back to the source and the refracted wave travels through the discontinuity. This is done in such away that energy is still conserved.

The amplitude of a travelling wave at a certain place along the line is determined by the superposition of the amplitudes of the waves that arrive at that place at that time. It follows then that a line voltage would not be univalued but would vary with the position on the line at any instant [12], [17]. To demonstrate these travelling wave phenomena, we consider the behaviour of the waves at line terminations.

### 3.7.1 Short Circuit Termination

When an incident voltage wave (original wave) reaches a short circuit at the end of a transmission line, the reflected wave precisely cancels out the incident wave so the refracted wave is zero. A short circuit by characterisation implies that a voltage cannot develop across the shorted terminals [12], [17], [31].

If the incident voltage wave is $V_1$ and the incident current wave is $I_1$, then the reflected voltage wave $V_2$ will be equal to $-V_1$ and the reflected current wave $I_2$ will equal $+I_1$. This effectively doubles the current flowing in the line, while the line voltage is forced to zero [12]. If the losses are ignored, then all the energy is stored in the magnetic field.

### 3.7.2 Open Circuit Termination

In contrast to a short circuit termination, an open circuit line termination demands that the current at the open point is zero. Thus, if the current wave of $+I_1$ arrives at an open circuit, a current wave of $-I_1$is reflected back towards the source. The incident voltage wave, $V_1$, is reflected back as $+V_1$. This results in a doubling of the line voltage and a net zero current along the transmission line. In which case, if the losses are ignored, all the energy is stored in the electric field.

### 3.7.3 General Termination

When a transmission line is terminated on some equipment with different impedance to the line, then the refraction and reflection coefficients are used to determine what happens when the travelling wave reaches the termination [12], [31].

Consider a junction between two lines of characteristic impedances $Z_A$ and $Z_B$, for instance a line terminating on a cable. The relationship between the incident wave and the reflected wave is determined by the reflection coefficient: $\frac{Z_B - Z_A}{Z_B + Z_A}$, while the relationship between the incident wave and the refracted wave is determined by the refraction coefficient is given by: $\frac{2Z_B}{Z_B + Z_A}$.

## 3.8 Frequency Range Associated with Switching Operations

Frequencies generated by transient phenomena on a network can range anywhere from 0Hz (DC) to 50MHz, including lightning surges and switching operations [24]. To represent all network components over this frequency range is not practical. Therefore, only specific network elements that have an effect on the transient phenomena being studied are given detailed consideration.

Cigre Brochure 39 [24] places the frequency range of line energisation and line reclosing between 50/60Hz – 20kHz. Additionally, the brochure puts disconnector switching (single re-strike) and faults in GIS in the frequency range of 100kHz to 50MHz. In contrast, the frequency range associated with lightning surges or faults in substations is 10kHz – 3MHz [24].

Wiggins and Wright [34] conducted and documented field tests where electric and magnetic fields of switching transients were characterised according to the type of voltage level, as well as the type of switch used for the operation. Among the tests conducted were switching operations involving air-insulated disconnectors. It was found that disconnector switching produced transients inside a substation of significantly larger amplitude and of a greater number than those produced by circuit breakers. The total number of transients produced by a slow disconnect switch were found to be as high as 10000, in contrast to 60 when a fast disconnector was used. The frequencies measured during the switching of air-insulated disconnect switches ranged from 120Hz to 40kHz [34].

When energising a line, if the main interest is concentrated on the maximum overvoltage which occurs, the line characteristics and the feeding network are of importance. However, if the details of the initial rate of rise of the overvoltages are of importance, then detailed characteristics of the substation, e.g. capacitances of the measuring transformers, the number of outgoing lines and their surge impedances are decisive to the travelling wave phenomena determining the initial shape of the overvoltage [24].

The simplest representation of a transmission line, one that considers the transmission line only from the terminal point of view and only at one frequency, would be a T or π circuit. Each phase can be represented by a resistor equal to the line surge impedance, $Z_0$.

However, it should be mentioned that the error generated when modelling a transmission line at frequencies other than the power system frequency is small, provided that the transmission line length is short when compared with the quarter wavelength of the highest frequency considered. At 20kHz, a quarter wavelength is 3.75km compared to 1500km at 50Hz.

## 3.9 Summary

Key aspects pertaining to switching operations in general were discussed in this chapter. Analysis of the RLC circuit shows that an interrupted current will have a transient component containing sinusoidal functions with an angular frequency that depends on the circuit elements that form $\eta$. These circuit elements define the characteristic impedance and angular frequency that contribute to irregular shape of the current after the switching operation.

Transient recovery voltage (TRV) was discussed. The voltage is formed across the switching contacts at current interruption is the difference between supply side voltage and load side voltage of the switching device. The TRV can be as high as 2p.u. and in cases where the switching contacts are overstressed, restrikes and/or reignitions are likely to occur.

Another aspect that is discussed is the distributed nature of overhead lines that supports the travelling voltage and current waves. Depending on the type of discontinuity the travelling wave arrives at, the amplitude of the wave is either greater or less than the incident wave. The returning wave in turn affects the magnitude of the TRV.

# Chapter 4 Modelling considerations

## 4.1 Introduction

As discussed in preceding chapters, overhead transmission lines play a critical role during switching operations where capacitive currents are interrupted. During a switching operation, the parameters and characteristics of the transmission line together with other network elements help determine the capacitance seen at the disconnector at either the load side or supply side. It is, therefore, necessary to concentrate on the transmission line and how it is modelled during a switching operation simulation.

The research approach used in this study is based on computer simulations of capacitive current switching. The choice to use this approach was guided by one of the objectives of the study, which was to develop a method by which the switching capability of disconnectors can be predicted. Computer simulation tools are used to model the network components and the behaviour of network during switching operations of unloaded transmission lines.

It was decided to use an EMTP based program to model the various line modelling techniques during the switching studies. ATP was chosen as the EMTP based simulation package, while DigSILENT PowerFactory was the other simulation tool used. The simulation packages are discussed in more detail in subsequent chapters. This chapter, however, will focus on how to model the network, in particular the overhead transmission lines for transient solutions. It will explore the different overhead line models that were simulated in the study.

## 4.2 Modelling of transmission lines for transient solutions

To begin with, consider overhead transmission lines that can be approximated using $R', L'$ and $C'$ parameters. The parameters $R', L'$ and $C'$ are evenly distributed along the line, where the "prime" in $R', L'$ and $C'$ is used to indicate distributed parameters in $\Omega$/km, $H$/km and $F$/km. These parameters are, in general, not lumped elements. Some of them, $R'$and $L'$, are functions of frequency and are not constant.

For steady state operations where lines of moderate "electrical" length, typically ≤ 100km at 60Hz or 50Hz [33], transmission lines can be approximated using lumped elements T or Π circuits. In a T circuit, half of the series impedance is lumped at each end of the line. In a Π circuit, the total shunt capacitance is lumped together and halved and each half is located at either end of the line.

However, for this thesis

$$z = R' + j\omega L' \quad \Omega/\text{km} \tag{4.1}$$

$$y = G' + j\omega C' \quad \text{S/km} \tag{4.2}$$

where:

$z$ is the series impedance of the transmission line in per unit length.

$y$ is the shunt admittance of the transmission line in per unit length.

$G'$ is the shunt conductance of the transmission line in Mhos/km.

Most transmission lines are represented using two-port networks where the sending-end voltage $V_S$ and current $I_S$ are related to the receiving-end voltage $V_R$ and current $I_R$ using well known *ABCD* parameters [32], [33]. If one considers Figure 4.1, then equation (4.3) shows this relation.

$$\begin{bmatrix} V_S \\ I_S \end{bmatrix} = \begin{bmatrix} A & B \\ C & D \end{bmatrix} \begin{bmatrix} V_R \\ I_R \end{bmatrix} \tag{4.3}$$

Then:

$$V_S = AV_R + BI_R \quad \text{volts} \tag{4.4}$$

$$I_S = CV_R + DI_R \quad \text{A} \tag{4.5}$$

In Figure 4.1 below, $Z_{\text{series}}$ is the series impedance of the line and $Y_{\text{shunt}}$ is the shunt impedance of the transmission line.

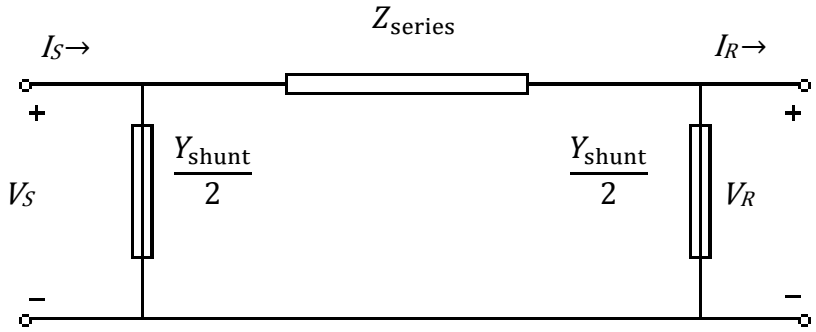


Figure 4.1 Equivalent π-circuit for ac steady state solution of a transmission line [33]

The *ABCD* parameters for an equivalent π-circuit are given in [32] as:

$$A = D = 1 + \frac{Y_{\text{shunt}} Z_{\text{series}}}{2} \quad \text{p.u.} \tag{4.6}$$

$$B = Z_{\text{series}} \quad \Omega \tag{4.7}$$

$$C = Y_{\text{shunt}} \left( 1 + \frac{Y_{\text{shunt}} Z_{\text{series}}}{4} \right) \quad \text{S} \tag{4.8}$$

For long lines (250km for 60Hz), $Z_{\text{series}}$ and $Y_{\text{shunt}}$ are given as follows [32], [33]:

$$Z_{\text{series}} = zl \frac{\sinh(\gamma l)}{\gamma l} \tag{4.9}$$

$$\frac{Y_{\text{shunt}}}{2} = \frac{yl}{2}\frac{\tanh(\gamma l/2)}{\gamma l/2} \tag{4.10}$$

where γ is the propagation constant of the transmission line.

$$\gamma = \sqrt{(R' + j\omega L')(G' + j\omega C')} \tag{4.11}$$

For a lossless line, where $R = 0$ and $G = 0$ then equations (4.9) and (4.10) become:

$$Z_{\text{series}} = (j\omega L' l)\left(\frac{\sin\left(\omega l\sqrt{L'C'}\right)}{\omega l\sqrt{L'C'}}\right) \tag{4.12}$$

$$\frac{Y_{\text{shunt}}}{2} = \frac{j\omega C' l}{2}\left(\frac{\tan\left(\frac{\omega l}{2}\sqrt{L'C'}\right)}{\frac{\omega l}{2}\sqrt{L'C'}}\right) \tag{4.13}$$

However, if equation (4.11) is rewritten for the transmission line:

$$\gamma = \sqrt{LC(R/L + j\omega)(G/C + j\omega)} \tag{4.14}$$

and, the term $(R/L)$ equals $(G/C)$, then the transmission line is said to be distortionless. The propagation constant along the transmission line, γ, reduces to:

$$\begin{aligned}\gamma &= \sqrt{LC(R/L + j\omega)(R/L + j\omega)} \\ &= (R/L + j\omega)\sqrt{LC} \\ &= \frac{R}{L}\sqrt{LC} + j\omega\sqrt{LC} \\ &= \sqrt{\frac{R^2 LC}{L^2}} + j\frac{\omega}{v} \\ &= \sqrt{RG} + j\frac{\omega}{v}\end{aligned} \tag{4.15}$$

From the result shown in equation (4.15), $\sqrt{RG}$ and $v = 1/\sqrt{LC}$ are constant for the transmission line. All frequencies travel at a constant velocity with a constant attenuation – that is, without distortion [32].

### 4.2.1 Nominal π-circuits

If the length of the transmission line is short, typically less than 100km, then $\gamma l$ term in equations (4.9) and (4.10) approaches the value 1. This approximation results in a simplified circuit called the nominal π-circuit [32], [33], as indicated with the equations below. This nominal π-circuit is also suitable for medium-length lines up to 250km at 60Hz [32].

$$Z_{\text{series}} = l(R' + j\omega L') \tag{4.16}$$

$$\frac{Y_{\text{shunt}}}{2} = \frac{l}{2}\left(G' + j\omega C'\right) \tag{4.17}$$

Nominal π-circuits are fairly accurate for steady state solutions if the line is "electrically" short. Longer lines will result in errors. Due to the approximations made with the nominal π model and the lumpiness of the model, spurious oscillations are found when this model is used for transient solutions [33].

The cascade connections of nominal π-circuits approximate the even distribution of the line parameters reasonably well up to a certain frequency and are useful for untransposed lines [33]. Having a nominal π-circuit divided into smaller nominal π-circuit that are cascaded, has the effect of shortening the length of the line 'seen' by equations (4.16) and (4.17). Yet this method for modelling overhead transmission lines does not allow for flexibility in modelling the frequency dependence of the line parameters [35]. The model still produces spurious oscillations.

When it comes to modelling cascaded connections of π-sections, the number of π-sections to include in the model is crucial. The CIGRE Working Group 33.02 [24] states that the number of π-sections needed depends on the expected maximum frequency of the transient oscillation [24]. According to the working group, the maximum frequency is suggested to be close to the

natural frequency of the line [35]. Nevertheless, the CIGRE Working Group recommends as a rule of thumb that the maximum length of a π-section, $s$, is derived using:

$$s = \frac{v}{5 f_{\max}} \tag{4.18}$$

Where $v = {}^{1}/_{\sqrt{L'C'}}$ and represents the propagation speed of the electromagnetic wave, while $f_{\max}$ is the maximum frequency of one individual π-section of the transmission line [24].

The CIGRE Working Group 33.02 [24] also advises that when modelling switching transients the time step at which the simulation is run is also critical. Digital computers cannot simulate transient phenomena continuously, but only at discrete intervals of time (step size Δt). Researchers who have studied switching transient simulations advise that the simulation step size, $\Delta t$, should be governed by [24], [27]:

$$\Delta t \leq \frac{1}{10 \times f_{\max}} \tag{4.19}$$

### 4.2.2 Distributed Line Model: Constant parameters

For transient solutions, though, travelling wave solutions are faster and usually more accurate than solutions using lumped line models. To make the travelling wave solutions useful for switching studies, Dommel [33] suggests using a simple single phase lossless line model which includes the total series resistance, $R$, lumped in three places. This model produces reasonably accurate results and are better than the results produced using nominal π-circuits at frequencies that are not at power frequency of 50Hz or 60Hz [33]. Furthermore, the model can be extended for use on *n*-phase lines, which can be achieved by transforming phase quantities to modal quantities. For the purpose of introduction and understanding details of how *n*-phase lines are decoupled to form modal quantities are discussed further in Appendix A. In this thesis, the transmission lines modelled are assumed to be 3-phase and balanced.

In the publication by the CIGRE Working Group 05 of Study Committee No 13 [35], it was found that the frequency dependence of overhead lines is smaller than with underground cables

and therefore it was not necessary to have the level of accuracy that distributing the resistance would achieve. As a result, the constant parameter distributed line model distributes $L'$and $C'$ along the length of the line and lumps the total line resistance, $R$, in three places. In this model, $R$ is lumped with: $R/2$ in the middle and $R/4$ at both ends of an otherwise lossless line [33] [36]. Then:

$$Z_{\text{modified}} = Z_{\text{phase}} + \frac{R}{4} \tag{4.20}$$

Due to the lumping of the series resistance, $R$, sections of the constant parameter line model are lossless. Dommel [33] suggests that the user leaves out the resistance of the line altogether at the risk of less accurate results. That is to say, model the line as a lossless line. For a lossless line, the equations (4.12) and (4.13) are valid. From these equations, $Z'_{\text{phase}}$ and $Y'_{\text{phase}}$ changes phase by 2π, consequently, from equations (4.4) and (4.5) so too does $V_S$ and $I_S$. Therefore:

$$\lambda = \frac{2\pi}{\omega l\sqrt{L'C'}} = \frac{1}{fl\sqrt{L'C'}} \tag{4.21}$$

where:

$\lambda$ is the wavelength of the for $V_S$ and $I_S$.

$f$ is the corresponding frequency.

$l$ is the length of the transmission line.

A lossless line, where $R = 0$ and $G = 0$, is similar to the LC circuit, discussed earlier in Chapter 3 where the frequency of the circuit is defined by equation (3.10). The natural frequency of the line, $f_n$, is then given with:

$$f_n = \frac{1}{2\pi l\sqrt{L'C'}} \tag{4.22}$$

Furthermore, the characteristic impedance of the lossless line, $Z_C$, is determined by:

$$Z_C = \sqrt{\frac{z}{y}} = \sqrt{\frac{j\omega L'}{j\omega C'}} = \sqrt{\frac{L'}{C'}} \tag{4.23}$$

Dommel [33] warns, however, that the lumped resistance model that is employed by the ATP-EMTP program only gives reasonable results if $R/4 \ll Z_C$. This is because when this line parameter is calculated at high frequencies, and because $R$ is frequency dependent, the likelihood of an erroneous line resistance existing on the line is much higher. The line resistance could be in the order of 10 times the characteristic impedance of the line being studied, depending on the frequency at which $R$ is calculated [33].

When dealing with constant parameter distributed models, especially in the ATP-EMTP model where $R$ is lumped in three places, the question then becomes at what frequency does one calculate the transformation matrix?

For switching surge studies, the preferred approach, as discussed by various studies [29], [33] [24], [28], is to calculate the transformation matrices at one particular frequency. In [35], the CIGRE Working Group 05 of Study Committee No 13 suggested that line parameters of the switched line should not be calculated at frequencies higher than the natural frequency. The CIGRE report, as do other authors [24], [26], [27], [37], proposed that the line parameters be evaluated at a frequency close to, or at the natural frequency of the line, as shown in (4.22). It was noted that models that were evaluated at the natural frequency produced satisfactory results.

### 4.2.3 Distributed Line Model: Frequency Line parameters

A frequency dependent parameter refers to the frequency response of the distributed series inductance and resistance on a transmission line.

At very high frequencies, the shunt capacitances of a transmission line are also influenced by earth conduction effects. At frequencies below 100kHz, the earth conduction effects are negligible and as a result the shunt capacitance is considered constant [33]. In contrast, series resistances and series inductances on a transmission line are functions of frequency [33].

Calculating the series impedance requires that the ground resistivity is taken into account. It is implied with the equations used to calculate the voltage across transmission lines that there is a return path or the existence of ground to which all voltages are referenced [33]. Carson's formula for homogeneous earth is discussed in various publications [12], [18], [33], and is often used when data for detailed multilayer earth return is seldom available. The formula is, however, deemed accurate enough for power system studies [33]. In the absence of actual data, it is common practice to use 100Ωm for the earth resistivity [33]. It is the value given for earth resistivity of average damp earth [32].

If one considers a solid cylindrical conductor, in dc, the current distribution is uniform throughout the conductor cross-sectional area. For ac, the current distribution is non-uniform. The current distribution tends to flow with greater density towards the outside of the conductor when the current is alternating. At high frequencies (in the order of tens of kilohertz), the current crowds the surface of the conductor and almost none flows in the interior of the conductor. This 'crowding' is known as the *skin effect*, the consequence of which is an increase of the effective resistance of the conductor and a decrease in its inductance [12], [32].

At power frequencies of 50Hz or 60Hz , for a series impedance matrix, $[Z]$:

$$[Z] = [R(\omega)] + j\omega[L(\omega)] \tag{4.24}$$

the ac resistance of a conductor is not appreciably higher than the conductor's dc resistance. However, for transient analysis, where frequencies can be higher than 1kHz, it is not appropriate to use the dc values of $R(\omega)$ and $L(\omega)$. Furthermore, several transient frequencies can be carried in a particular model, making the task of choosing one frequency at which to calculate the transmission line parameters difficult [12]. The solution is then to use a frequency dependent line model with values calculated over a range of frequencies.

A frequency dependent line model was developed in Marti and published in [38]. Based on Figure 4.2, if one uses the equivalent π circuit equations then:

$$\begin{bmatrix} V_{\mathrm{k}} \\ I_{\mathrm{km}} \end{bmatrix} = \begin{bmatrix} \cosh(\gamma l) & Z_{\mathrm{C}}(\omega)\sinh(\gamma l) \\ \dfrac{1}{Z_{\mathrm{C}}(\omega)}\sin(\gamma l) & \cosh(\gamma l) \end{bmatrix} \begin{bmatrix} V_{\mathrm{m}} \\ -I_{\mathrm{mk}} \end{bmatrix} \tag{4.25}$$

Here, two important parameters for wave propagation are: the characteristic impedance which is given by equation (4.26):

$$Z_C = \sqrt{\frac{R' + j\omega L'}{G' + j\omega C'}} \tag{4.26}$$

and, the propagation constant which is given by equation (4.27)

$$\gamma = \sqrt{(R' + j\omega L')(G' + j\omega C')} \tag{4.27}$$

Both parameters are functions of frequency, even for constant distributed parameters $R', L', C', G'$.

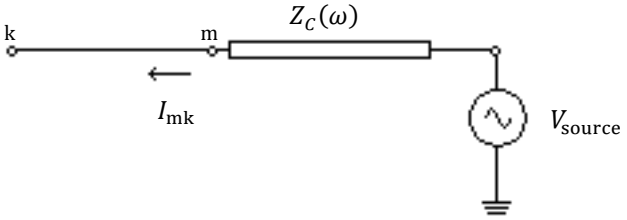


Figure 4.2 Voltage source connected to end m through matching impedance [33]

If one rewrites the equation for the voltage from (4.25), then:

$$\begin{aligned} V_{\mathrm{k}} - Z_{\mathrm{C}} I_{\mathrm{km}} &= (V_{\mathrm{m}} + Z_{\mathrm{C}} I_{\mathrm{mk}})\, A(\omega) \\ I_{\mathrm{km}} &= \frac{V_{\mathrm{k}}}{Z_{\mathrm{C}}} - \left(\frac{V_{\mathrm{m}}}{Z_{\mathrm{C}}} + I_{\mathrm{mk}}\right) A(\omega) \end{aligned} \tag{4.28}$$

where $A(\omega)$ is the propagation factor and is defined as:

$$A(\omega) = e^{-\gamma l} \tag{4.29}$$

Furthermore, if the propagation factor $A(\omega)$ is transformed from the frequency domain to the time domain, then:

$$a(t) = \mathbb{F}^{-1}\{A(\omega)\} \tag{4.30}$$

and $a(t)$ is a weighting function.

The time domain form of equation (4.29) , $a(t)$, should be evaluated by means of a convolution integral, which depends on past history terms. The weighting function $a(t)$ can be written down explicitly as a sum of exponentials. The method by which this weighting function is determined is discussed in detail in [33] and [38]. Also discussed in the publications [33] and [38] is how the characteristic impedance, $Z_C(\omega)$, can be approximated in the complex plane using *R-C* combinations by a rational function [38]:

$$Z_C(\omega) = \frac{N(s)}{D(s)} = H\,\frac{(s+z_1)(s+z_2)\ldots(s+z_n)}{(s+p_1)(s+p_2)\ldots(s+p_n)} \tag{4.31}$$

where $z_i$ and $p_i$ are real, positive and simple.

The frequency dependent model used for the simulations in ATP and PowerFactory are based on the J.Marti model described above. The intricacies of this model are detailed in a paper [38] which was published in 1982.

The frequency dependence of the line parameters needs to be accounted for in order to achieve accurate results with transient simulations. Previous studies by other researchers [33], [37], [38] have shown that the constant-parameter representation produces magnification of the higher harmonics of the signals and, as a consequence, a general distortion of the wave shapes and exaggerated magnitude peaks.

However, it is noted that the frequency dependence of the resistance and inductance of a line is most pronounced in the zero-sequence mode [33]. In cases where the types of transients that are simulated contain appreciable zero sequence voltages and currents, e.g. single line-to-ground faults, frequency dependent models are important.

With regard to zero-sequence modes, in some cases overhead transmission lines are fitted with ground wires or shield wires. Ground wires are useful during fault conditions and lightning conditions where high zero-sequence currents are experienced. Modelling the ground wires as part of the transmission line reduces the ground resistivity. During switching studies, however, it has been documented and tested that ground resistivity plays a minor role in transient studies related to switching operations as the zero-sequence mode currents are very small [18], [33]. For this reason, ground wires are not included in the simulation studies in this thesis.

In other words, for the accurate simulation of the characteristic impedance for open-ended lines, similar to those in this study, it is not as necessary to model the transmission line as a frequency dependent line [33], [38]. It is sufficient to model the line with a constant parameter model that is calculated at the natural frequency. But because the frequency dependent model is deemed more accurate, the transmission lines are modelled with them for comparison purposes.

### 4.2.4 Application of the 600kVA rule

It was mentioned in Chapter 2 that the 600kVA was used as a guideline for switching studies involving capacitive currents [4], [8]. This rule is applied by running a load flow study with the switch that is initially operated in an open position to determine voltages on either end of the switching contacts. In this position, the line-to-line voltage on the supply side $V_S$ of the switch would be measured, $V_L$ (i.e. the voltage on the load side of the disconnector) is assumed to be zero. The load flow studies are performed to estimate the voltage stress across the contacts of the switch.

Another load flow study is performed with the same switch in the closed position. In this position the current $I$ that would have been interrupted by the switch is measured. This load flow study is performed with the loads disconnected, thereafter the disconnector is operated.

With $V_S$, $V_L$ and $I$, the voltage across the switch contacts is taken as $V_S - V_L$. Using the equation provided in (2.2):

$$\sqrt{3}\left(\left|V_S - V_L\right|\right) I < 600\text{kVA} \tag{4.32}$$

The guideline stipulates that if the condition in the above equation is met, the disconnect switch could be operated on successfully. However, at voltages at 120kV and above, resistors had to be installed in series with the switch for a successful operation [8]. At 40kV, all the switching operations were successful [8].

The problem with using the 600kVA rule as a guideline is that it did not take the transient overvoltage into account as the voltages and currents used were obtained using steady state methods. Nor did it consider how the transmission lines were modelled. For steady state analyses, lumped transmission line models were sufficient and were used accordingly. However, when it came to transient analysis, lumped models were not adequate, as has been previously discussed. Moreover, the 600kVA rule also showed to be inadequate when compared to field results performed in other studies [9], [39].

## 4.3 Methodology

The method in which the simulations were based during this study can be summarised follows:

- First, a suitable network where a disconnector was used to switch capacitive current was identified. A network that forms part of the Eskom Distribution system was used and is described in more detail in the next chapter.

- Second, information about the network elements had to be gathered to facilitate the modelling of the network in both simulation software tools. Additionally, the network elements identified in preceding chapters to be critical to the modelling of switching transients were identified. These were the transmission line and the disconnector, in particular. Fortunately, because the network was part of the Eskom System, the network with all its elements had already been modelled and verified in PowerFactory for use in other studies like load flows and steady state studies.

- Next, the power system model was simulated in ATPDraw and in PowerFactory. Load flow studies were performed on the models in both simulation packages and results were compared. For these load flow studies the overhead transmission lines in the

network were modelled using lumped parameters. The load flow studies were run so as to verify the correctness of the ATP model in comparison to the PowerFactory model.

- Thereafter, the model was setup to run the switching studies. First, the disconnectors were modelled as ideal switches, where the current was interrupted immediately. In order to ensure that the transmission line being switched by the disconnector was unloaded, switching operations had to be made to unload the line. Consequently, it was important to note the sequence of the switching procedure and to note that breakers were used to switch load.

- Furthermore, the time step of the simulation was set to satisfy the equation given in (4.19). It was important that the time step for the simulation was less than the travel time of the shortest line being in the model. Thereafter, in ATPDraw, an ATP simulation was run, while in PowerFactory, an EMT simulation was run.

- Once the simulation was run, the voltages and currents at the source side and load side of the disconnector were measured. The highest overvoltage as well as the current was recorded.

When all the simulations were run, the tests were analysed and discussed. Before the results are discussed, the next chapter introduces the power system model used in the study and how its various components that make up the power system model were modelled.

# Chapter 5 Power System Model

## 5.1 Introduction

An existing network, where switching of a disconnector is often practised, was identified as a test circuit for this study. The circuit was modelled in ATP and PowerFactory. This chapter discusses how the network was modelled, including the sequence in which the simulations were performed on the network.

## 5.2 The System Model

Figure 5.1shows a system configuration of the network that was modelled for this study. The network forms part of the Eskom Distribution 66kV Western Grid. The customer base that is supplied by this network includes a few district municipalities as well as rural farmer schemes.

From Figure 5.1, substation *A* is a 132/66kV substation. Two 66kV single circuit lines are interconnected between this substation, *A*, and substation *D*. Breakers at the substations are indicated with an '×' in the figure. On the one 66kV line, line number 1, the loads at substations *B* and *C* are supplied, while on the other 66kV line, line number 2, substations *E* and *F* are connected.

The study focuses on switching line number 2. The line disconnector that is the subject of this study is also marked in the figure.

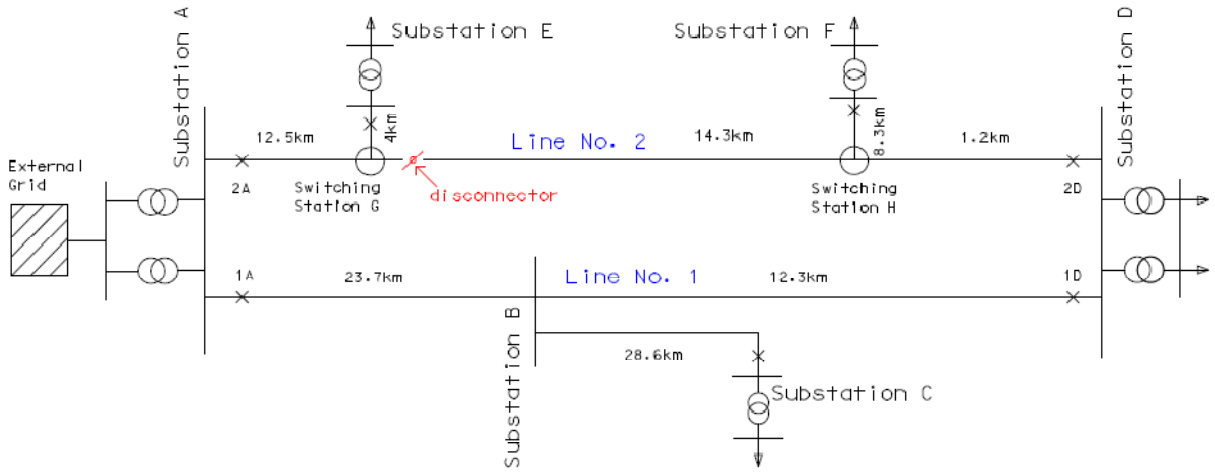


Figure 5.1 System configuration of a 66kV Network

Line number 2 is a single circuit line built on a combination of wooden structures and steel lattice structures. The conductor type used for lines 1 and 2 is an ACSR type conductor, Hare conductor.

The conductors are arranged in a horizontal flat configuration and spaced 3.8m apart. The conductor attachment heights along the line route differ according to the terrain. However, the average conductor attachment height is taken as 9.6m above ground.

On line number 2, there are two switching stations: Switching Station *G* and Switching Station *H*. These switching stations are fitted with disconnectors. These allow for switching operations to isolate the line from either substation *A* or substation *D*.

The distance from substation *A* to the switching station *G* is 12.5km. The distance from the switching station to the substation *E* is 4km. From switching station *G* to *H* is another 14.3km, and substation *D* is located at 1.2 km from switching station *H*. Substation *F* is 8.3km from the switching station *H*.

The network in Figure 5.1 presents a scenario in which a disconnector can be used to interrupt current, in this case capacitive current from a no-load line. This is described in the next section.

## 5.3 Switching Operations on the System Model

Assume that it is desired that maintenance work be performed on the section of line between Substation *D* and switching station *H*, with limited supply interruption to customers at substation *F*. The network configuration, as shown in Figure 5.1, is such that several switching operations are performed in order to isolate the desired portion of line. One of the operations requires that a disconnector at switching station *G* is used to interrupt the current associated with the unloaded transmission line between switching station *G* and substation *D*.

The first switching operation for a scenario depicted in the previous paragraph, is to disconnect any load at substation *D* by opening the breaker *2D* at substation *D* on line number 2. Then the breaker at substation *F* is opened. This is done to ensure that the disconnector at switching station *G* is not operated under load conditions. As discussed in previous chapters, disconnectors are only capable of opening and closing a circuit when either negligible current is broken or made.

After removing the loads at substations *D* and *F*, the line number 2 between switching station *G* and substation *D* is unloaded. At this point, the line disconnector at *G* is opened. Then the portion of line between *H* and substation *D* can be isolated and maintenance work can resume on the line as originally intended and required.

Thereafter, once it is no longer required that the portion of the line between switching station *H* and substation *D* is isolated, the line disconnector at switching station *G* can be closed. Following that, the breaker at substation *F* and breaker *2D* can be closed to pick up the load at the respective substations.

The sequence of switching operations discussed above is a switching procedure that Eskom Distribution would follow according to the operating regulations [14]. This sequence of switching operation is what is simulated in ATP and PowerFactory.

In the simulations, the phase voltages and phase currents are monitored for overvoltages and switching transients as a result of the switching operation of the disconnector at switching station *G*. Overvoltages that are greater than 2.0p.u., as suggested by previous researchers [4],

are deemed severe. For the purpose of this study, if the overvoltages are greater than 2.0p.u. at the point of the operation (switching station *G*), then the switching operation is considered unlikely to succeed.

Before discussing the simulation package and the results, the next section of this chapter examines how the power system network shown in Figure 5.1 was modelled in both simulation packages.

## 5.4 Simulated Power System Model

In the circuit, the current that the line disconnector at switching station *G* would interrupt, is a capacitive current that is associated with an unloaded overhead transmission line. Because the transmission line is an integral part of the initiation of the capacitive current, how the transmission line is modelled is an important aspect of simulations performed. An inaccurate model of the transmission line could result in exaggerated or understated switching overvoltages and transients being recorded. It is for this reason that the first part of the simulated tests was to simulate the response of the simulated network to different transmission line models in both the ATP and PowerFactory simulation tools. Modelling of the system model will be discussed in subsequent chapters, but before that the various elements which constitute the system model are discussed.

### 5.4.1 External Grid

The external grid to which the simulated power system model is connected, was modelled as a source at substation *A*. It was modelled as an ideal source with an input voltage of 1.056p.u. and a power frequency of 50Hz. In other words, the input voltage is 5.6% above the rated voltage. This input voltage coincides with the voltage level at the 66kV bus-bar at substation *A* after a load flow study is performed.

### 5.4.2 Loads

The simulated loads at the different substations were generated from a load study of the existing network on which the power system model is based. The simulated loads are shown in Table

5.1. For use in ATP, the loads shown in Table 5.1 are converted into equivalent delta connected resistance and inductance values.

Table 5.1 Test Circuit Loads at the substations

| | Active Power (MW) | Reactive Power (MVAr) | $R$ (Ω) (delta) | X (Ω) (delta) |
|---|---|---|---|---|
| Load at Substation *F* | 1.58 | 0.52 | 7420.93 | 2442.73 |
| Load at Substation *C* | 3.58 | 1.30 | 3207.29 | 1164.82 |
| Load at Substation *D* | 2.23 | 0.84 | 5130.83 | 1932.64 |
| | 8.57 | 2.63 | 1393.59 | 427.66 |
| Load at Substation *A* | 28.45 | 8.79 | 419.31 | 129.56 |
| Load at Substation *E* | 0.77 | 0.17 | 16165.50 | 3592.68 |

### 5.4.3 Disconnector

The breakers at substations *D* and *F* and the disconnector at switching station *G* are simulated as switches. The sequence of switching operations used for the study is shown in Table 5.2. First, the loads at *F* and *D* substations are disconnected, and then the line is de-energised. After this, the line is energised and the loads at *F* and *D* are picked up.

An important point to keep in mind is that because the sub-transmission lines are short (less than 80km) and in order to satisfy equation (4.19), where $f_{\max}$ is calculated using the shortest line in the network [27], the time-step to use during the simulation gets very small, in the order of microseconds. Thus, if the switching times and simulations times are set for longer periods (greater than 1 second), the time taken to run one simulation is long. The simulation time can be as high as 10 minutes depending on the processing speed of the computer being used to run the simulation. Consequently, to prevent long simulation times for the simulation runs, switching times were chosen where each switching operation lasted at least one cycle of the power frequency voltage or current.

Table 5.2 Simulated switch operating times

| Switch to operate | Time of operation (s) | Type of operation |
|---|---|---|
| Line number 2, 66kV breaker at substation $D$ | 0.026 | Open |
| Breaker at substation $F$ | 0.064 | Open |
| Disconnector at switching station $G$ | 0.085 | Open |
| Disconnector at switching station $G$ | 0.13 | Close |
| Breaker at substation $F$ | 0.185 | Close |
| Line number 2, 66kV breaker at substation $D$ | 0.2 | Close |

### 5.4.4 Conductors

It was pointed out earlier that the conductors for line number 1 of the test circuit had a horizontal flat formation. It should be noted that the conductor attachment height is not the same for the entire line route. However, for the purposes of this study, it is assumed that the tower geometry is the same for the whole circuit. The average conductor attachment height above ground and the average tower geometry are used to model the transmission line.

Tower geometry and conductor characteristics are used to determine the line parameters, namely the series impedance matrix as well as the shunt capacitance matrix. This tower geometry is shown in Figure 5.2. In this figure, the conductor attachment height is shown as 9.6m above ground. The phase spacing between conductors is 3.8m. The conductor attachment height above ground is calculated at 8.145m, i.e. conductor sag of 1.455m, for an average span length of 200m of Hare conductor.

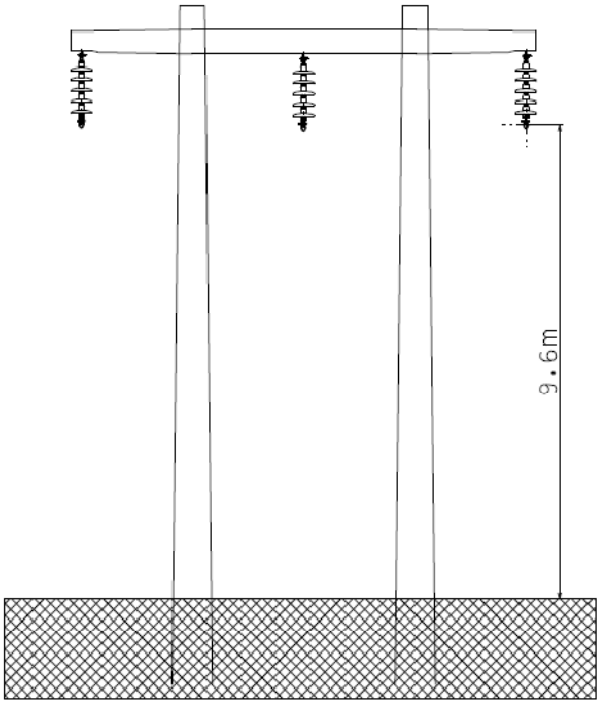


Figure 5.2 Structure showing conductor attachment height from ground.

The conductor characteristics used for modelling the Hare conductor are listed below:

- $R_{out}$ (outer radius of conductor) = 0.708 cm
- $R_{in}$ (inner radius of conductor) = 0.236 cm
- Conductor resistance at DC = 0.2733 Ω/km
- GMR (geometric mean radius) = 0.5437 cm
- Conductor unit weight = 4.19 N/m
- Ultimate tensile strength = 36000 N

Modelling was done for only the 3 phase conductors. No earth wire was modelled for these lines. The line parameters $R'$ and $L'$ of overhead lines are not constant but functions of frequency. In the simulations performed, skin effect is taken into account.

There is no available data for ground resistivity for the test circuit. It is assumed, for the purposes of this study, that ground resistivity is uniform. The value of 100Ωm is used.

The transmission lines in the test circuits are relatively short for the generated impedance matrix to have unsymmetrices at power frequency [33]. Therefore, the lines are modelled as transposed lines.

The next section will explore the different transmission line models that were simulated.

### 5.4.5 Transmission line models

As mentioned before, the way in which the transmission line is modelled in the simulation greatly influences the accuracy of the simulation results. For this study, the different transmission line models were simulated in ATP, purely because ATP is the more recognised and widely used simulation tool for electromagnetic transient simulation studies.

Transmission line can be modelled either as lumped parameter models (T or π models or cascaded π-section transmission line models) or as distributed parameter models (constant parameter models or frequency dependent models). Due to the frequency dependence of line parameters and the higher frequencies associated with transient simulations, lumped parameter models are not suited for transient simulations. Nevertheless, the various transmission line models were simulated in ATP.

The different transmission line models that were simulated in ATP and PowerFactory are listed below:

1. Lumped π model
2. Cascaded 2 π-section model
3. Constant parameter model at 50Hz
4. Constant parameter model at 1.5kHz
5. Frequency Dependent model with a frequency range from dc to 5kHz

The lumped π models calculate the line parameters at the power frequency, in this case, 50Hz. The constant parameter model calculates the line parameters at a user defined frequency, in this case the natural frequency. Some researchers suggest that the natural frequency of the line be used to calculate the line parameter [22], [24], [28]. However, the lines in this test circuit are

short lines. As a result, the natural frequency is in the order of tens of kilohertz (46.6kHz) using the equation (4.22). When the resistance is calculated in ATP at this natural frequency, it produces an error since $R/4 > Z_C$ at the frequency of 46.6kHz. As a result, the ATP simulation does not run, thus another frequency was chosen. The decision of which frequency to use was guided by frequency scans on the lines. It should be mentioned, this error is only true for ATP and not PowerFactory. The simulation was performed in PowerFactory at 46.6kHz and no errors similar to those experienced during the ATP simulations were flagged.

Because the lumped parameter models do not provide a travelling wave solution, for comparison reasons, a constant parameter model is simulated at 50Hz. Another constant parameter model is simulated at 1.5kHz, which was the approximate natural frequency of the network as simulated from the frequency scans performed in ATP.

The last simulations performed are using frequency dependent models. The frequency range for the first simulation was from 0.001Hz (DC) to 5kHz. The frequency of 0.001Hz is used as ATP does not allow an entry of 0Hz for DC.

The simulations in ATP and PowerFactory require that the step size Δt used in the simulations be less than the travel time of the shortest line in the network [37]. The shortest line in the power system model used in the study satisfies equation (4.19).

The test circuit shown in Figure 5.1 is also simulated in PowerFactory. An electromagnetic transient simulation is simulated for a period from 0 to 0.25s, the same time period that was used for the ATP simulation.

### 5.4.6 Mitigation techniques

In the literature review discussed in Chapters 2 and 3, some techniques are identified as having a possibility of reducing the switching overvoltages that are experienced on a power system network as a result of a switching operation using a disconnector. These are briefly highlighted below:

- The first technique is for a disconnector to interrupt current at the ‘natural zero’ of the phase current. For a manually operated disconnector this is not possible as the current

crosses the zero point every 0.2ms for a 50Hz power frequency. However, if the disconnector can be modified in such a manner, using discrete signal processing methods, the disconnector only interrupts the current at the natural zero. This is in contrast to operating the disconnector to interrupt all of the three phase currents at the same time. Due to the phase shift on the phase currents, if interruption on all three phases occurs simultaneously then it is only possible to have one phase at its natural zero during the switching operation, while the other two phases are not. To model this mitigation technique, the disconnector considered in the simulation is modelled to operate only at the natural zero.

- The second technique is based on the findings by Knobloch [23] and Peelo [4] who stated that the highest overvoltages occur when the source-side capacitance ($C_S$) is less than the load side capacitance ($C_L$). This mitigation technique is modelled by introducing a source-side capacitor ($C_S$) at switching station *G*. The size of capacitor chosen is a 500kVAr or 0.365μF at 66kV. This value was chosen so as not to produce excessively high voltages at the various substations, yet still have an effect to the switching operation for simulation purposes.

These simulation techniques were tested in this study using the power system model, already discussed in this chapter. The simulation tests were run on both ATP and PowerFactory simulation tools. The next chapter will describe the two simulation packages used during the study.

# Chapter 6 Description of Simulation Tools Used in this Study

## 6.1 Introduction

In this chapter, the Alternative Transient Program (ATP) is assessed and the modelling techniques for different transmission line models are examined. The power system model simulated in ATP to test the switching capability of a disconnector while energising and de-energising an unloaded transmission line is also presented. Furthermore, this chapter introduces the simulation tool DigSILENT PowerFactory. Modelling features of the simulation tool are discussed, in particular the modelling of the power system model used in this study.

## 6.2 The Alternative Transient Program

The Alternative Transient Program (ATP) is a royalty free version of the Electromagnetic Transients Program (EMTP). ATP has a graphical, mouse-driven pre-processor called ATPDraw, which was developed by Hans K. Hoidalen. In ATPDraw, the user can construct an electrical circuit using the mouse and selecting components from the menu [40]. ATPDraw runs on a MS-Windows platform. The version of ATPDraw used in this study is Windows version 4.2p1.

Figure 6.1 shows the main window of ATPDraw and its menus. A circuit gets constructed in ATPDraw, and ATPDraw generates an ATP input file in the appropriate format based on "what you see is what you get" [40]. An ATP simulation is run. ATPDraw is able to integrate both the simulation tool ATP and whichever plotting program the user chooses to use. The plotting program used in this thesis is the PlotXY program. The user interface for the PlotXY program is shown in Figure 6.2, where the user can select which variable to display.

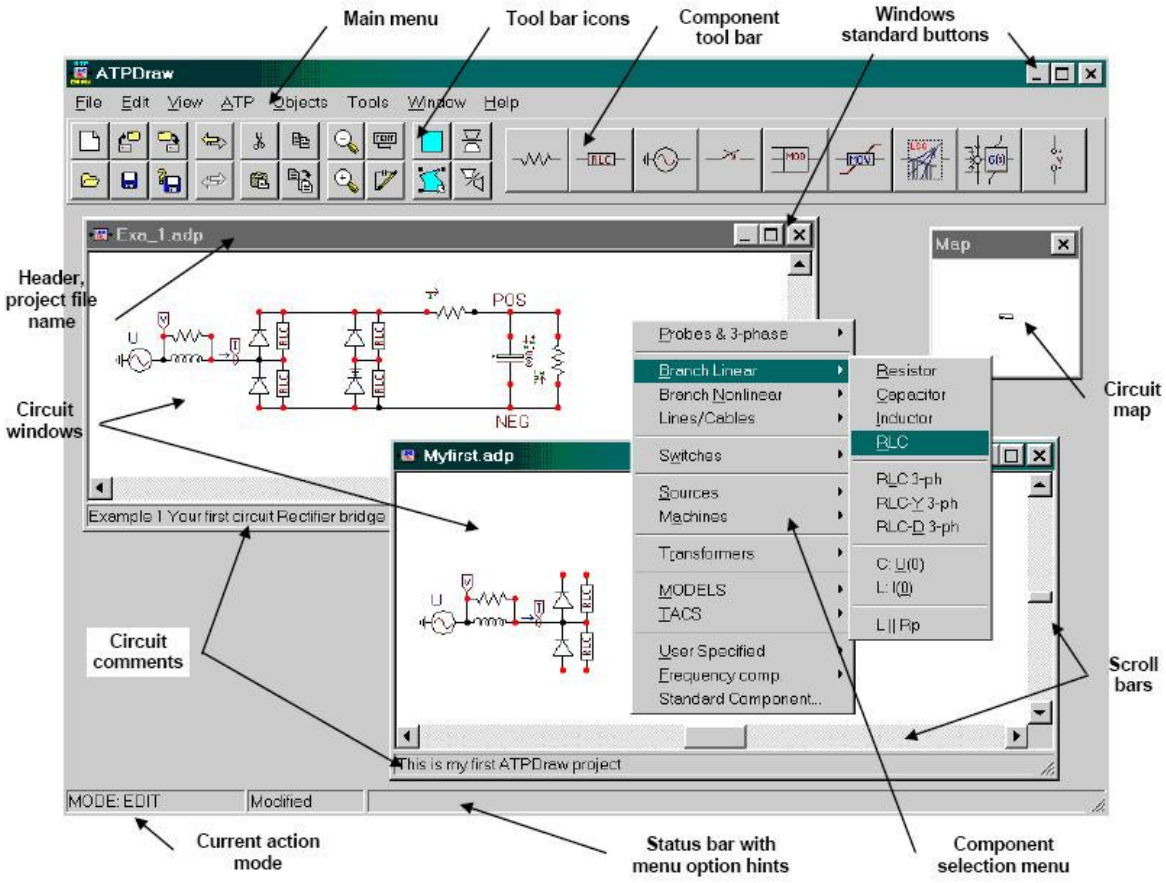


Figure 6.1 ATPDraw main window and floating component selection menu [15]

ATPDraw was developed in a manner such that most of the standard components of ATP, like the line/cable modelling (LCC) component, are supported. The LCC component is based on the supporting routine of ATP-EMTP namely, LINE CONSTANTS. With the LCC component, as shown in Figure 6.3 and Figure 6.4, the user is able to describe the transmission line model parameters and provide data that describes the material constants as well as the geometry of the transmission line or cable. ATPDraw converts the data into a format on which an ATP simulation run is performed [15], [40]. Using the LINE CONSTANTS supporting routine, the ATP

simulation is able to produce detailed line parameters. These line parameters are then used for different types of applications, including transient problem analysis, such as switching studies and lightning surge studies [33].

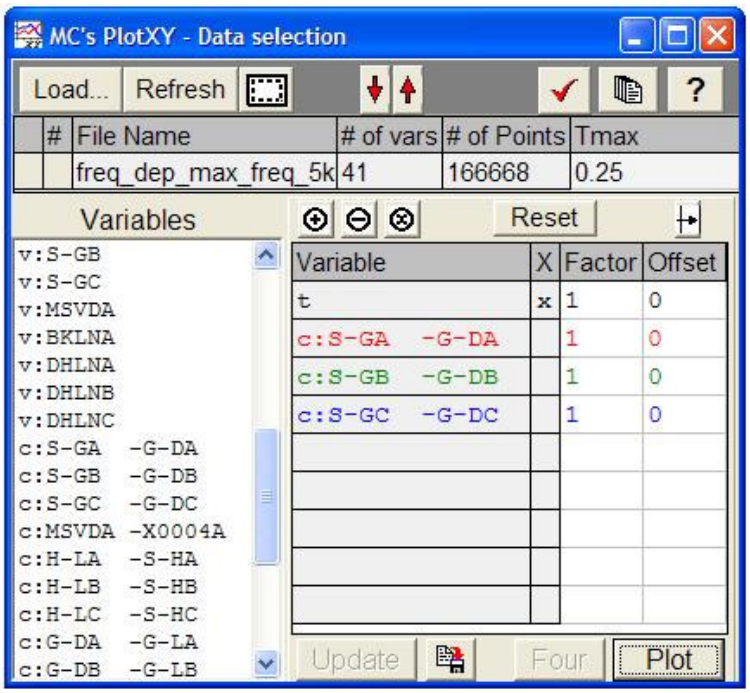


Figure 6.2 PlotXY dialog box in ATP

The advantage of using ATPDraw is that it hides the ATP execution files as much as possible and lets the user work directly with the geometrical and material data in the circuit. This allows ease of use to the user of the program, as the user does not have to learn how to apply and utilise the cumbersome data cards and formats used in ATP-EMTP. A drawback in using ATPDraw is that only cases producing electrical models of the transmission lines are supported [40].

The ATPDraw line modelling component (LCC) is accessed by double-clicking on the LCC graphic in the main window. Figure 6.3 shows the LCC graphical symbol and its dialog box, in ATPDraw. This is where line data pertaining to the network can be entered. Figure 6.4 shows the dialog box where actual line configuration and parameters are entered. A viewer window is also available to allow the user to confirm that correct entries of the configuration have been made.

As shown in Figure 6.3, the LCC supports the following electrical models [15] [33] [40]:

- *Bergeron*: Constant parameter KCLee (untransposed lines) or Clarke (transposed lines)
- *PI*: Nominal PI-equivalent (short lines)
- *JMarti*: Frequency dependent model with constant transformation matrix
- *Noda*: Frequency dependent model (not supported in CABLE CONSTANTS)
- *Semlyen*: Frequency dependent simple fitted model (not supported in CABLE PARAMETERS)

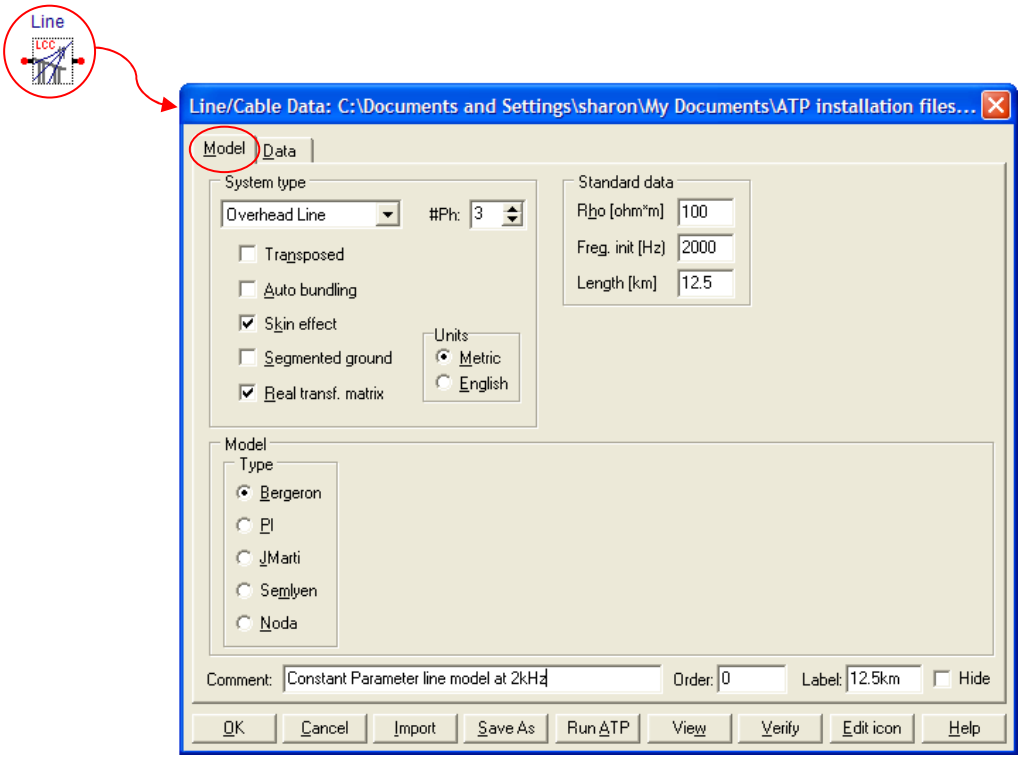


Figure 6.3 LCC in ATPDraw: Model and Parameter setting dialog box

### 6.2.1 Simulated Network in ATP

The ATP model of the power system model discussed in the previous chapter is shown in Figure 6.5. The substations *A*, *B*, *C*, *D*, *E* and *F* as well as the switching stations *G* and *H* are framed in the figure to show their positions in the ATP model relative to the figure of the model

shown in Figure 5.1. The disconnector studied in this thesis is also pointed out in Figure 6.5. Voltage and current probes are specified with *V* and *I* flags at the element nodes in the figure.

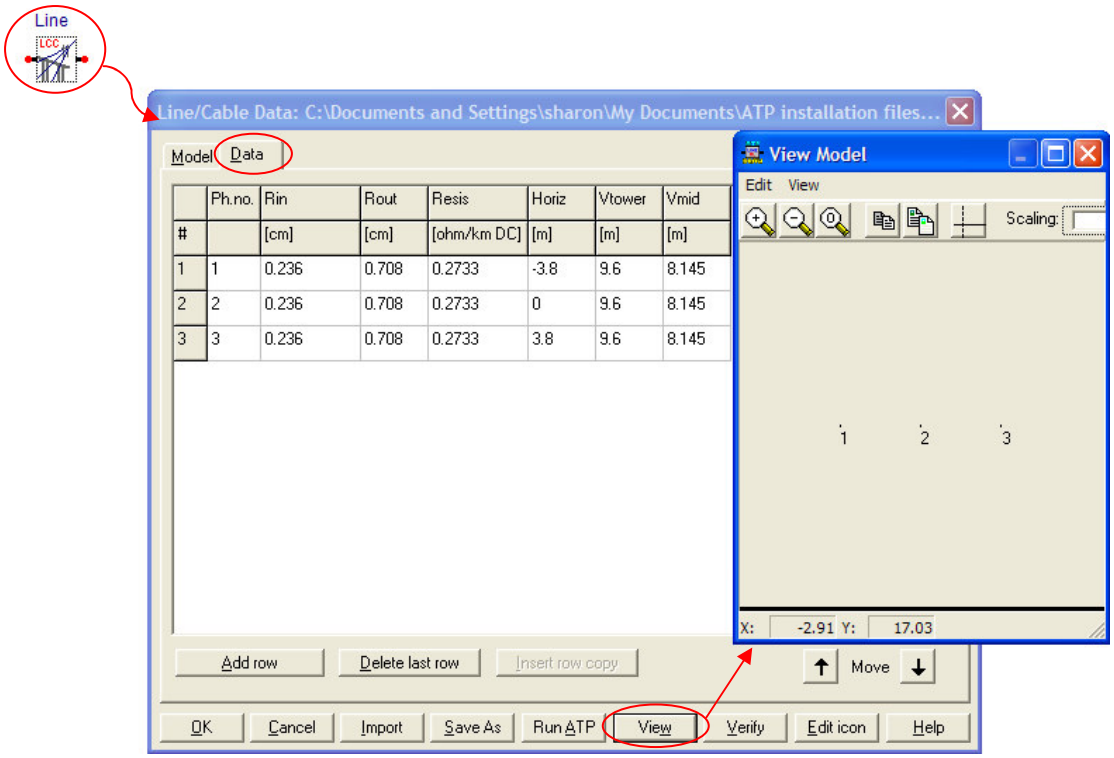


Figure 6.4 LCC in ATPDraw: Line Data dialog box for 3-phase line with a "View Model" window

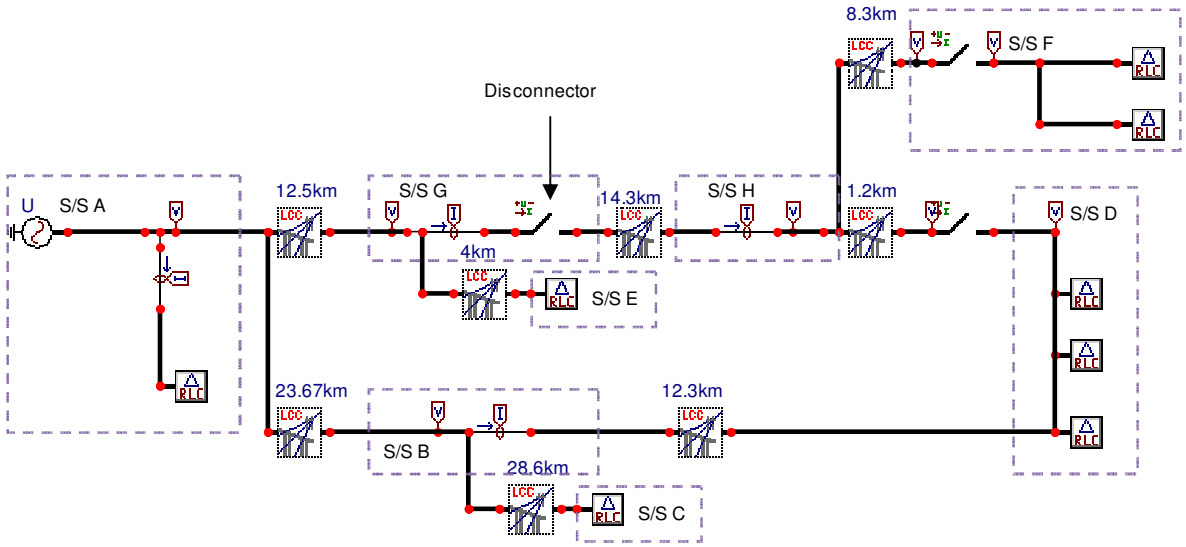


Figure 6.5 Simulated network in ATP

The voltage and current readings shown in the simulations results that follow in Chapter 8 are taken at switching station *G* and at switching station *H*. Readings are taken at switching station

*G* as this is where the switching operation of the disconnector takes place, while at switching station *H*, readings are taken to observe the effects that the switching operation of the unloaded line has at the receiving end of the line. The current that is interrupted by the disconnector in the ATP simulations is 2.56A.

The sequence of the switching operations simulated in ATP are shown again in Table 6.1.The switch operation times of the breakers at substations *D* and *F* are to unload the line; thereafter the disconnector is opened.. Then the operations are reversed, i.e. the disconnector is closed to energise the line, and subsequent to that the breakers are closed. Figure 6.6 is an example of a phase current plot showing how the switching times in Table 6.1 correlate when examining an ATP simulation plot from the PlotXY program.

Table 6.1 Switching operation times in ATP and PowerFactory

| Switch to operate | Time of operation (s) | Type of operation |
|---|---|---|
| Line number 2, 66kV breaker at substation *D* | 0.026 | Open |
| Breaker at substation *F* | 0.064 | Open |
| Disconnector at switching station *G* | 0.098 | Open |
| Disconnector at switching station *G* | 0.143 | Close |
| Breaker at substation *F* | 0.185 | Close |
| Line number 2, 66kV breaker at substation *D* | 0.2 | Close |

## 6.3 PowerFactory

PowerFactory is a power system simulation software tool developed by DigSILENT. This software is capable of performing load flow studies in radial and meshed networks (balanced and unbalanced), short circuit analysis and electromagnetic transient simulation studies, to name but a few [16]. The version of PowerFactory used for this study is version 13.2 Build 326 or 13.2 (B326).

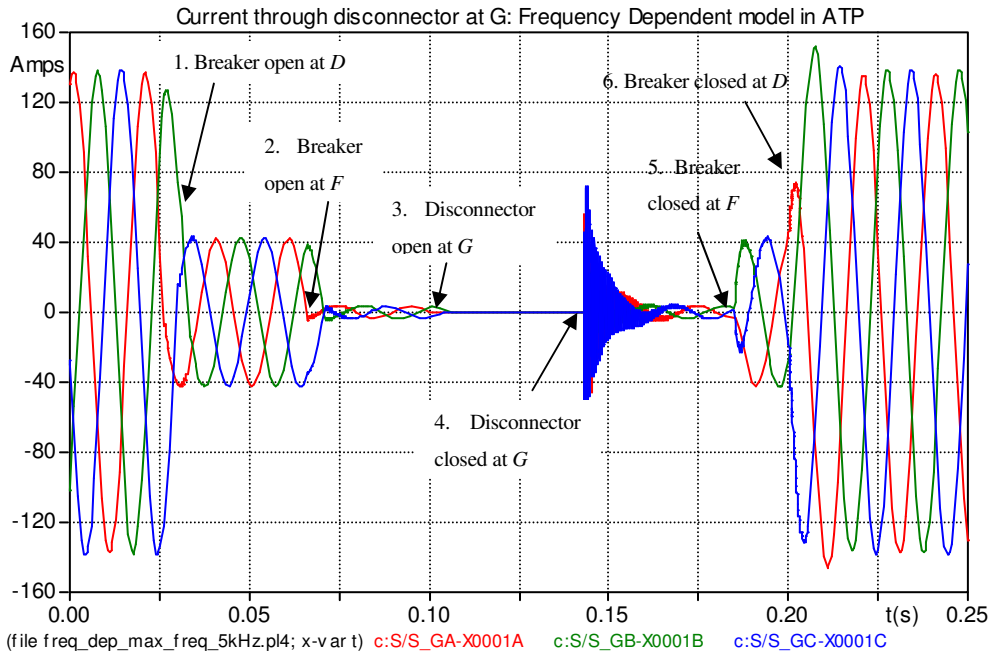


Figure 6.6 An example showing the sequence of the simulated switch operating times taken: phase current at switching station *G*

Eskom, the power utility in South Africa, acquired a corporate licence for PowerFactory. The tool is used mainly for steady state simulations and rarely for transient studies related to switching operations. PowerFactory already has extensive use within the utility, for steady state and stability studies. One of the aims of this study is to determine whether or not the use of PowerFactory within the utility could be extended to switching studies.

The advantage of using PowerFactory was the fact that the utility's network was already fully modelled in the simulation tool. All that would be required to run the switching studies would be to re-model the portion of the network being studied to suit transient simulation. However, the main drawback in using PowerFactory would be the limited literature available on the use of PowerFactory and limited knowledge of how the models could be manipulated for transient analysis. Literature used for PowerFactory modelling was only available via the user manuals and technical manuals.

PowerFactory makes use of a single database that contains all the required data for all equipment within a power system. The significance is that the user gets accustomed to one user interface as all activities are controlled and accessed via the main program window [16]. PowerFactory is intended to be used and operated in a graphical environment. Data entries are

performed by drawing the network under study and then editing the objects to assign data to them. If more modification is required, data can be manipulated using a data viewer called the Data manager. Some of the PowerFactory windows are shown in Figure 6.7.

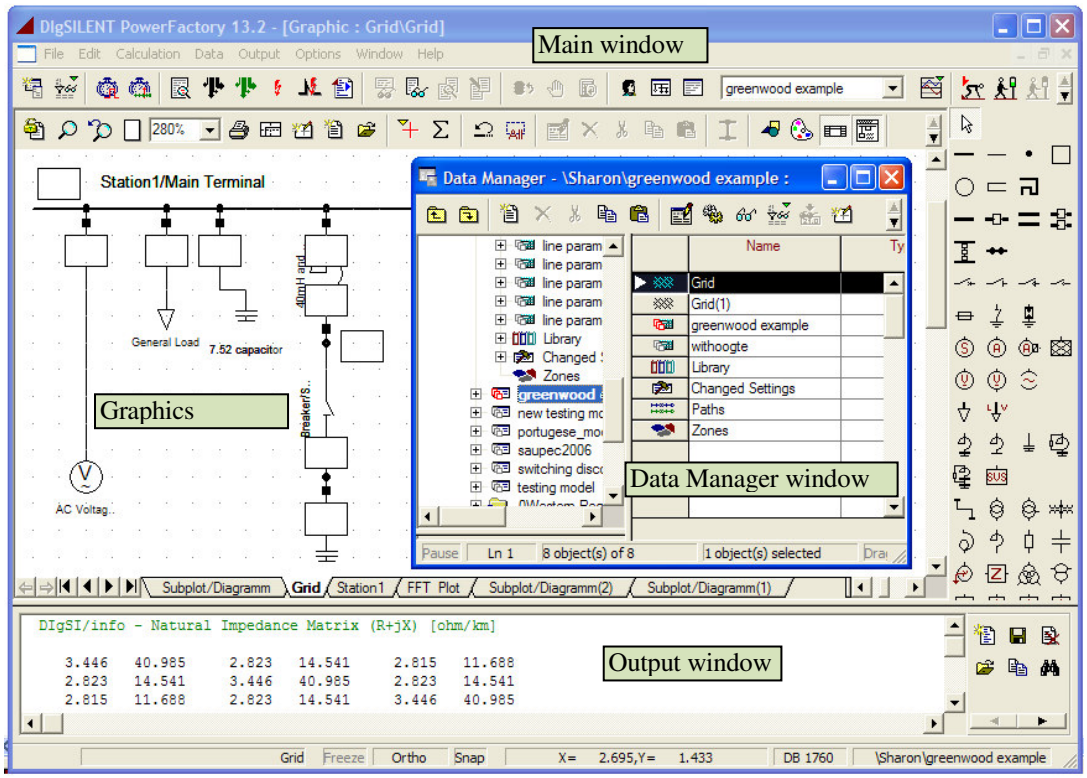


Figure 6.7 PowerFactory Window

The data structure in PowerFactory is such that the data is split into two main groups: *type* data and *element* data. Without delving too much into the structure, a brief summation of the structure follows. *Type* data is data that is common to several items in a network, for example, the type of conductor used in a network [16]. *Element* data is data that is specific to the installation of a particular type of item, for example the length of a conductor used, the manner of installation of the conductor (in air or ground), or the element that the conductor is connected to at either end, etc [16].

In the graphics window in PowerFactory, data is accessed by double-clicking the object in question. This is similar to the ATPDraw simulation tool. Double-clicking an object opens up an input dialog box, see Figure 6.8, where the details of the object can be entered. Figure 6.8 shows a dialog box for a 14.3 km transmission line.

Figure 6.9 shows an element data dialog box for a particular transmission line PowerFactory. It also shows the type of line models supported: lumped or distributed. If the model is distributed, it allows the user to determine if the transmission line is modelled using constant parameters or frequency dependent parameters.

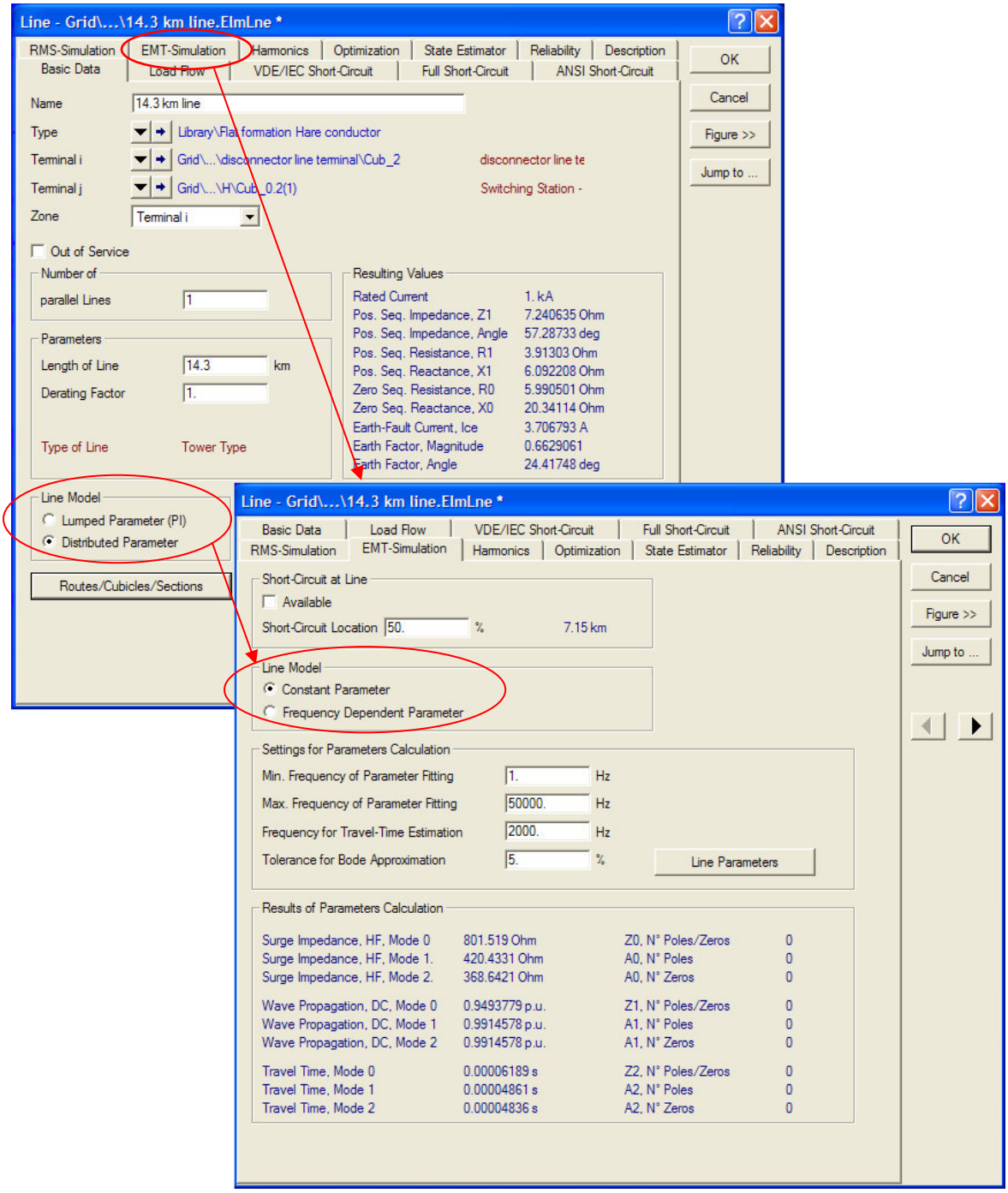


Figure 6.8 Element data dialog box for a transmission line in PowerFactory

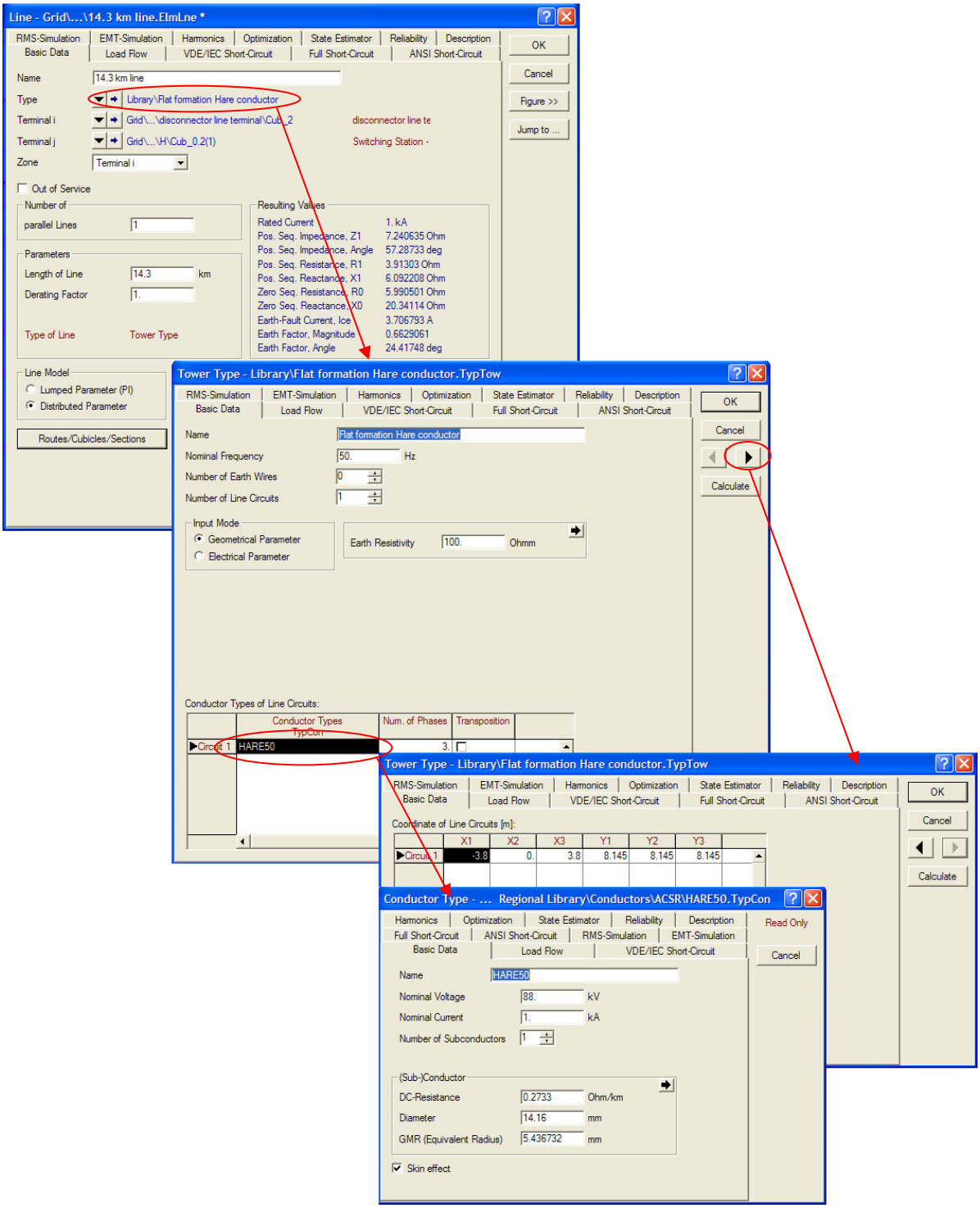


Figure 6.9 Type data dialog box for a transmission line in PowerFactory

According to the DigSILENT Technical Documentation on Overhead line models [41], PowerFactory supports a nominal π model for the lumped transmission line models. The Bergeron approach is used for the distributed line model with constant parameters. The

frequency dependent distributed parameter line mode uses the J. Marti approach that is discussed in [33], [38], [41].

Figure 6.9 shows the *type* data related to the element shown in Figure 6.8. In the *element* data dialog box, the user is able to select the *type* data for that element by either creating a new one or selecting one already in use in network. *Type* data allows the user to define the parameters of the transmission line either geometrically or electrically as well as allowing the user to define the type conductor. This is shown in Figure 6.9. In this case, the *element* is a line that is 14.3km long. The characteristics of the line: tower configuration, conductor type, phase spacings at the tower, constitutes the *type*.

### 6.3.1 Simulated Network in PowerFactory

The same power system model that was modelled in ATP was also modelled in PowerFactory and is shown in Figure 6.10. The dotted boxes in the figure show where the various substations and switching stations are in the PowerFactory model in relation to the system model that was shown earlier in Figure 5.1. A regular PowerFactory user would be accustomed to seeing simulation result boxes on the model, although these are not shown in Figure 6.10. These simulation result boxes were hidden in the figure for display purposes only. Only the elements of power system model are shown.

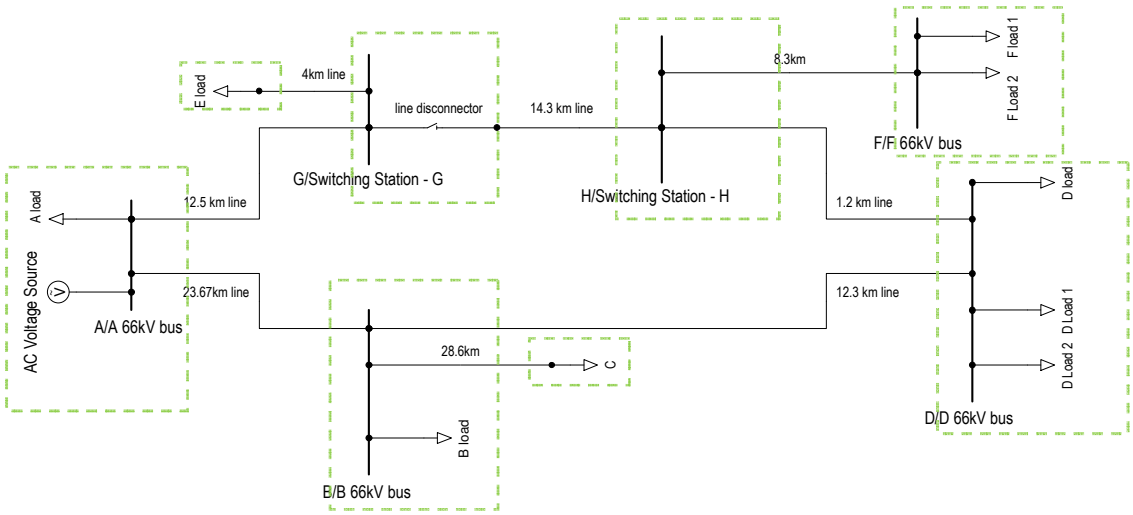


Figure 6.10 Simulated network in PowerFactory

The same switching operation run in ATP are run in PowerFactory to monitor the effect on the phase voltages and currents at switching station *G* and *H* due to switching operations of the line disconnector at switching station *G*. The switching operation run in PowerFactory and the times of the switching operation are shown in Figure 6.11. The current that is interrupted by the disconnector in the PowerFactory simulations is 2.73A.

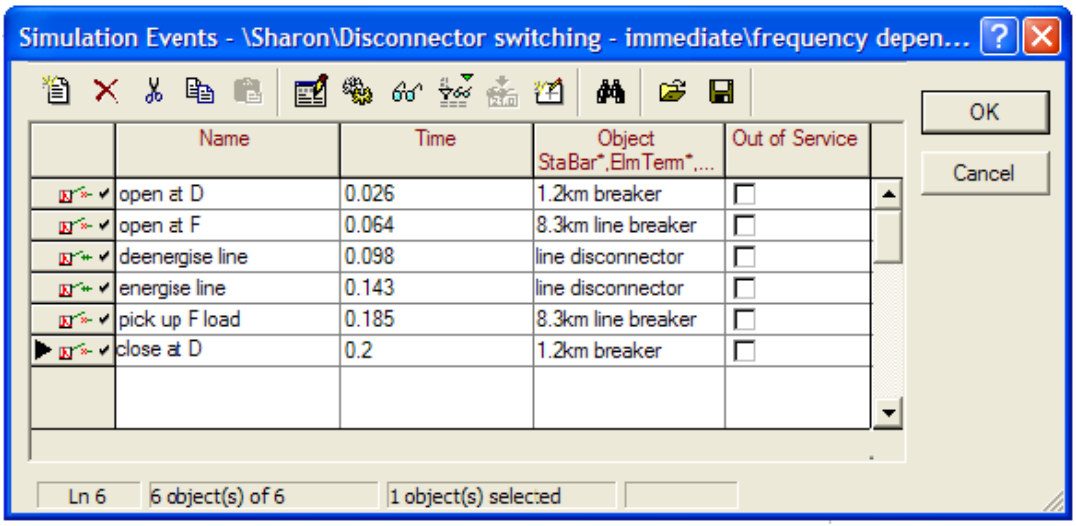


Figure 6.11 Switching operation times in PowerFactory

## 6.4 Summary

As mentioned before, ATP is recognised and widely used for transient simulation studies. It is used in this study for this reason. The PowerFactory simulation tool allows the user to model the power system model used in this study with the same parameters as those modelled in ATP. PowerFactory also allows the user to simulate the same operation times used for the disconnector and breakers in the power system model simulated in ATP. The likeness of both the ATP and PowerFactory power system models allows for a comparative study of the simulation results to be performed. The next chapter presents the simulation results of the power system model in both simulation tools and discusses the similarities and differences thereof.

# Chapter 7 Simulation Results and Discussions

## 7.1 Introduction

For this study, if overvoltages at the point of the disconnector switching operation (switching station *G*) are greater than 2.0pu, the switching operation of the disconnector was deemed unlikely to succeed. Taking this into consideration, this chapter presents the results of disconnector switching operation simulations of the network shown in Figure 5.1, using both the ATP and PowerFactory simulation tools. As mentioned in the previous chapters, the power system models in both simulation tools were simulated for various transmission line models, the results of which are discussed in this chapter. The simulation results from ATP are presented first, followed by the results from PowerFactory software package. Thereafter, the results from simulations of the mitigation techniques are discussed.

## 7.2 ATP simulation results

### 7.2.1 Lumped Transmission Line Model

The first disconnector switching test simulation in ATP used a lumped transmission line model for the overhead lines. The disconnector simulated in the ATP, was modelled to interrupt the current through it immediately and not at the 'natural zero' of the sinusoidal current waveform. The simulation was done in this way in order to investigate the effectiveness of the mitigation techniques that will be discussed later in the thesis.

The voltage and current plots of the phase voltages and phase currents drawn up from the Plot XY program used by ATP, were taken from voltage and current probes positioned at switching station *G* and switching station *H*. The positioning of these probes is shown in Figure 6.5 which displays the simulated power system model.

The first voltage plot, shown in Figure 7.1, is the phase voltage computed at switching station *G*. The second voltage plot, shown in Figure 7.2 is the phase voltage computed at switching station *H*. In these voltage plots, it is distinguishable that re-energising the unloaded transmission line results in transient overvoltages at the point of switching (switching station *G*) and at end of the unloaded line (at switching station *H*). It is also noticeable, from the figures, that there is a difference in the voltage plots at $0.098s < t < 0.143s$ at switching stations *G* and *H*. This is due to the residual voltage on the transmission line after the disconnector has operated. Furthermore, the transient overvoltages are higher at *H* than at *G*. The maximum peak magnitude at switching station *G* is 93.5kV or 1.73p.u. While at switching station *H*, the maximum peak magnitude is 113.6kV or 2.11p.u.

Based on the theory, higher overvoltages at switching station *H* than at switching station *G*, are not unexpected. A combination of reflected travelling waves as well as trapped charge on the line contribute to the higher stresses experienced at switching station *H*. However, due to the operating practice of earthing of equipment after de-energising for safety purposes, the likelihood of trapped charge existing on the de-energised line is diminished, and as a result the possibility of higher overvoltages in reality at switching station *H* than at switching station *G* is doubtful.

Figure 7.3 and Figure 7.4 show current waveforms calculated using a lumped transmission line model. Figure 7.3 shows the phase current waveforms through the disconnector at switching station *G*, while Figure 7.4 shows the phase current at the end of the unloaded line, at switching station *H*. As expected, the lumped transmission line model produces exaggerated and misleading peak phase current reading at switching station *G* when the disconnector is closed to re-energise the unloaded transmission line. The phase current remains at the high magnitude and is highly oscillatory even after all the load has fully restored at $t = 0.2s$. The peak current for the lumped model at switching station *G*, from Figure 7.3 is 3645A, which is very high when compared to the steady state peak current of 138A.

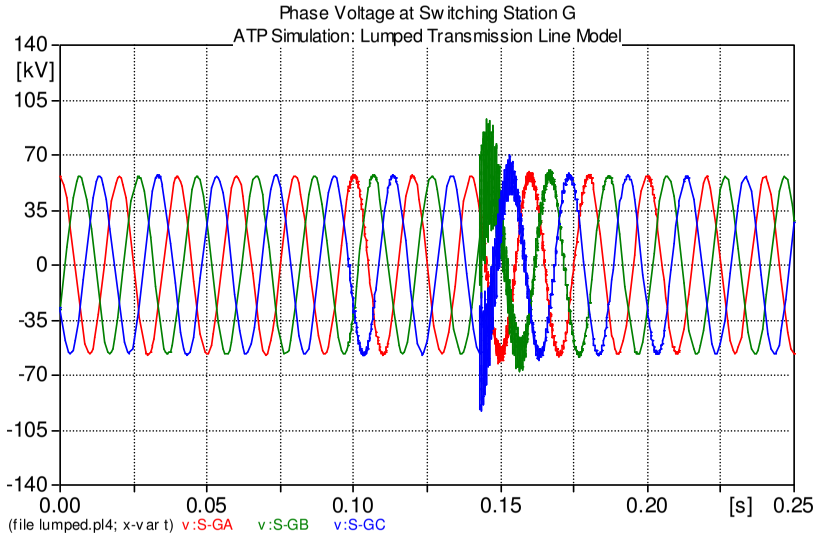


Figure 7.1 ATP Lumped transmission line model: Phase voltage at Switching Station *G*

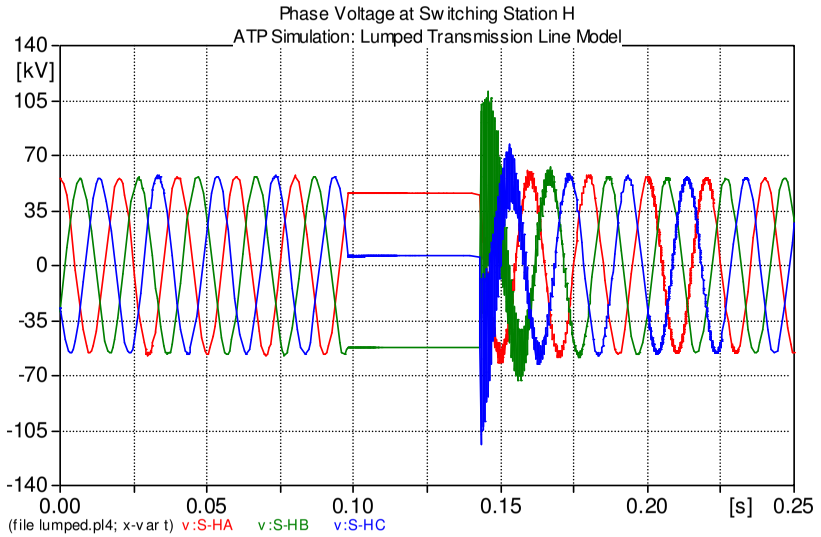


Figure 7.2 ATP Lumped transmission line model: Phase voltage at Switching Station *H*

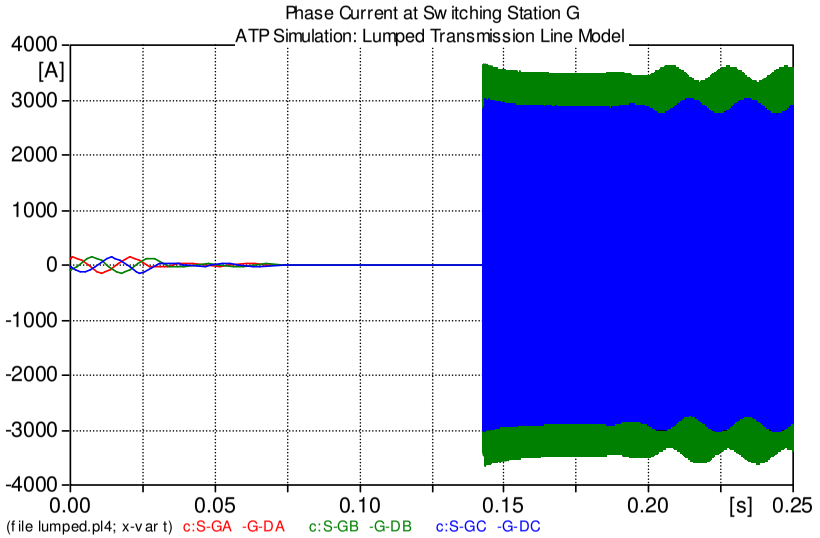


Figure 7.3 ATP Lumped transmission line model: Phase current at Switching Station *G*

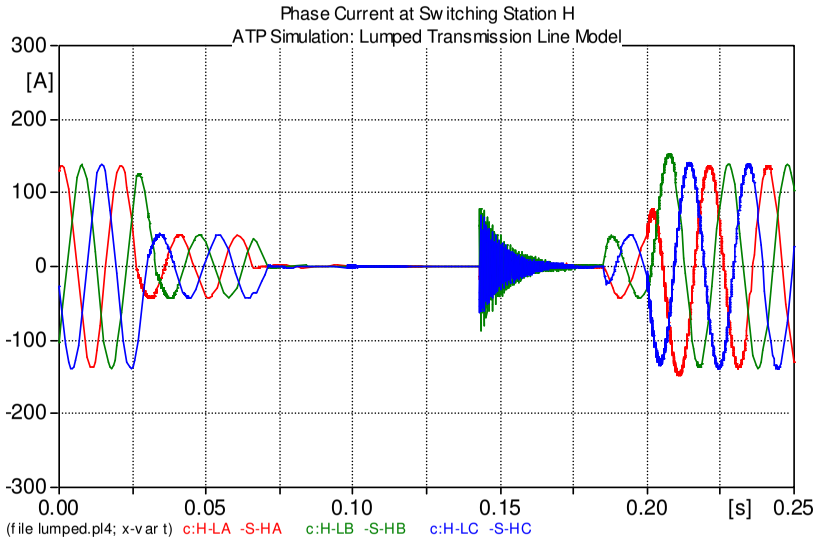


Figure 7.4 ATP Lumped transmission line model: Phase current at Switching Station *H*

### 7.2.2 Cascaded 2-π Transmission line model

Figure 7.5 - Figure 7.8 show the simulation results obtained when the transmission lines are modelled with cascaded 2-π line models to simulate disconnector switching. The variation in results between the cascaded 2-π model and lumped model are highlighted by the difference between the phase current results of the cascaded 2-π model and the lumped. Similar to the lumped model results, the phase current at switching station *G* in the cascaded 2-π model is overstated and misleading. However, the peak phase current for the cascaded 2-π simulated model is almost half that of the lumped simulated model at 1952A.

Comparison of the phase voltage results of both the lumped and cascaded 2-π transmission line models at switching station *G* shows the phase voltages are higher using the cascaded 2-π transmission line model with a peak phase voltage of -102.5kV which translates to -1.88p.u., when compared to -93.5kV peak phase voltage or 1.73p.u. recorded using a lumped model. For easy reference, the maximum phase voltages experienced at both switching stations for both the lumped and cascaded 2-π transmission line are tabulated in Table 7.1.

Table 7.1 Magnitudes of Peak Transient overvoltages and currents for lumped parameter transmission line models in ATP

| Transmission Line Model in ATP | Switching Station *G* | | | Switching Station *H* | | |
|---|---|---|---|---|---|---|
| | Voltage [kV] | Voltage [p.u.] | Current [A] | Voltage [kV] | Voltage [p.u.] | Current [A] |
| Lumped OHL model | 93.5 | 1.73 | 3645 | 113.6 | 2.11 | 86.7 |
| Cascaded 2-π OHL model | 101.5 | 1.88 | 1952 | 115.8 | 2.12 | 130.7 |

### 7.2.3 Constant Parameter Transmission Line Model

After running the simulations using lumped parameters, the transmission lines in the power system model were modelled using distributed parameters. Two types of distributed parameters were considered for the simulations, namely: the constant parameter model and the frequency dependent model. The literature discussed in previous chapters indicated a preference for the use of distributed parameters for the transmission line modelling where switching operations are expected [24], [28].

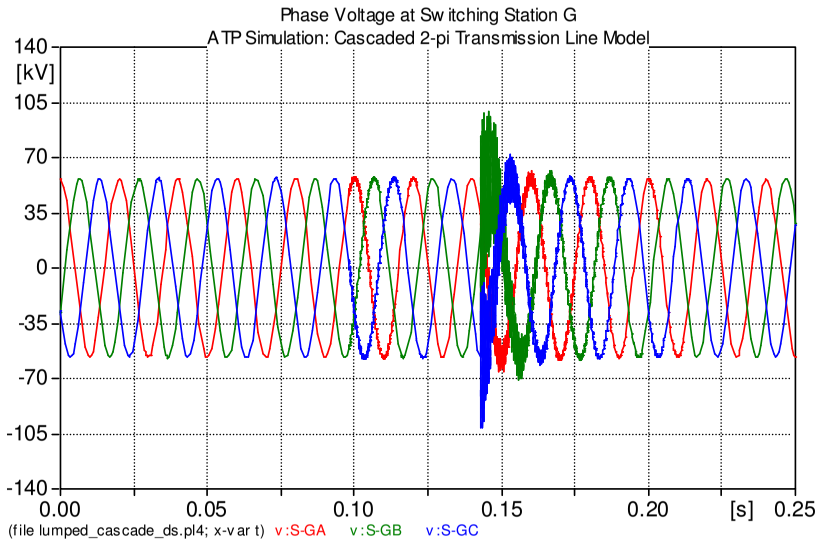


Figure 7.5 ATP: Cascaded 2-π model – Phase voltage at Switching Station *G*

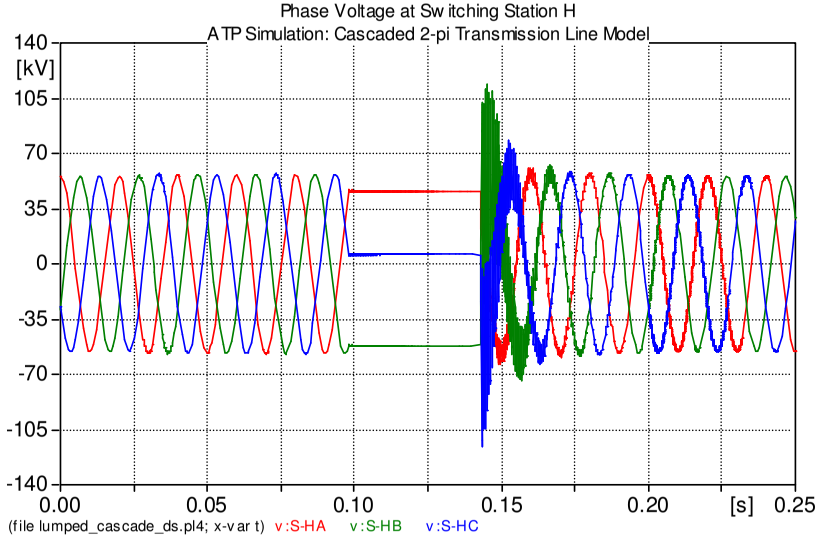


Figure 7.6 ATP: Cascaded 2-π model – Phase voltage at Switching Station *H*

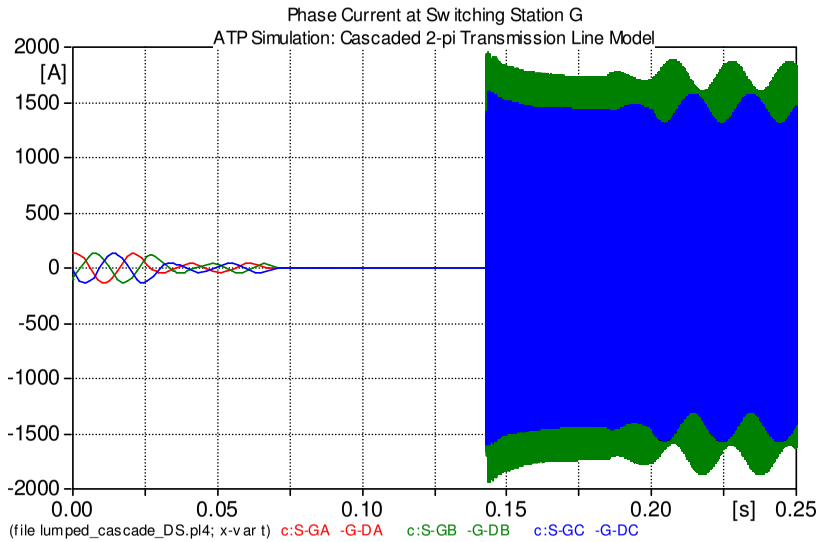


Figure 7.7 ATP: Cascaded 2-π model – Phase current at Switching Station *G*

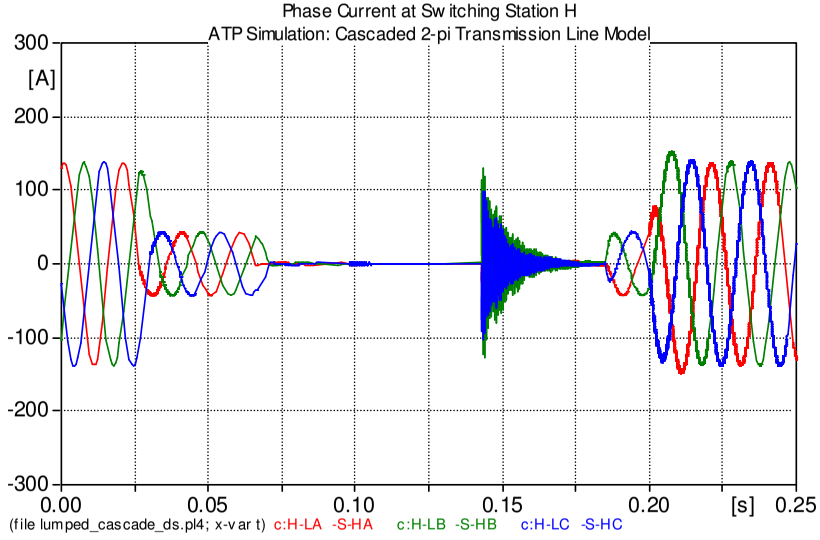


Figure 7.8 ATP: Cascaded 2-π model – Phase current at Switching Station *H*

This preference stemmed from the travelling wave nature of switching operations along transmission lines.

The first distributed parameter simulation run was that of the constant parameter transmission line model. This line model was computed at two frequencies: first, at the power frequency of 50Hz, and secondly, at the approximate natural frequency of the network (≈1.5kHz). Similar to the lumped parameters in the previous section, phase currents and phase voltages were observed at switching station *G* and switching station *H*. For the simulation results for the constant parameter models at 50Hz, the results are displayed in Figure 7.9 – Figure 7.12, while Figure 7.13 – Figure 7.16 shows the results for the constant parameter models calculated at 1.5kHz.

In the same manner as the lumped parameter model, the phase voltages are higher at switching station *H* (at the end of the transmission line) than at switching station *G*. There is no overvoltage when the disconnector is opened – i.e. at de-energisation. However, when the unloaded line is re-energised, switching transient overvoltages are experienced. This evidenced at $t = 0.143$s in Figure 7.9, Figure 7.10, Figure 7.13 and Figure 7.14.

Furthermore, unlike the lumped model that produced spurious phase current results, the phase currents at switching station *G* showed higher currents than at switching station *H*. The highest peak phase current magnitude simulated at switching station *G* for the 50Hz constant parameter model is 252A. Correspondingly, for the 1.5kHz constant parameter model, the highest peak current magnitude is 248A.

The transmission lines modelled using constant parameter calculated at 50Hz and 1.5kHz did, however, produce electro-magnetic transients for the phase currents and voltages. Fourier transforms of the phase voltages and phase currents revealed frequencies up to 2kHz, when the transmission line was re-energised.

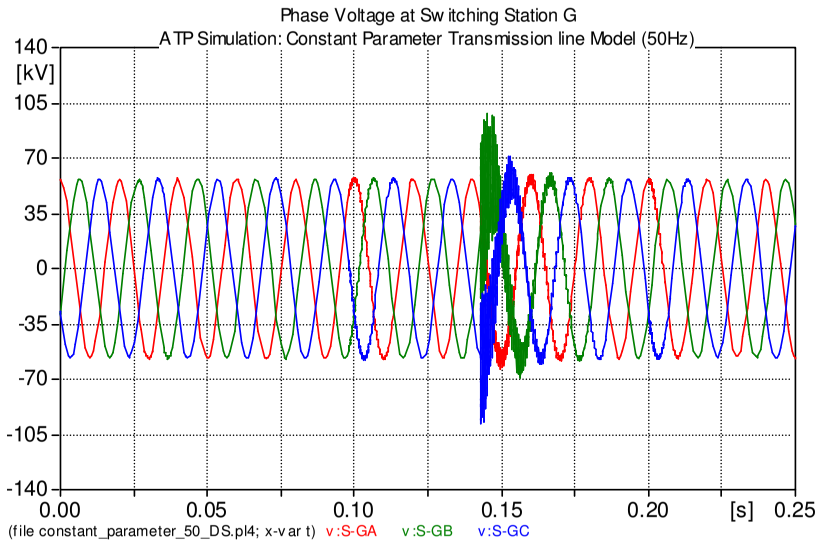


Figure 7.9 ATP: Constant Parameter (50Hz) model – Phase voltage at Switching Station *G*

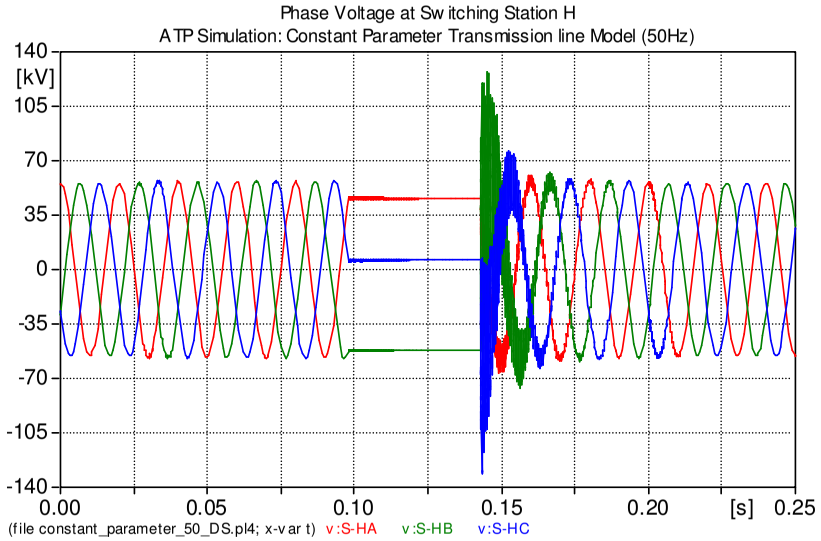


Figure 7.10 ATP: Constant Parameter (50Hz) model – Phase voltage at Switching Station *H*

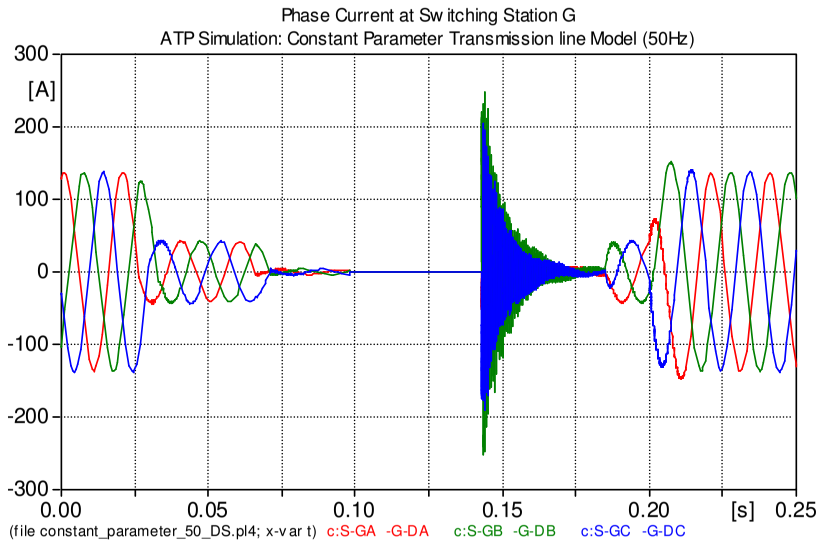


Figure 7.11 ATP: Constant Parameter (50Hz) model – Phase current at Switching Station *G*

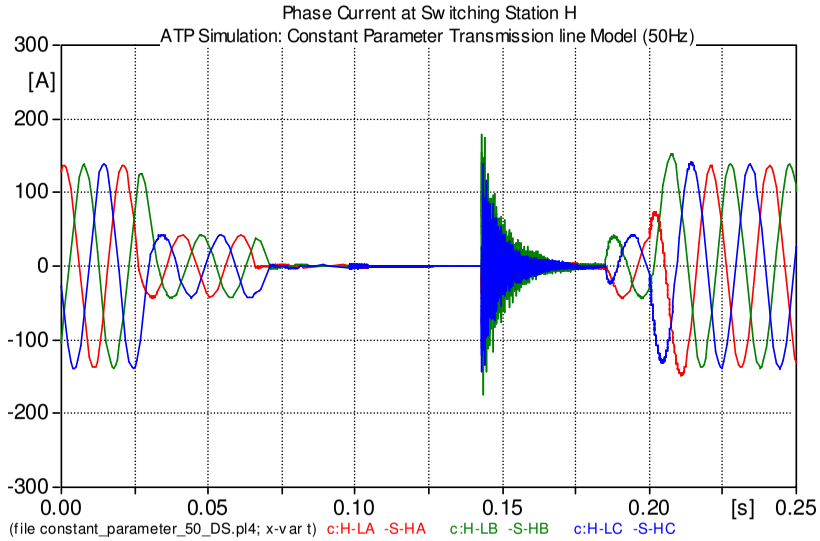


Figure 7.12 ATP: Constant Parameter (50Hz) model – Phase current at Switching Station *H*

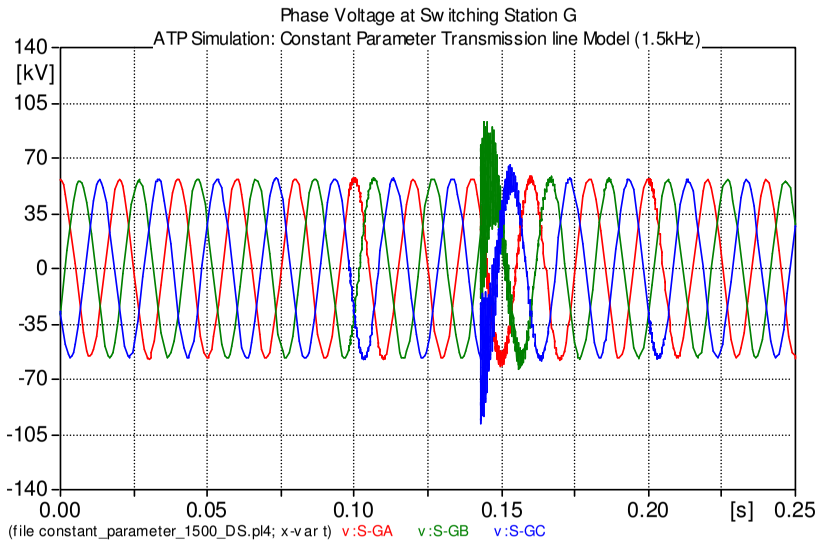


Figure 7.13 ATP: Constant Parameter (1.5kHz) model – Phase voltage at Switching Station *G*

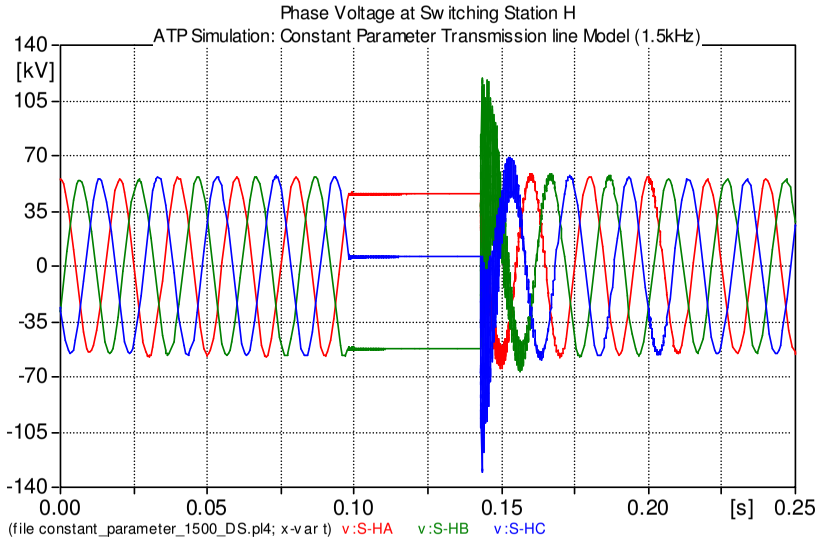


Figure 7.14 ATP: Constant Parameter (1.5kHz) model – Phase voltage at Switching Station *H*

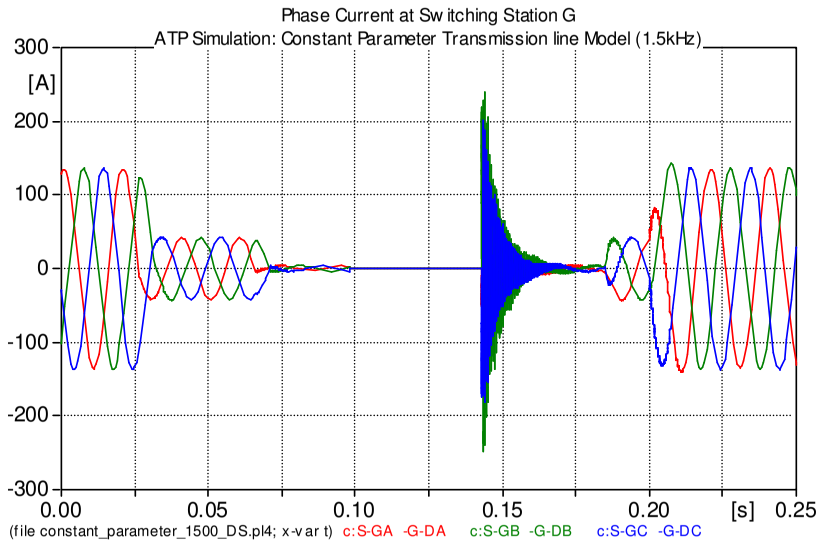


Figure 7.15 ATP: Constant Parameter (1.5kHz) model – Phase current at Switching Station *G*

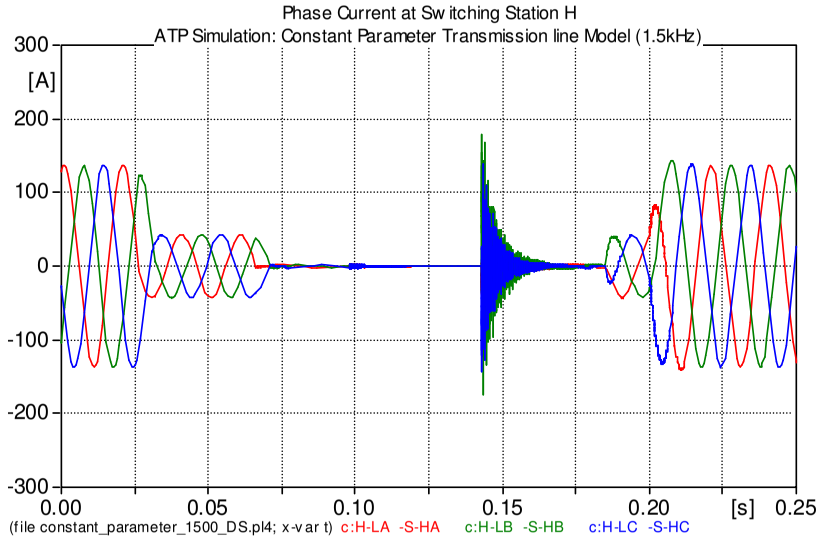


Figure 7.16 ATP: Constant Parameter (1.5kHz) model – Phase current at Switching Station *H*

### 7.2.4 Frequency Dependent Transmission Line Model

The final transmission line model simulated for a switching operation was for the frequency dependent model, based on the J. Marti model [33], [38]. The simulated phase voltages and phase currents produced using this type of transmission line model are shown in Figure 7.17 – Figure 7.20.

Again, similar to the results presented before, the transient overvoltages caused by the disconnector switching operation are more severe at re-energisation than that de-energisation. In addition, what is evident from the plots shown in Figure 7.17 and Figure 7.18, is the overvoltages are 31.5% higher at switching station *H* than at switching station *G*.

Also, in agreement with the results produced using the other transmission line models in ATP, the frequency dependent transmission line model results in higher phase current switching transients at switching station *G* than at switching station *H*. Yet what is different between the results of the frequency dependent model and the other transmission line models is that the period is shorter in which the phase current experiences high phase current transients, although not significantly so.

Table 7.2 shows the maximum peak magnitude phase currents and maximum peak magnitude phase voltage results from the simulations using the constant parameter and frequency dependent transmission line models.

Table 7.2 Magnitudes of Peak Transient overvoltages and currents for distributed parameter transmission line models in ATP

| Transmission Line Model in ATP | Switching Station *G* | | | Switching Station *H* | | |
|---|---|---|---|---|---|---|
| | Voltage [kV] | Voltage [p.u.] | Current [A] | Voltage [kV] | Voltage [p.u.] | Current [A] |
| Constant Parameter at 50Hz | 98.2 | 1.82 | 253.1 | 131.4 | 2.44 | 174.2 |
| Constant Parameter at 1.5kHz | 98.3 | 1.82 | 248.8 | 130.7 | 2.44 | 175.4 |
| Frequency Dependent | 95.8 | 1.78 | 234.2 | 125.6 | 2.34 | 162.5 |

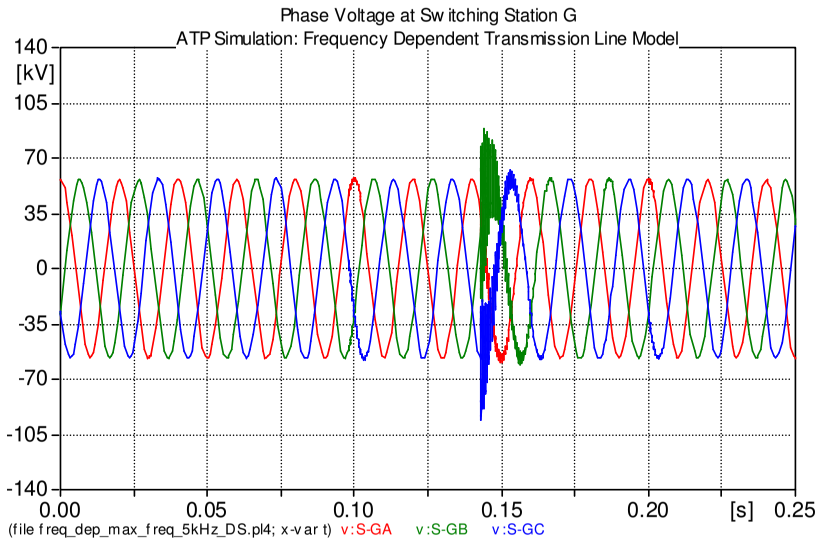


Figure 7.17 ATP: Frequency Dependent model – Phase voltage at Switching Station *G*

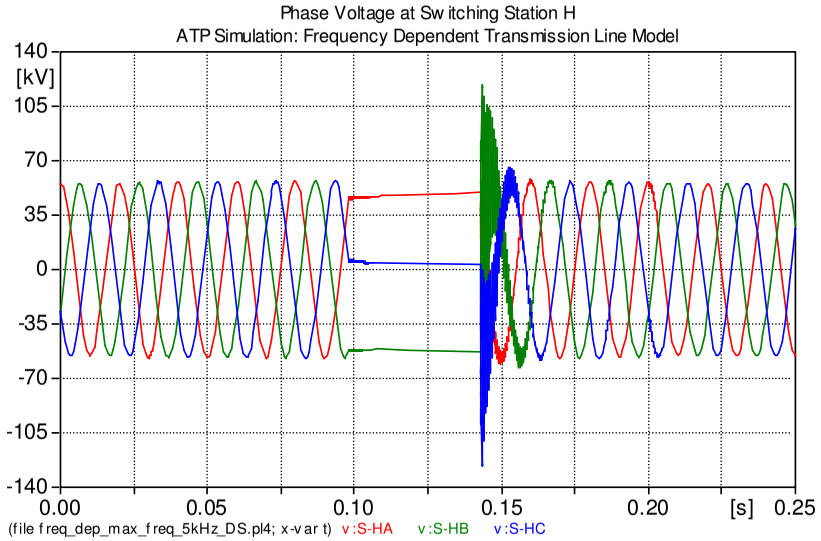


Figure 7.18 ATP: Frequency Dependent model – Phase voltage at Switching Station *H*

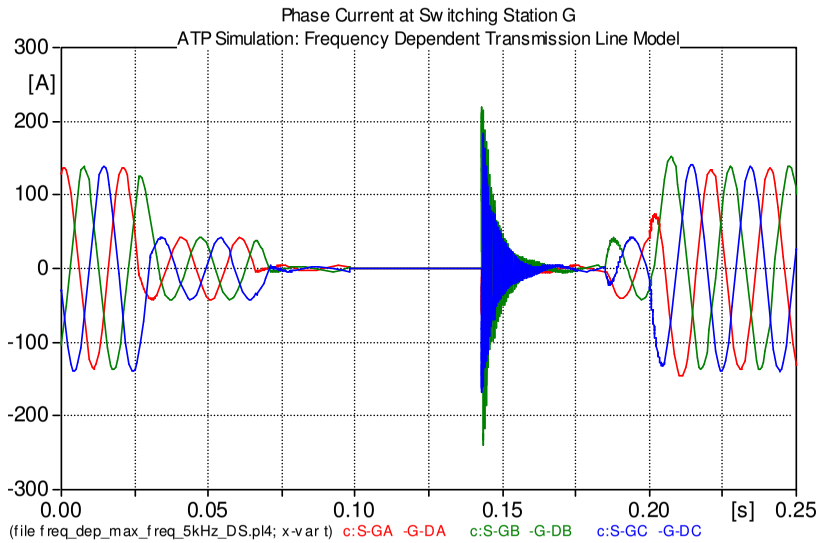


Figure 7.19 ATP: Frequency Dependent model – Phase current at Switching Station *G*

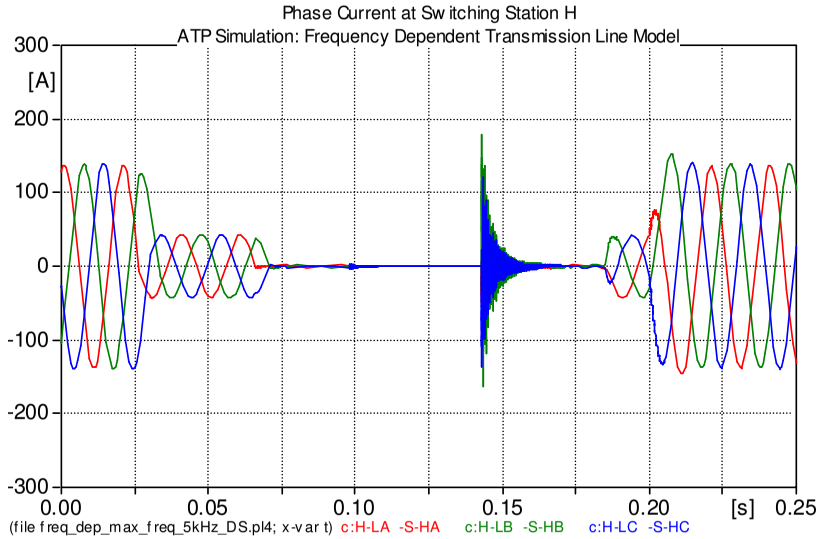


Figure 7.20 ATP: Frequency Dependent model – Phase current at Switching Station *H*

## 7.3 PowerFactory Simulation Results

### 7.3.1 Lumped transmission line model

This section of the chapter presents the simulation results of the power system model shown in Chapter 5, but using the PowerFactory simulation tool. Much like the ATP simulations discussed before, the PowerFactory simulations are performed for the various transmission line models.

The first transmission line model simulated using the power system model in PowerFactory was the lumped transmission line model. The simulation results for the lumped transmission line model are shown in Figure 7.21 – Figure 7.24 for the phase voltages and phase currents at switching station *G* and switching station *H*, respectively.

In the same manner as the ATP simulation results, PowerFactory simulation results indicate higher transient overvoltages when the disconnector is operated to re-energise the transmission line. Furthermore, the transient overvoltages are higher at switching station *H* than at switching station *G*. The maximum peak phase voltage at switching station *G* is 92.0kV or 1.72p.u., while at switching station *H*, the maximum peak phase voltage is 113.4kV or 2.10p.u. Moreover, the lumped transmission line model in PowerFactory yields onerous peak phase current results at switching station *G*, with the maximum peak phase current of 1295.6A when the line is re-energised. The maximum peak phase current of 1295.6A in PowerFactory is still less than the maximum peak phase current of 3645A recorded using ATP. However, the computed phase current for the PowerFactory simulation does not show the same oscillatory behaviour as seen in Figure 7.3 during the ATP simulation.

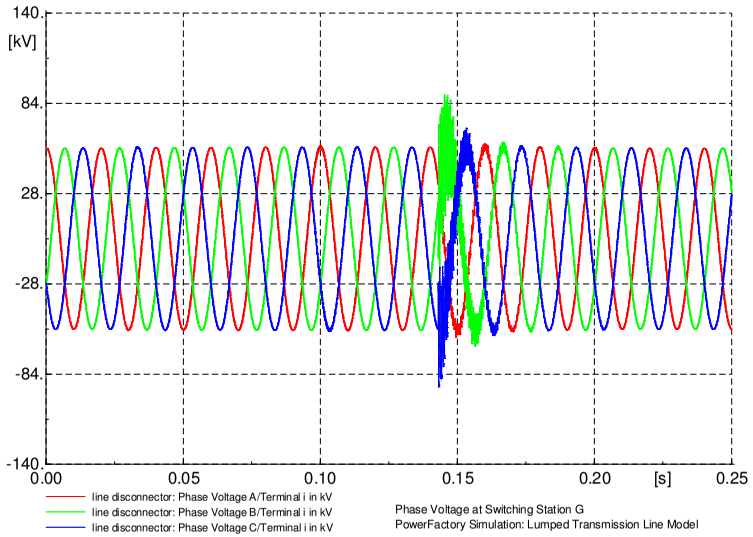


Figure 7.21 PF: Lumped model – Phase voltage at Switching Station *G*

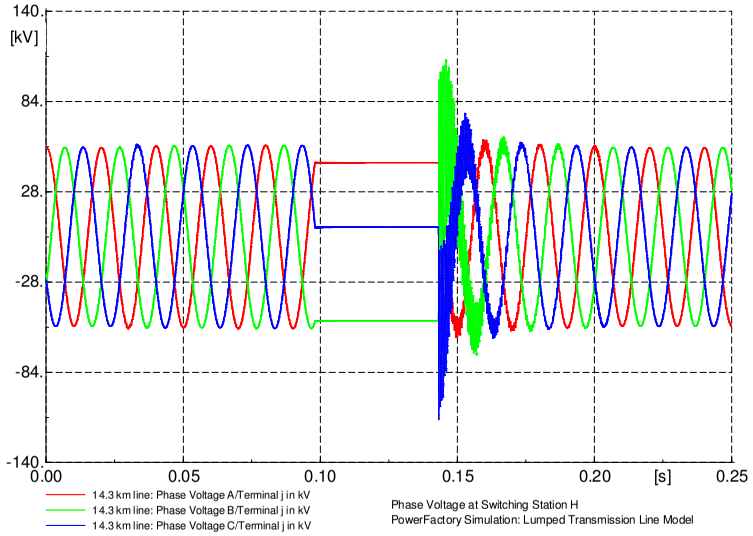


Figure 7.22 PF: Lumped model – Phase voltage at Switching Station *H*

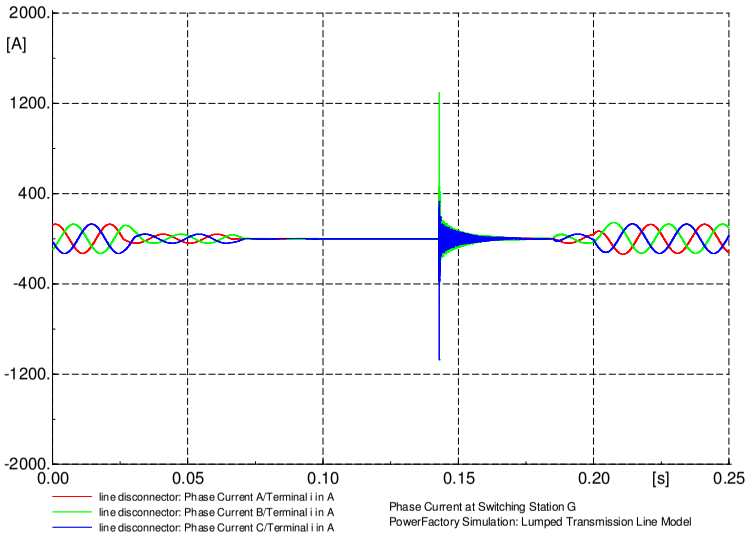


Figure 7.23 PF: Lumped model – Phase current at Switching Station *G*

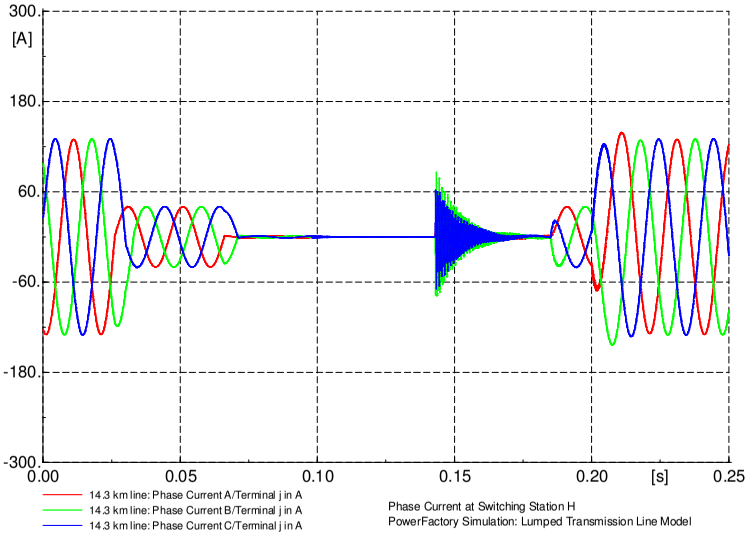


Figure 7.24 PF: Lumped model – Phase current at Switching Station *H*

### 7.3.2 Cascaded 2-π Transmission line model

Figure 7.25 – Figure 7.28 show the results of the disconnector switching operations from the PowerFactory simulation when the transmission lines are modelled using cascaded 2-π transmission line.

When a cascaded 2-π transmission line model is simulated in PowerFactory, the peak phase current of 662.8A is observed at switching station *G*. This peak phase current is considerably less than the 1295.6A recorded using the lumped simulation. In addition to that, unlike the results obtained from the simulations in ATP, the high frequency oscillations in the PowerFactory simulations are not present when full load is restored.

The resultant phase voltages at switching station *G* of the switching operations simulated in PowerFactory for cascaded 2-π model showed that the most significant transient voltages occurred when the unloaded transmission line was re-energised. The cascaded 2-π model showed an overvoltage of -101.2kV or -1.88p.u. at switching station *G* and 116.3kV or 2.16p.u. at switching station *H*.

In Table 7.3, the maximum phase voltages in magnitude and per unit values as well as the maximum phase currents experienced when the disconnector is operated, are tabulated. The results shown are taken at switching stations *G* and at the switching station *H*.

Table 7.3 Magnitudes of Peak Transient overvoltages and currents for lumped parameter transmission line models in PowerFactory

| Transmission Line Model in PowerFactory | Switching Station *G* | | | Switching Station *H* | | |
|---|---|---|---|---|---|---|
| | Voltage [kV] | Voltage [p.u.] | Current [A] | Voltage [kV] | Voltage [p.u.] | Current [A] |
| **Lumped OHL model** | 92.0 | 1.71 | 1295.6 | 113.4 | 2.10 | 78.6 |
| **Cascaded 2-π OHL model** | 101.2 | 1.88 | 662.8 | 116.3 | 2.16 | 140.8 |

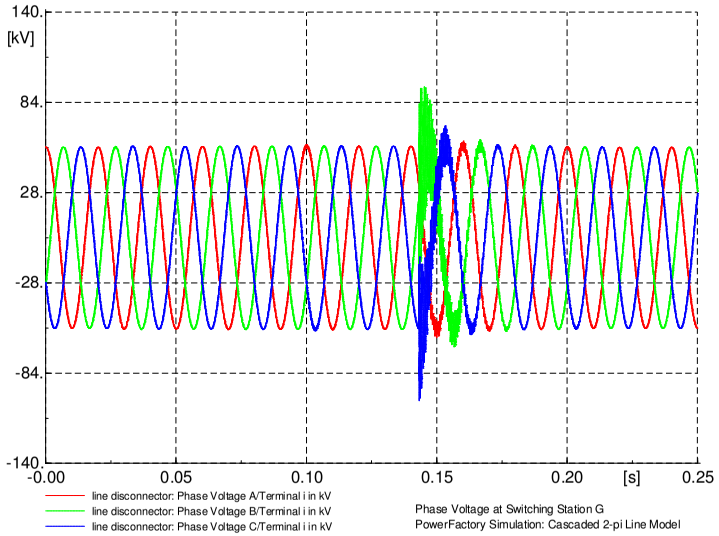


Figure 7.25 PF: Cascaded 2-π model – Phase voltage at Switching Station *G*

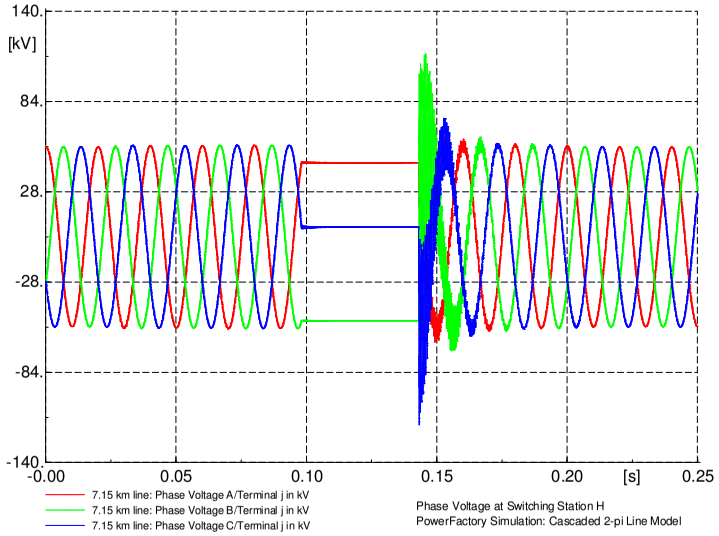


Figure 7.26 PF: Cascaded 2-π model – Phase voltage at Switching Station *H*

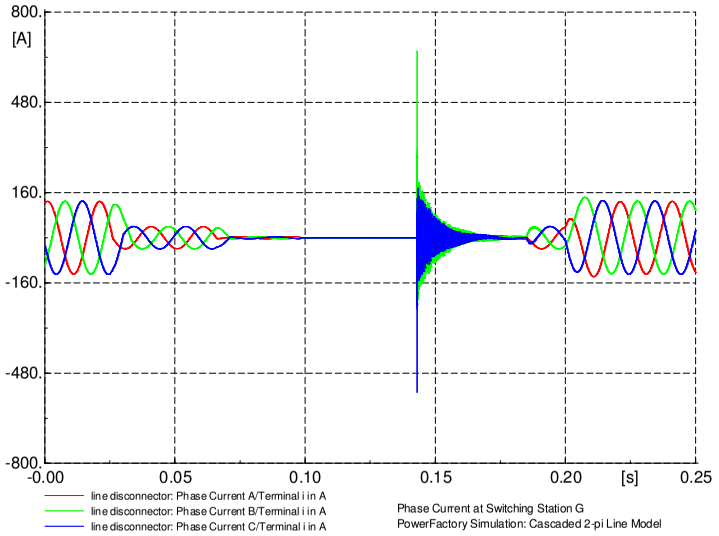


Figure 7.27 PF: Cascaded 2-π model – Phase current at Switching Station *G*

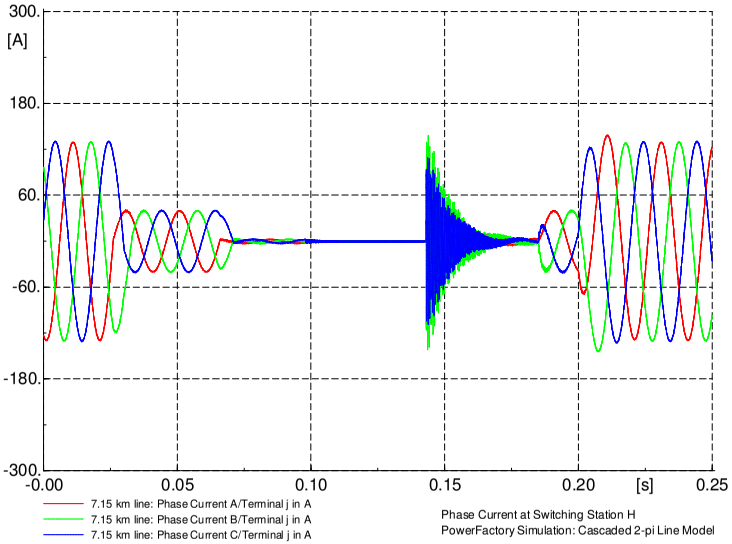


Figure 7.28 PF: Cascaded 2-π model – Phase current at Switching Station *H*

### 7.3.3 Constant Parameter Transmission Line Model

The next simulations run in PowerFactory used constant parameter transmission line models. The constant parameters were calculated at 50Hz and 1.5kHz, in the same manner as the simulations run in ATP. The results from the constant parameter transmission models calculated at 50Hz are shown in Figure 7.29 – Figure 7.32. Figure 7.33 – Figure 7.36 show the results from the constant parameter transmission line models calculated at 1.5kHz.

The results using the constant parameter models are, in general, in agreement with the results obtained with the ATP simulations. The overvoltages are higher at switching station *H*, at the receiving end of the unloaded transmission line, than at switching station *G*, where the switching operation takes place. Yet, the current transients are higher at switching station *G* than at switching station *H*. The maximum peak phase voltages and currents are summarised in Table 7.4.

An observation of the phase voltages calculated at switching station *H* using PowerFactory, shows that the phase voltage on the unloaded line does not remain unchanged after the disconnector is switched open, see Figure 7.30 and Figure 7.34. This is in contrast to the corresponding results obtained using the ATP simulation tool, see Figure 7.10 and Figure 7.14.

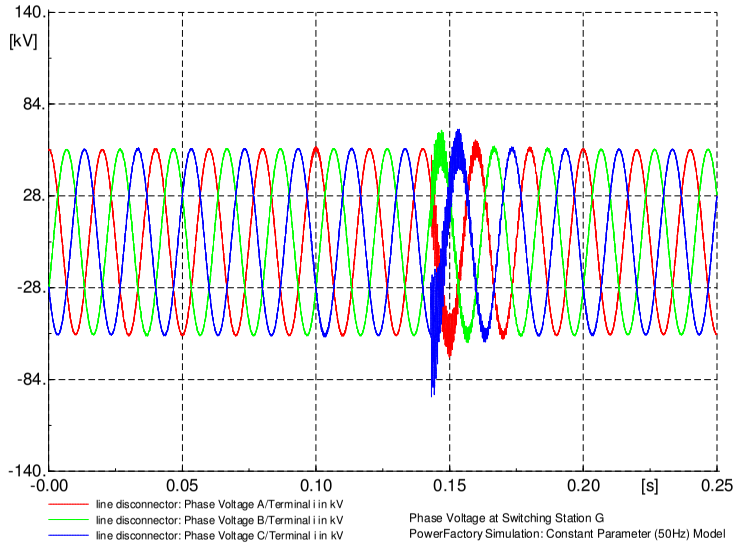


Figure 7.29 PF: Constant parameter (50Hz) model – Phase voltage at Switching Station *G*

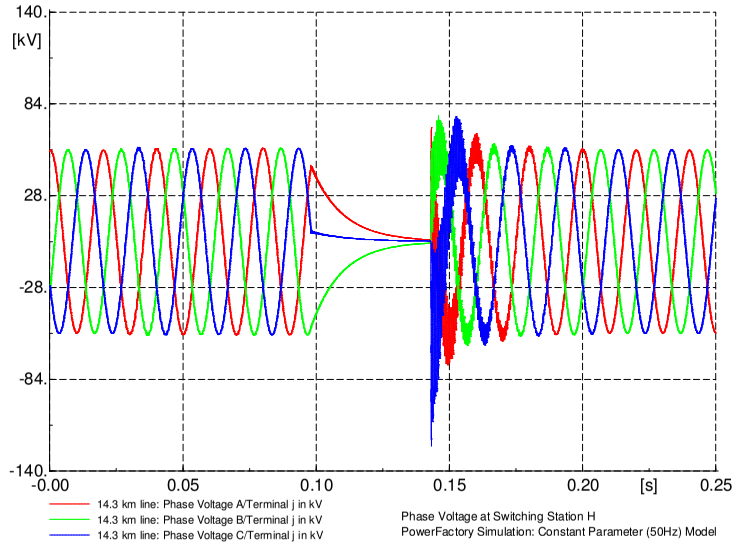


Figure 7.30 PF: Constant parameter (50Hz) model – Phase voltage at Switching Station *H*

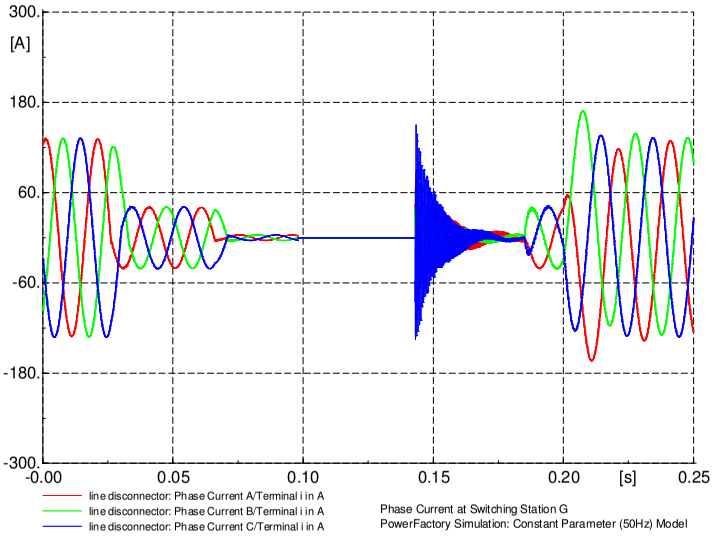


Figure 7.31 PF: Constant parameter (50Hz) model – Phase current at Switching Station *G*

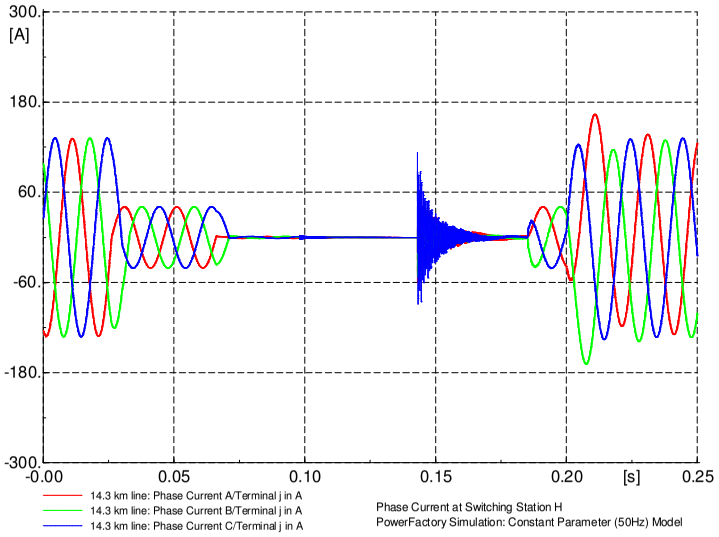


Figure 7.32 PF: Constant parameter (50Hz) model – Phase current at Switching Station *H*

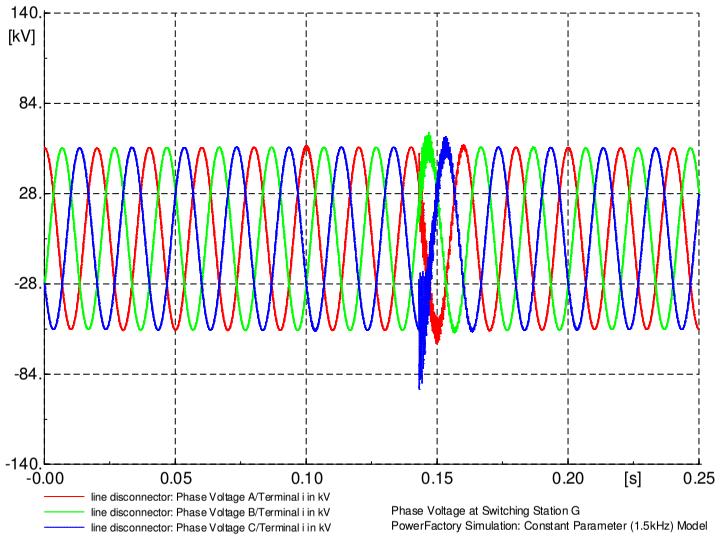


Figure 7.33 PF: Constant parameter (1.5kHz) model – Phase voltage at Switching Station *G*

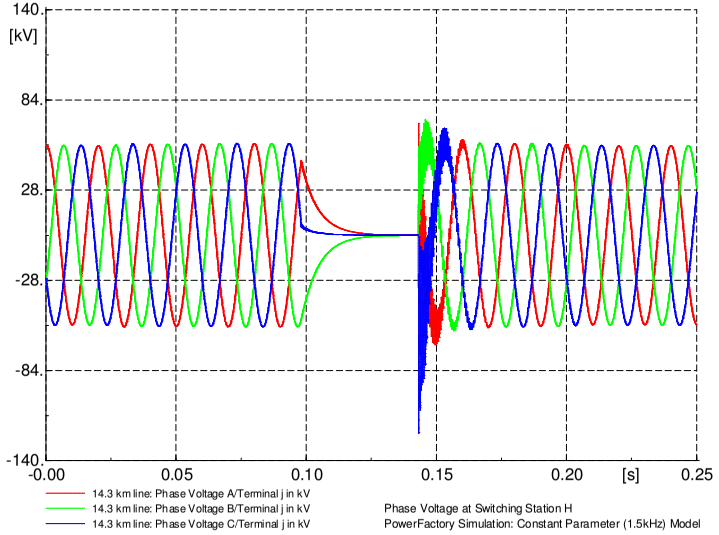


Figure 7.34 PF: Constant parameter (1.5kHz) model – Phase voltage at Switching Station *H*

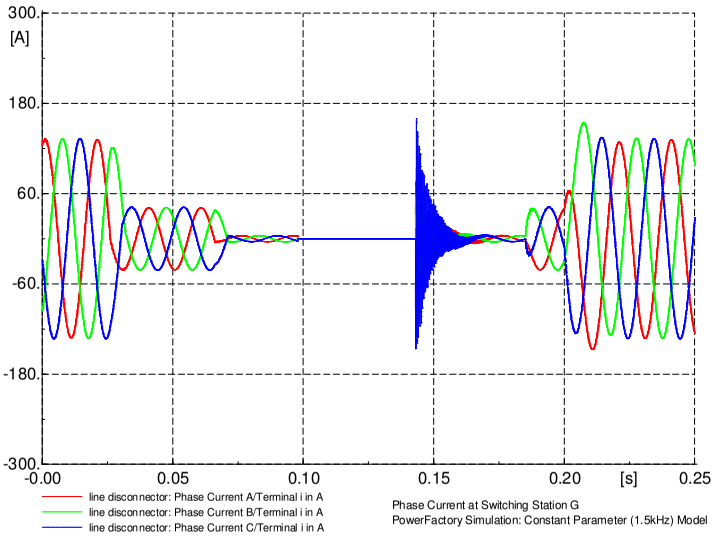


Figure 7.35 PF: Constant parameter (1.5kHz) model – Phase current at Switching Station *G*

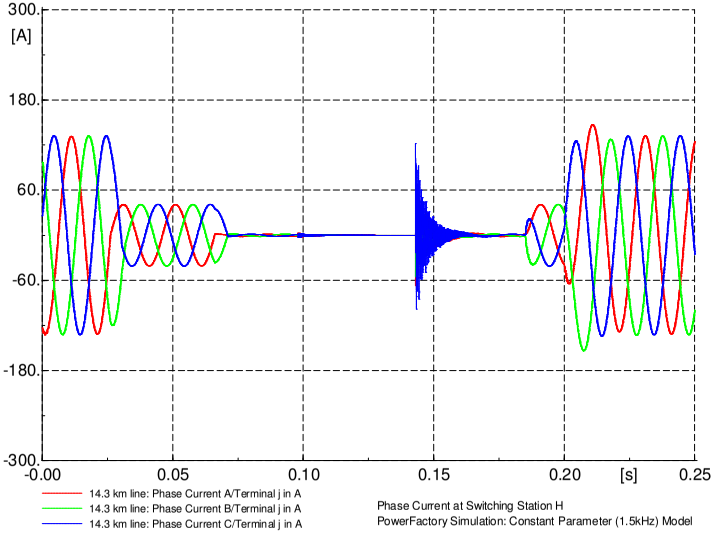


Figure 7.36 PF: Constant parameter (1.5kHz) model – Phase current at Switching Station *H*

### 7.3.4 Frequency Dependent Transmission Line Model

The last transmission line model to be simulated in PowerFactory is the frequency dependent line model based on the model proposed by J. Marti [38]. The simulation results produced results similar to those observed when using the constant parameter model. This is as expected for this type of simulation, where no appreciable zero sequence voltages and currents occur.

The phase voltage and phase current results from the frequency dependent simulation in PowerFactory are shown in Figure 7.37 – Figure 7.40. At switching station *H*, high transient overvoltages at 118.9kV or 2.21p.u are shown. The magnitude of the highest peak phase voltage at switching station *G* is 90.2kV or 1.67p.u. Table 7.4 tabulates the frequency dependent simulation results with those obtained using the constant parameter line models used in PowerFactory.

Table 7.4 Magnitudes of Peak Transient overvoltages and currents for distributed parameter transmission line models in PowerFactory

| Transmission Line Model in PowerFactory | Switching Station *G* | | | Switching Station *H* | | |
|---|---|---|---|---|---|---|
| | Voltage [kV] | Voltage [p.u.] | Current [A] | Voltage [kV] | Voltage [p.u.] | Current [A] |
| **Constant Parameter at 50Hz** | 93.9 | 1.74 | 135.5 | 124.6 | 2.31 | 112.7 |
| **Constant Parameter at 1.5kHz** | 93.5 | 1.73 | 159.6 | 122.9 | 2.28 | 123.0 |
| **Frequency Dependent** | 90.2 | 1.67 | 150.1 | 118.9 | 2.21 | 123.0 |

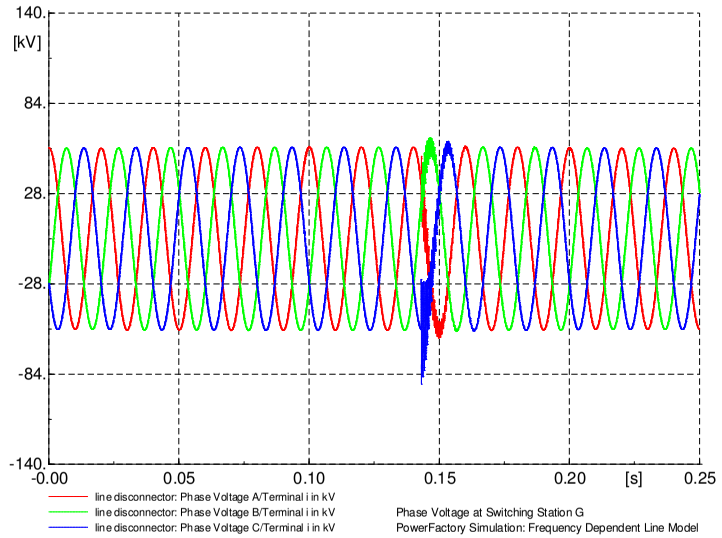


Figure 7.37 PF: Frequency Dependent model – Phase voltage at Switching Station *G*

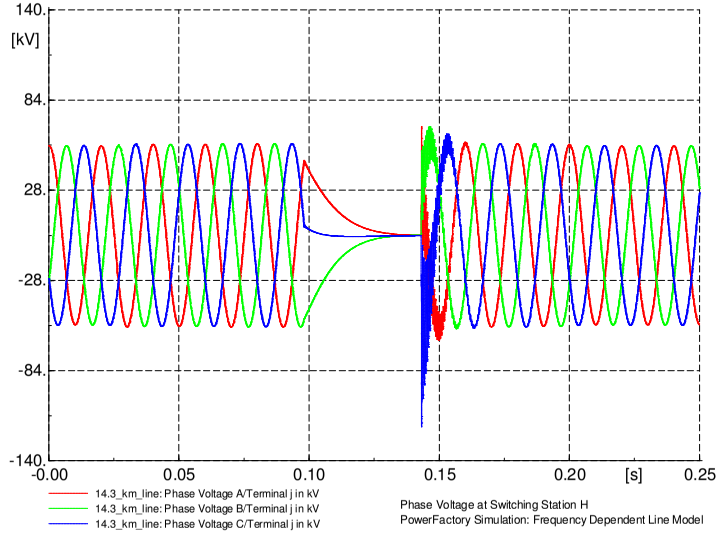


Figure 7.38 PF: Frequency Dependent model – Phase voltage at Switching Station *H*

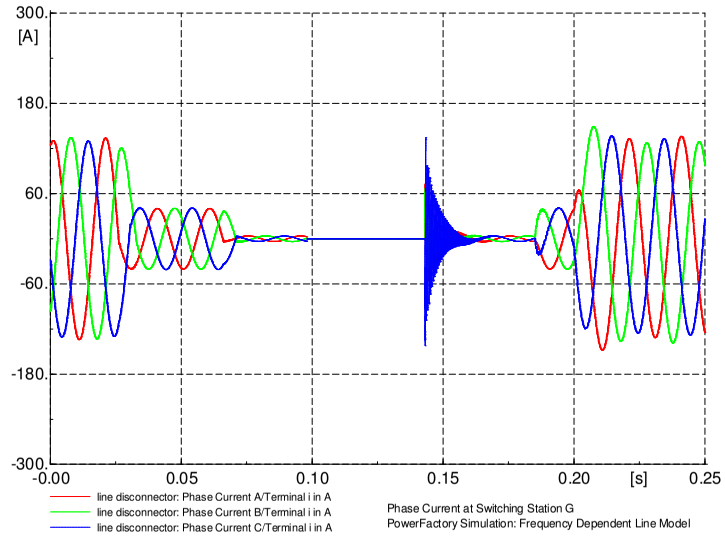


Figure 7.39 PF: Frequency Dependent model – Phase current at Switching Station *G*

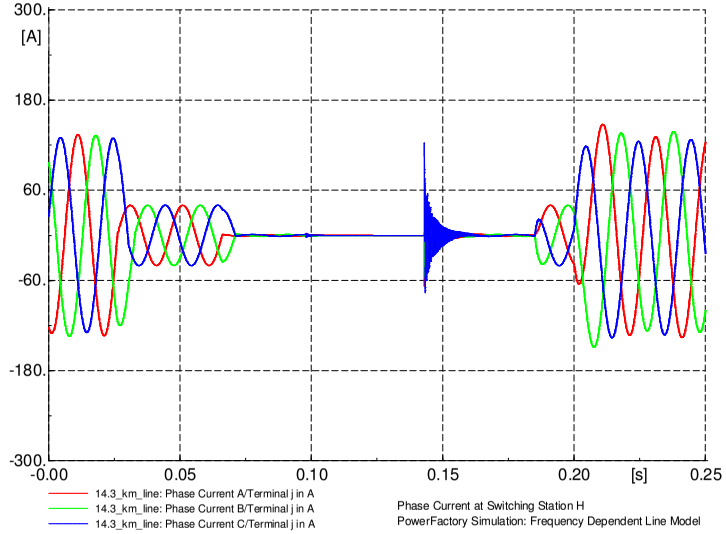


Figure 7.40 PF: Frequency Dependent model – Phase current at Switching Station *H*

## 7.4 Discussion of Simulation Results in ATP and PowerFactory

The results tabulated in Table 7.1 and Table 7.4 are combined to produce the chart shown in Figure 7.41. Figure 7.41 shows the magnitudes, in per unit, of the maximum peak phase voltages calculated at switching station *G* and station *H* for the different types of transmission line models used to simulate the disconnector switching of an unloaded transmission line. The bar chart also shows the results taken at the two switching stations, *G* and *H*, from the two simulation tools used in this thesis, ATP and PowerFactory (indicated in the bar chart as PF).

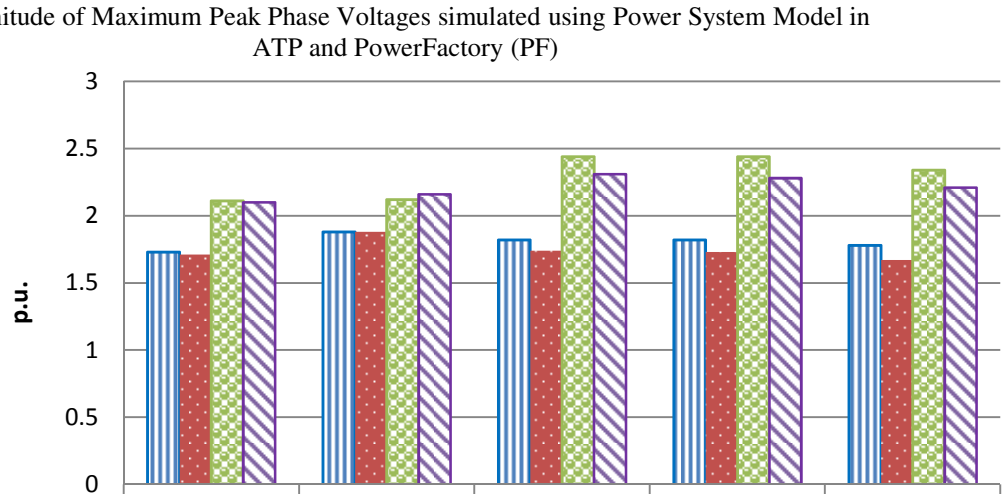


| | Lumped OHL model | Cascaded 2 - π OHL model | Constant Parameter at 50Hz | Constant Parameter at 1.5kHz | Frequecy Denpendent |
|---|---|---|---|---|---|
| ATP:Switching Station G | 1.73 | 1.88 | 1.82 | 1.82 | 1.78 |
| PF: Switching Station G | 1.71 | 1.88 | 1.74 | 1.73 | 1.67 |
| ATP:Switching Station H | 2.11 | 2.12 | 2.44 | 2.44 | 2.34 |
| PF: Switching Station H | 2.1 | 2.16 | 2.31 | 2.28 | 2.21 |

Figure 7.41 Bar chart comparing the magnitudes of phase voltages at switching station *G* and *H* for ATP and PowerFactory

Owing to the onerous and spurious simulation results from the phase currents taken from the lumped and cascaded 2π models, the results from these models are generally disregarded, although are shown for the sake of completeness. The results of the distributed parameter

models, namely: constant parameter model and frequency dependent model, are discussed further in this chapter.

From the chart, it is evident that the phase voltages at switching station *G* are less than 2.0pu irrespective of the transmission line model or software package that was used to run the simulation. It was stated earlier that a switching operation in this study is unlikely to succeed if overvoltages greater than 2.0pu are observed at the point of the switching operation. Based on this criteria, the switching operation of the disconnector, shown in Figure 5.1, should succeed.

However, taken from a personnel safety perspective, where an operator would manually operate a disconnector switch, the arcing due to switching transients at switching station *G* would be of concern to the operator. The current interrupted by the disconnector in the ATP simulation is 2.56A, while it is 2.73A in PowerFactory. In his publication, Peelo [4] warns that currents up to 2A can be interrupted provided that it is understood and accepted by the user that the disconnector may be close to fully open position at current interruption.

Unfortunately, the results presented in the study did not relate the overvoltages, switching transients or high frequency oscillations shown in the simulation results to arcing. However, it is thought that if the period of arcing can be related to the period where the phase voltages experience high frequency oscillations or transient oscillations, then one can formulate a method to assist field operators to gauge when a disconnector is safe to operate, where negligible currents are involved.

Moreover, one has to bear in mind that based on the simulation results higher overvoltages are experienced at switching station *H*. These overvoltages at switching station *H* are greater than 2.0p.u., but they do not last longer than a full cycle of the power frequency. Despite this, there is an indication from the simulation results that equipment that is stationed further from the origin of the switching operation will experience higher overvoltages than at the source.

One finding from the simulation results from both the ATP and PowerFactory simulations is that the re-energising of the transmission line results in higher overvoltages than de-energising of the transmission line. This is in contrast to findings by Knobloch [23] who states in his paper that higher values of overvoltages are measured during a “switching off” or de-energising

operation than during an energising operation. Peelo [4] made no comment of this finding by Knobloch despite agreeing with him on various other findings, such as the use of a source-side capacitor to reduce transient overvoltages.

Based on ease by which one can set up the power system model, the frequency dependent line model is the preferred model to use. This model eliminates the need to choose a frequency at which to model the transmission line by calculating the behaviour of the line over a range of frequencies. Furthermore, the user is not restricted to only use the model for steady state studies or studies that do not involve high zero sequence voltages or currents. Due to the fact that there is no significant difference in the maximum overvoltages presented in the simulation results in Figure 7.41, the frequency dependent line model is still the preferred model to simulate a switching operation where a disconnector is used.

For all the distributed parameter model results, the ATP simulation tools produce higher transient voltages than PowerFactory, despite using the same parameters in modelling the power system model in both simulation tools. Many of the principles used in ATP are also used in PowerFactory. For example, the use of the J. Marti model for the frequency dependent EMT simulations or the EMTP based line models for the constant parameter line models. For the user to decide which simulation tool is preferred will have to be a decision based on the user's level of competency with the simulation tool.

Ultimately, to establish whether the results simulated using both simulation tools are enough to determine the success of a disconnector switching operation for an unloaded transmission line, the simulation results would have to be verified by field or laboratory tests. Unfortunately, field tests did not form part of the scope for this study, but they are recommended to ascertain which simulation package produces results that are closer to reality in the field.

## 7.5 Simulation results of Mitigating techniques

Two techniques that can mitigate the effect of the switching overvoltages experienced during disconnector switching were highlighted in previous chapters. These are current interruption of the disconnector at the zero crossing and the introduction of a source-side capacitor ($C_S$).

For comparative reasons, the same power system model used in the previous simulations was used to simulate the models for mitigating techniques. The frequency dependent line model was used for the simulations in ATP and PowerFactory.

### 7.5.1 Disconnector Switching at Current Zero-Crossing

Figure 7.50 shows a bar graph that compares the results of the simulations run in ATP and PowerFactory. The graph compares the results previously shown for a frequency dependent model where the phase currents of the disconnector are interrupted at the same time, and the results of the simulation where the disconnector operates at the phase current zero-crossing. From the chart, it is evident that the interruption of the disconnector at the zero-crossing produces lower transient overvoltages than those produced when the disconnector is operated immediately. For example, when the power system model is simulated in ATP using a zero-crossing disconnector, the magnitude of the maximum peak phase voltage at switching station *G* is 1.29p.u. The equivalent model in PowerFactory is 1.47p.u. In contrast, the first simulations without zero-crossing disconnector models (indicated on the chart by 'Disconnector switch'), yielded maximum peak phase voltages at switching station *G* of 1.78p.u. and 1.67p.u in ATP and PowerFactory, respectively.

The simulation results where the zero-crossing disconnector model is used in the ATP simulation tool are shown in Figure 7.42 – Figure 7.45, while the results from the PowerFactory simulation tool are shown in Figure 7.46 – Figure 7.49.

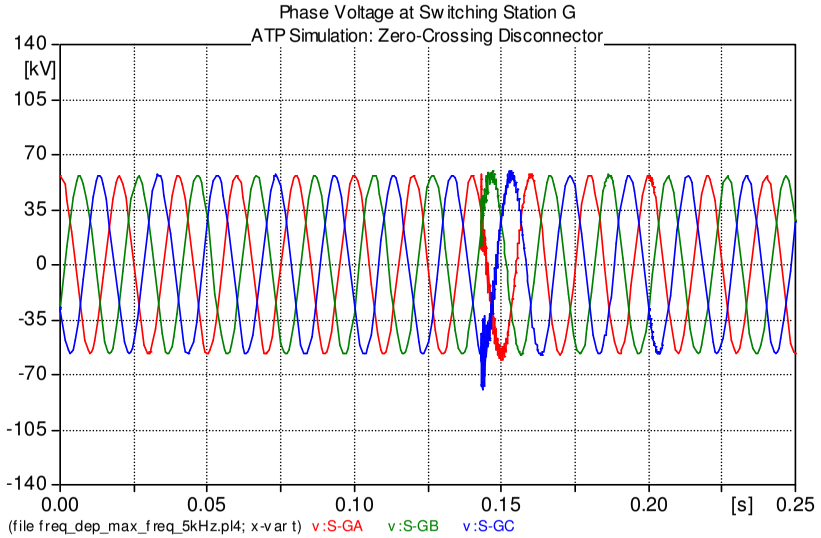


Figure 7.42 ATP: Zero-crossing disconnector model – Phase voltage at Switching Station *G*

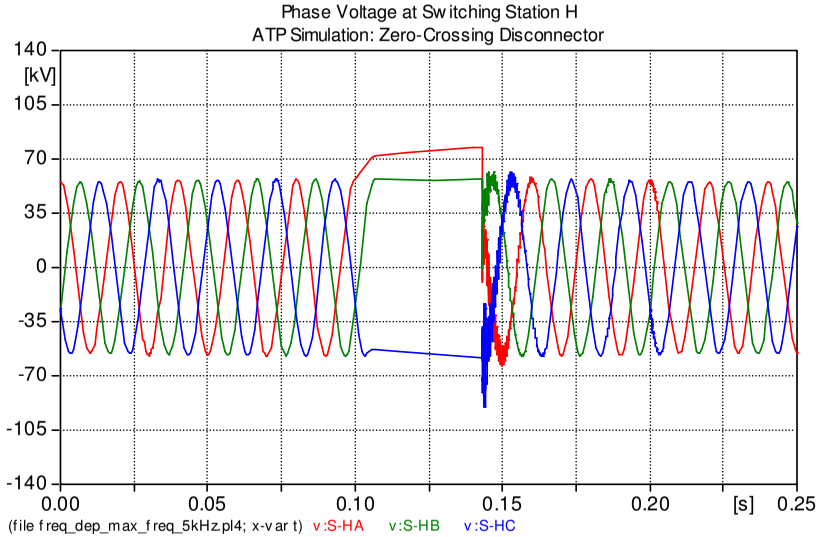


Figure 7.43 ATP: Zero-crossing disconnector model – Phase voltage at Switching Station *H*

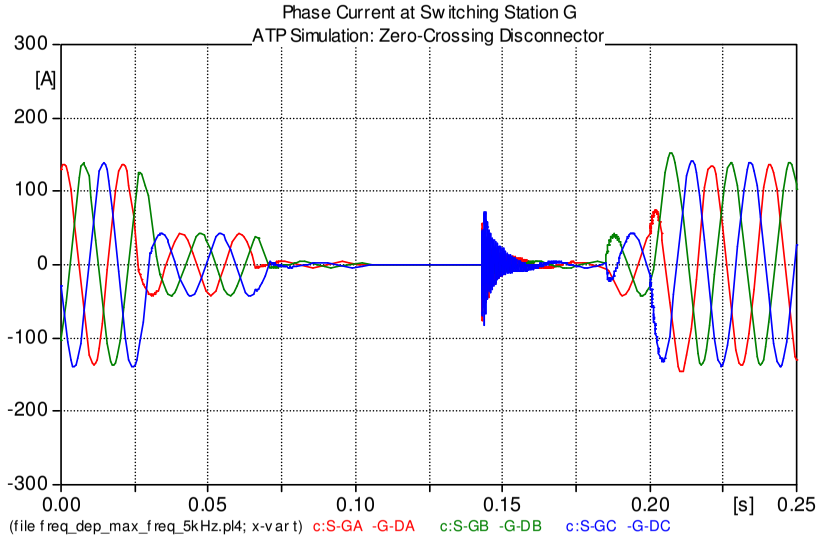


Figure 7.44 ATP: Zero-crossing disconnector model – Phase current at Switching Station *G*

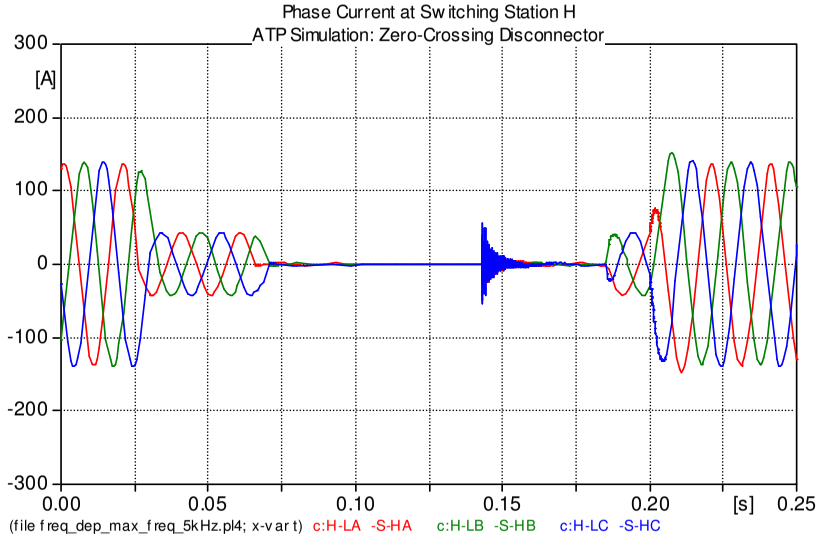


Figure 7.45 ATP: Zero-crossing disconnector model – Phase current at Switching Station *H*

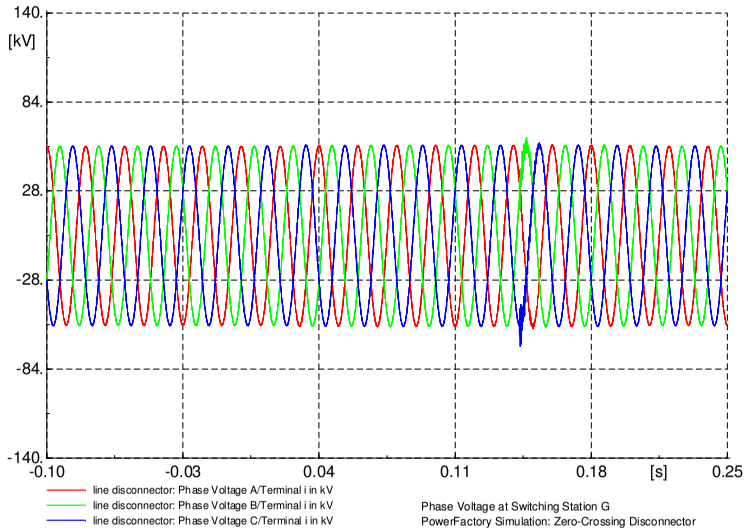


Figure 7.46 PF: Zero-crossing disconnector model – Phase voltage at Switching Station *G*

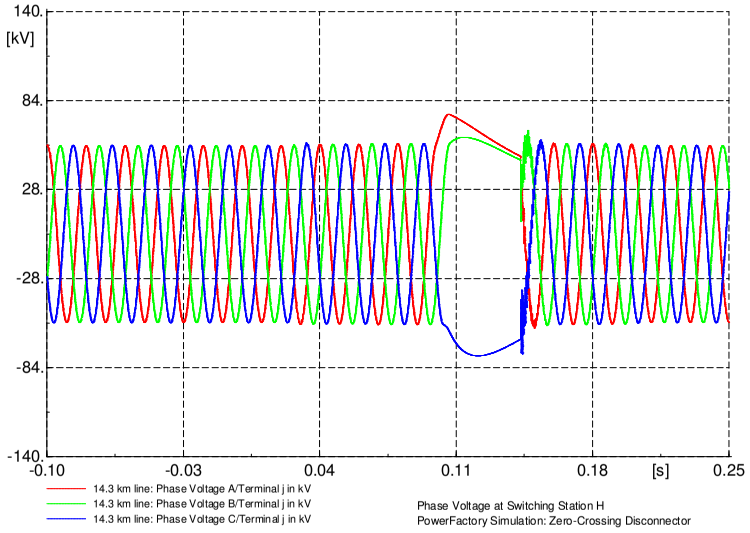


Figure 7.47 PF: Zero-crossing disconnector model – Phase voltage at Switching Station *H*

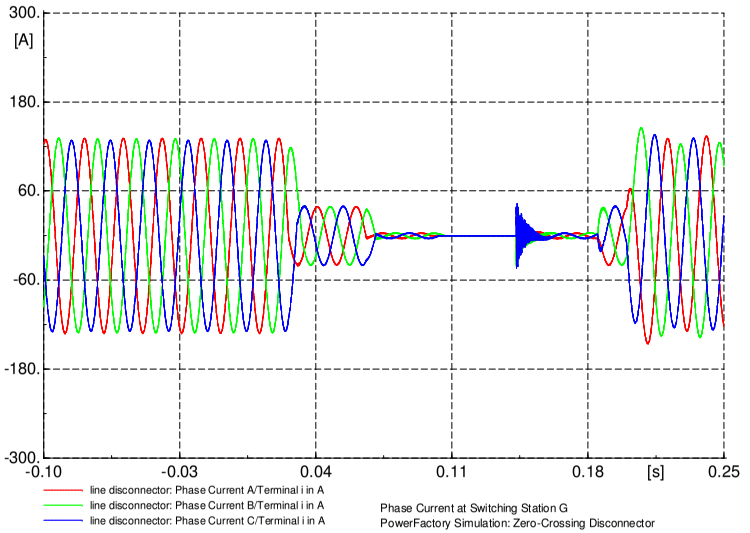


Figure 7.48 PF: Zero-crossing disconnector model – Phase current at Switching Station *G*

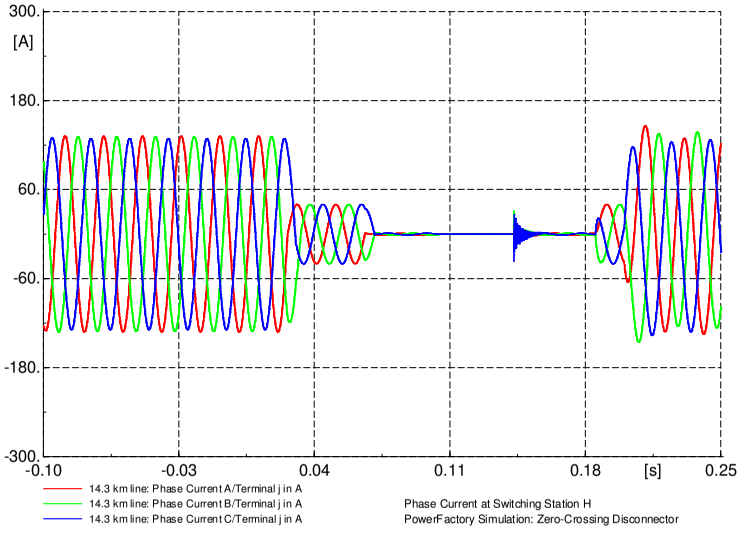


Figure 7.49 PF: Zero-crossing disconnector model – Phase current at Switching Station *H*

The most significant reduction in overvoltages occurs at switching station *H*. In the previous simulations run with the disconnector being switched when the current was interrupted immediately, the overvoltages at switching station *H* were in excess of 2.0p.u. After the zero-crossing simulations for the disconnector, the overvoltages reduced by 31.5% to 1.68p.u. using PowerFactory and by 66.4% to 1.40p.u. using ATP.

The practicality of having disconnectors interrupt current at the natural zero of the current cycle is highly unlikely for a manually operated disconnector, although it is possible for a motor-operated disconnector to achieve this as it can be controlled using discrete signal processing (DSP) means.

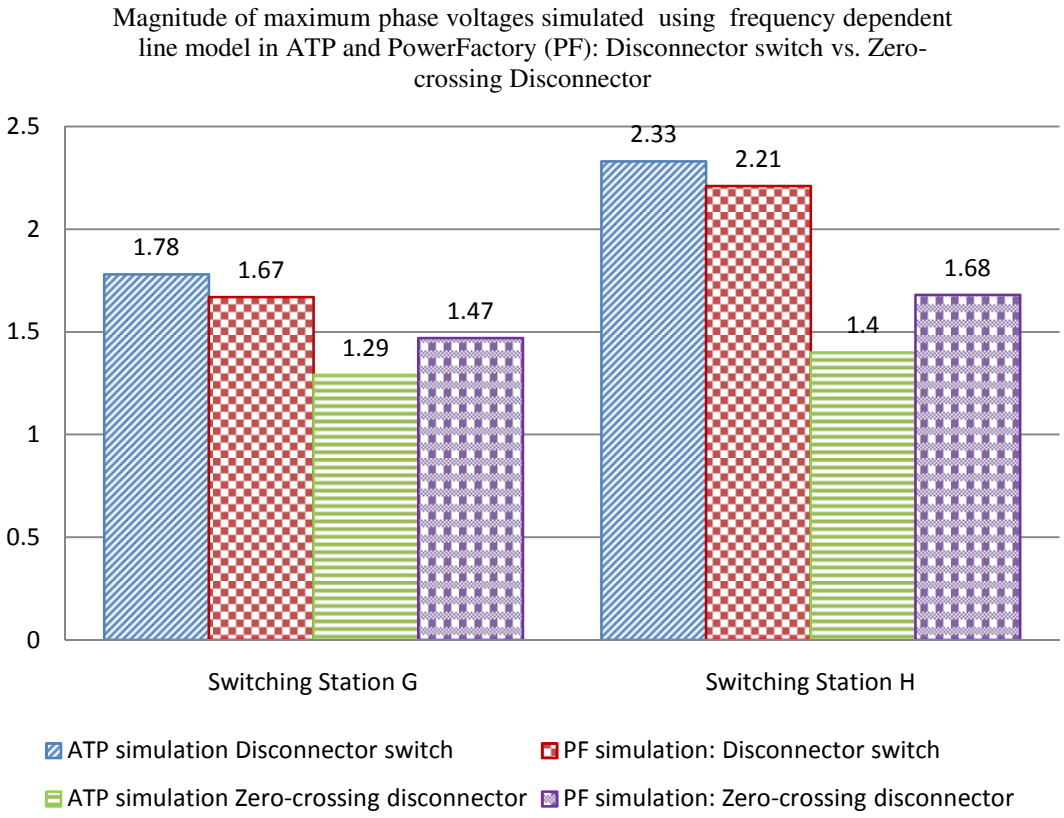


Figure 7.50 Bar Chart comparing the simulation results produced in ATP and PowerFactory (PF) for disconnector zero crossing

### 7.5.2 Increase of Source-Side Capacitance

As mentioned before, the second mitigation technique was tested by introducing a source-side capacitor ($C_S$) connected in parallel at switching station *G* in the power system model. The power system model was simulated using a source-side capacitor with a power rating of 500kVAr or $C_S = 0.365\mu F$ at 66kV. Figure 7.59 shows a bar graph that compares the per unit values of the magnitudes of the maximum phase voltages for the source-side capacitor simulations run in ATP and PowerFactory with the per unit values of the corresponding simulations without a source-side capacitor. The phase voltages are taken at switching station *G* and *H*. The graph also shows the results of the previous frequency dependent line model simulation where the disconnector was operated immediately alongside the source-side capacitor simulation results. In addition to the graph, Figure 7.51 – Figure 7.54 are the simulation results of the phase voltage results from the ATP simulation. Figure 7.55 – Figure 7.58 show the simulation results from the PowerFactory simulation.

From the chart, there is a slight reduction in the magnitudes of the phase voltages when the source-side capacitance is introduced at switching station *G*. This reduction in phase voltages, however, is not as evident as the reduction observed when the disconnector is changed to interrupt current at the zero crossing. In ATP, the transient overvoltage at switching station *G* is reduced from 1.78p.u. to 1.74p.u. In PowerFactory, the transient overvoltage is reduced from 1.67p.u. to 1.61p.u.

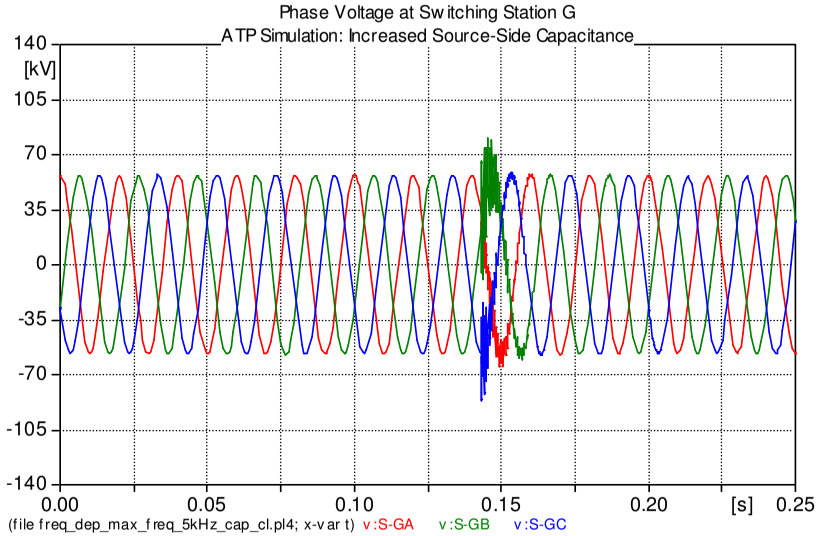


Figure 7.51 ATP Simulation with increased $C_s$: Phase Voltage at Switching Station *G*

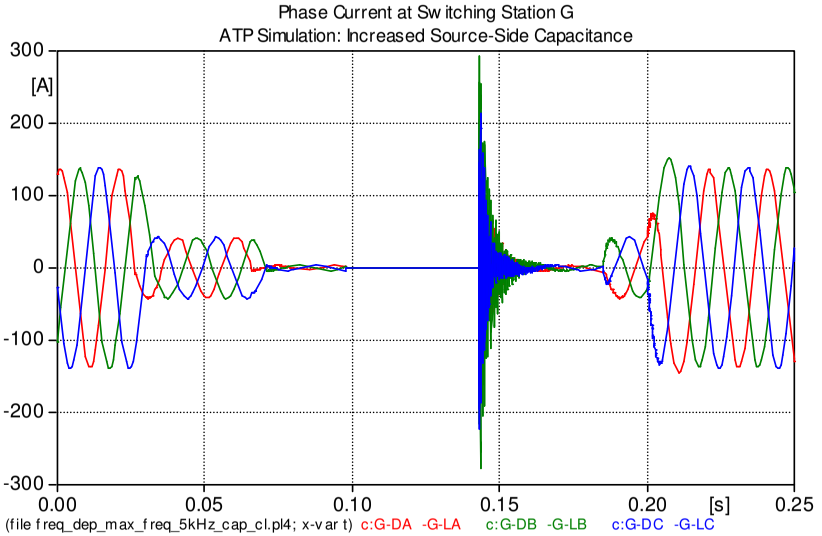


Figure 7.53 ATP Simulation with increased $C_s$: Phase Current at Switching Station *G*

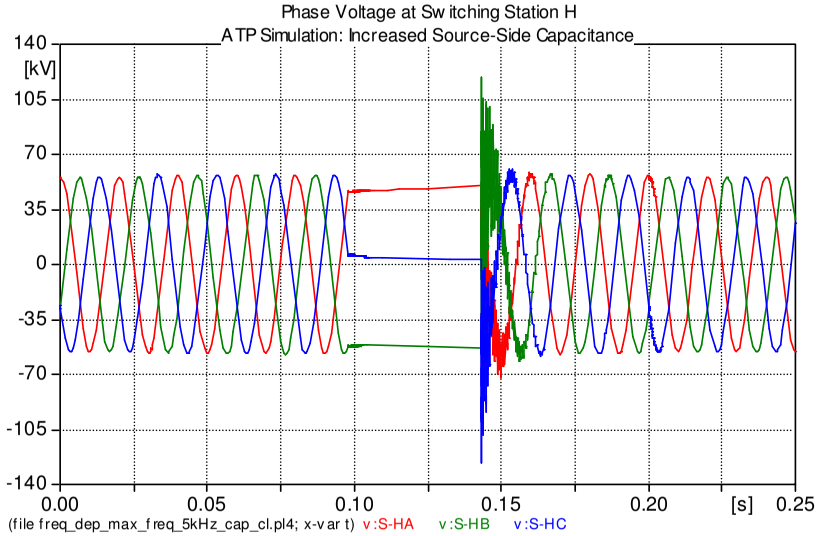


Figure 7.52 ATP Simulation with increased $C_s$: Phase Voltage at Switching Station *H*

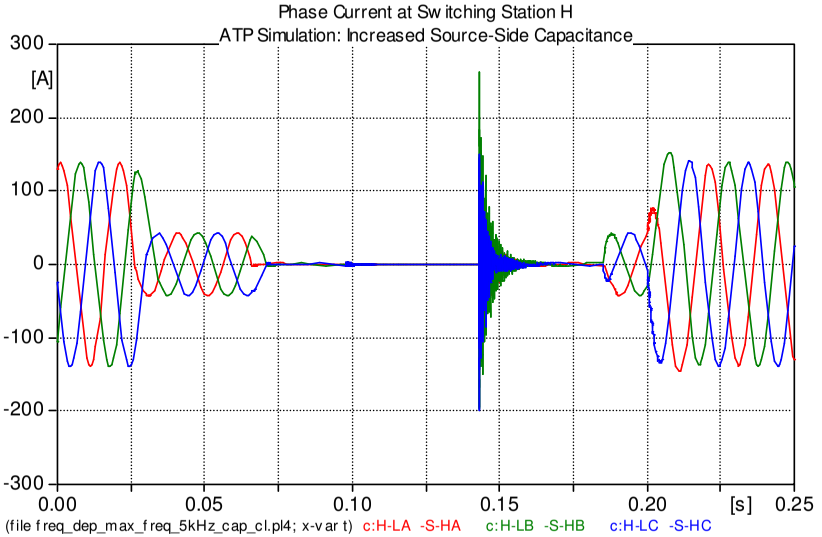


Figure 7.54 ATP Simulation with increased $C_s$: Phase Current at Switching Station *H*

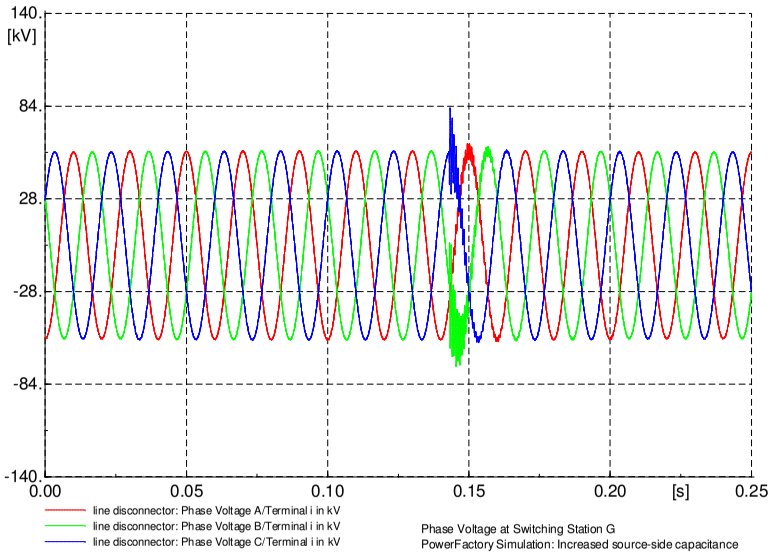


Figure 7.55 PF Simulation with increased $C_s$: Phase Voltage at Switching Station *G*

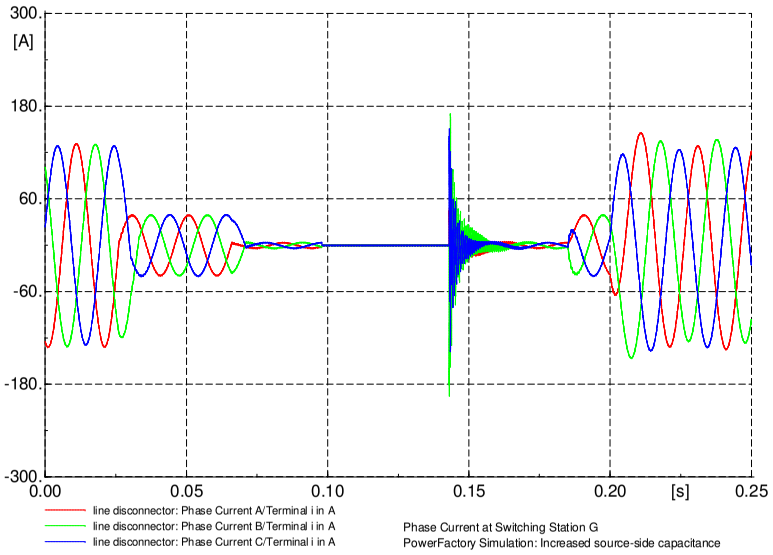


Figure 7.57 PF Simulation with increased $C_s$: Phase Current at Switching Station *G*

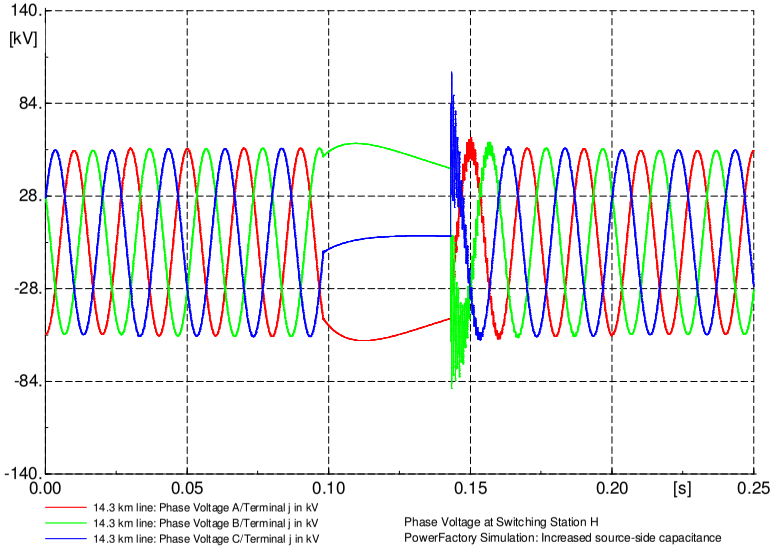


Figure 7.56 PF Simulation with increased $C_s$: Phase Voltage at Switching Station *H*

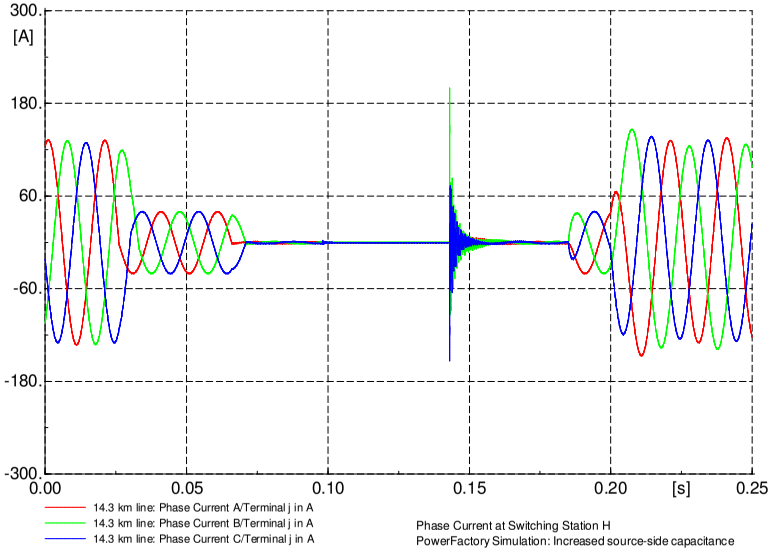


Figure 7.58 PF Simulation with increased $C_s$: Phase Current at Switching Station *H*

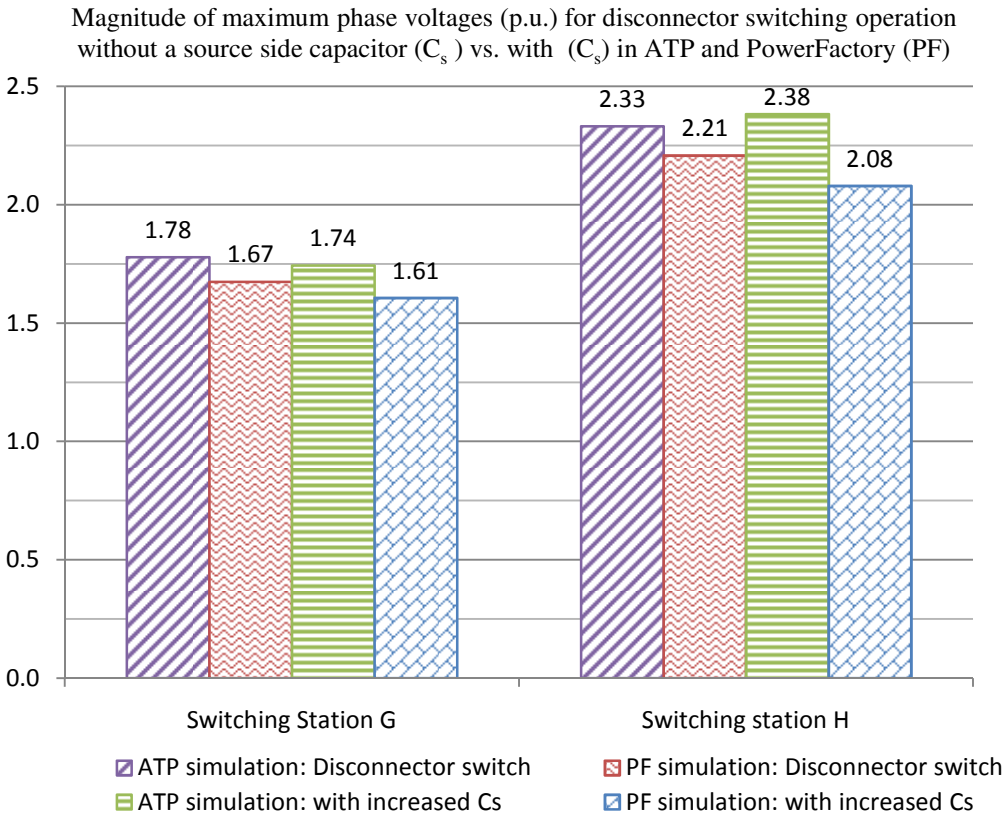


Figure 7.59 Bar chart comparing the simulation results produced in ATP and PowerFactory (PF) for increasing ($C_S$) at switching station

At switching station *H*, however, the reduction of the magnitude of the phase voltage is only apparent in the PowerFactory simulation and not the ATP simulation. However, the continued overvoltages experienced at switching station *H* can be attributed to how the introduction of the capacitor at switching station *G* was simulated. The capacitor that is simulated at switching station *G*, is simulated to remain connected to the network even after the disconnector switching operation. As a result, when the transmission line is unloaded, the phase voltages at switching station *H* (receiving end of the unloaded line) has higher phase voltages. Thus any transients experienced are superimposed on a higher power frequency phase voltage.

The ideal situation would be to only introduce the capacitor at switching station *G* during the disconnector switching operation. Another method of increasing the supply side capacitor would be to increase the bus-bar lengths or line length on the source side of the switching operation. However, the practicalities of this technique (having a supply side capacitor) would need further research if it is to be properly implemented.

Other tests, not shown here, indicate that if the size of the capacitor inserted at the switching station *G* is increased, the transient overvoltages at switching station *G* are decreased even further. The limitation, however, with increasing the size of the capacitor is the practicality of such an installation on a power system network. For instance, availability of space on an existing network, physical dimensions of the capacitor could limit the size of capacitor that can be installed on the network in question.

## 7.6 Summary

In this chapter, the findings of the disconnector switching simulations run in both ATP and PowerFactory simulation tools were presented. The simulations were run to test disconnector switching of unloaded transmission lines.

The first simulations run in both simulation tools were done in order to compare the results of simulations where different transmission line models were used to model the power system network. Lumped transmission line models as well as distributed parameter models were simulated. The lumped models proved to be onerous. Yet for the type of simulation where the zero-sequence voltages and currents were low, there was no significant difference in the results presented by the different distributed parameter models. Nonetheless, supported with the literature discussed, the frequency dependent model was preferred.

Preference between the simulation tools ATP/EMTP and DigSILENT PowerFactory from the results presented in this study are inconclusive without field or laboratory tests.

The next simulations assessed in the study were to investigate the effectiveness of mitigation techniques identified in the literature. Switching a disconnector at the current's natural zero reduced the transient overvoltages experienced at switching station *G* and *H*. The introduction of a source-side capacitor during the switching operation also reduced the transient overvoltages at switching station *G* and *H*. However, the reduction of overvoltages relies on the size of the capacitor installed, when $C_S$ is increased, the overvoltages are further reduced.

# Chapter 8 Conclusions and Recommendations

Disconnectors have been identified as being able to interrupt negligible currents such as capacitive currents associated with unloaded transmission lines. The objectives of this study were to model capacitive current switching using a disconnector; additionally, to simulate the developed model using two software tools to predict the capability of the disconnector to switch capacitive currents. The software tools were ATP, a widely used transient software program and PowerFactory, a relatively new power systems software tool. The model that was used in the study was based on an existing network that forms part of the South African sub-transmission network. The conclusions drawn from this thesis are presented below.

## 8.1 Conclusions

Switching operations with disconnectors involve switching transients and overvoltages. Therefore, the model chosen for simulation in both software packages needed to be modelled for transient solutions, in particular the transmission line model. There are different manners in which transmission line have been modelled in the two software packages. The simulation results presented in this thesis show that distributed parameter line models produced more meaningful results for switching studies than lumped parameter line models. This is in agreement with what was reported in the literature. Seeing as a frequency dependent line model

is easily set up in both software packages, it was the preferred method for modelling of the transmission lines.

For this study, a switching operation was deemed unlikely to succeed if overvoltages observed at the point of the switching were greater than 2.0p.u. Using the simulated model both ATP and PowerFactory produced overvoltages that were less than 2.0p.u at the point of switching (switching station *G* in the simulated network). Thus, based on the criteria for success stated above, the switching operation simulated in this study was deemed likely to succeed. However, overvoltages greater than 2.0p.u. were observed at the receiving of the line (switching station *H* in the simulated network). Higher overvoltages at the end of the line could prove to be problematic for equipment at this point.

In both simulation tools, re-energising the line or "switching on" operation produced higher overvoltages than de-energising of the transmission line or "switching off" operation. This is in contrast to findings made by Knobloch [23], where it is stated that higher values of overvoltages are measured during a "switching off" or de-energising operation.

Furthermore, the current interrupted by the disconnector in the ATP simulation is 2.56A, while it is 2.73A in PowerFactory. This equates to a 6% difference in the interrupted current and based on the literature, this level of current is acceptable provided that it is understood and accepted by the user that the disconnector may be close to fully open position at current interruption.

It should be mentioned that the success of the simulated switching operations in ATP and PowerFactory are not conclusive unless accompanied with field tests. Based on the theory, the higher overvoltages at switching station *H* than at switching station *G* as well as the higher overvoltages experienced during re-energisation were not unexpected. A combination of reflected travelling waves as well as trapped charge on the line contributed to the higher stresses experienced at switching station *H*. However, due to the operating practice of earthing of equipment after de-energising, the likelihood of trapped charge existing on the de-energised line is diminished, and as a result the possibility of higher overvoltages in reality at switching station *H* than at switching station *G* is doubtful. The field tests would be necessary to verify the results achieved in both software packages. These tests would also provide confirmation as to whether

or not a de-energising operation produces higher overvoltages than an energising switching operation. It is expected that de-energising ("switching off") operation will produce higher overvoltage values, in accordance with literature.

Two mitigation techniques were also investigated in this thesis. One of the techniques was for the disconnector to interrupt the capacitive current at the zero-crossing of the sinusoidally waveform across all phases instead of "chopping" the current in one instant. The other technique recommended increasing the source-side capacitance ($C_S$) of the disconnector being switched. The capacitor was introduced to the network in order to reduce the switching overvoltages experienced at the point where the switching operation takes place.

The technique of increasing the source-side capacitance ($C_S$) did reduce the overvoltages. However, the reduction in overvoltages was not as significant as the reduction seen when the current is interrupted at the zero-crossing. Using ATP, the results from the zero-crossing current method showed a 27.5% reduction in overvoltages at the point of switching, while the introduction of source-side capacitance ($C_S$) yielded a reduction of 2.25%. On the other hand, using PowerFactory resulted in a 11.9% reduction in overvoltages at the point of switching for the zero-crossing current method, whereas a reduction of 3.59% was only seen when the other technique was used. The reduction in overvoltages at the end of line, at switching station *H*, were even greater using the zero-crossing technique. ATP showed a 66% reduction in overvoltages while PowerFactory showed a 31.5% reduction in overvoltages at the end of the line. In comparison, increasing the source-side capacitance ($C_S$) resulted in an increase of 2.14% in overvoltages using ATP and a decrease of 5.88% in overvoltages using PowerFactory at the end of the line (switching station *H*). Owing to the significant reduction in overvoltages, the zero-crossing current technique is the recommended method.

## 8.2 Recommendations and Future work

Based on the findings and conclusions of this study, some recommendations can be made:

- Although the results presented in this study give an indication of what could be expected, field tests are required for verification. It is recommended that similar networks where capacitive current interruption is performed using disconnectors are

also simulated in ATP and PowerFactory and then tested in the field for verification. Furthermore, the field tests should include the mitigating techniques.

- There is scope to investigate and extend the simulations and modelling techniques used to test the switching of magnetising currents and loop current switching using disconnector.

- Additionally, more research is required to investigate how to simulate the arc that is drawn by a disconnector during a switching operation. The investigation needs to be conducted in such a way that the behaviour and duration of the arc drawn can be monitored along with the overvoltages and switching transients produced. If the arc that is drawn can be modelled correctly, then the next step would be to relate the arcing times with the simulation results. The purpose of shaping this relation could then assist even further in determining the success of a switching operation.

# References


[1] IEC 60050-441:1984, "Amendment 1 - International Electrotechnical Vocabulary. Switchgear, Controlgear and fuses - Second Edition," 2000-07.

[2] IEC 62271-1:2007, "High Voltage Switchgear and Controlgear. Part 1: Common specifications," 2007.

[3] IEEE C37.36b-1990, "IEEE Guide to Current Interruption with Horn-Gap Air Switches," 1990.

[4] D. F. Peelo, "Current interruption using high voltage air-break disconnectors," PhD Thesis, Eindhoven University of Technology, 2004.

[5] "IEEE Guide to Current Interruption with Horn-Gap Air Switches," IEEE C37.36b-1990, 1990.

[6] "IEEE Standards for High Voltage Switches," IEEE C37.30-1997, 1997.

[7] "High-voltage switchgear and controlgear - Part 102: Alternating current disconnectors and earthing switches," IEC Standard 62271-102, 2001-12.

[8] F. E. Andrews, L. R. Janes, and M. A. Andersson, "Interrupting Ability of Horn-Gap Switches," *AIEE Transactions*, vol. 69, pp. 1016-1027, 1950.

[9] D. F. Peelo, et al., "Current Interruption with High Voltage Air-Break Disconnectors," in *CIGRE Paper No. A3-301*, Paris, 2004.

[10] IEEE Committee Report, "Results of survey on interrupting Ability of Air Break Switches," *IEEE Transactions on Power Apparatus and Systems*, vol. PAS-85, no. No. 9, pp. 1008-1019, Sep. 1966.

[11] D. F. Peelo, "Current Interrupting Capability of Air-Break Disconnect Switches," *IEEE Transactions on Power Delivery*, vol. PWRD-1, no. 1, pp. 212-216, Jan. 1986.

[12] A. Greenwood, *Electrical Transients in Power Systems*, 2nd ed. New York: John Wiley & Sons, Inc., 1991.

[13] Eskom Distribution Materials Price Database. (2009, Oct.)

[14] D. de Beer, "Operating Regulations for High Voltage Systems," Eskom Working Instruction ESKAPVAEY6 Rev 0, 2005.

[15] M. Kizilcay. (2008, Aug.) Alternative Transients Program. [Online]. www.emtp.org

[16] DigSILENT GmbH. (2008) [Online]. http://digsilent.de/Software/PowerFactory_Features/

[17] L. van der Sluis, *Transients in Power Systems*. Chichester: John Wiley & Sons Ltd., 2001.

[18] J. A. Martinez, B. Gustavsen, and D. Durbak, "Parameter Determination for Modeling System Transients - Part I: Overhead Lines," *IEEE Transactions on Power Delivery*, vol. 20, no. 3, pp. 2038-2044, Jul. 2005.

[19] S. G. Patel, W. F. Holcombe Jr., and D. E. Parr, "Application of Air-Break Switches for De-Energizing Transmissions Lines," *IEEE Transactions on Power Delivery*, vol. 4, no. 1, pp. 368-374, Jan. 1989.

[20] A. Foti and J. M. Lakas, "EHV Switch Tests and Switching Surges," *IEEE Transactions on Power Apparatus and Systems*, vol. 83, no. 3, pp. 266-271, Mar. 1964.

[21] E. C. Rankin, "Experience with methods of extending the capability of High-Voltage Air Break Switches," *AIEE Transactions*, vol. 79, pp. 1634-1637, Feb. 1960.

[22] CIGRE Working Group 13.05, "The Calculation of Switching Surges. III. Transmission line representation for energization adn re-energization studies with complex feeding networks.," *Electra*, no. 62, pp. 45-78, 1979.

[23] H. Knobloch, "Switching of Capacitive Currents by Outdoor Disconnectors," in *Fifth International Symposium on High Voltage Engineering*, Braunschweig, Aug. 1987.

[24] CIGRE Working Group 33.02, "Guidelines for Representation Network Elements when Calculating Transients," CIGRE Brochure 39, 1990.

[25] S. Carsimamovic, Z. Bajramovic, M. Ljevak, M. Veledar, and N. Halilhodzic, "Current Switching with High Voltage Air Disconnector," in *International Conference on Power System Transients (IPST 05-229)*, Montreal, Canada, 2005.

[26] S. Sadovic, M. Heleta, M. Abadzic, and S. Djulic, "Computer and Experimental Investigations of Switching Overvoltages on HV transmission lines," in *CIGRE Paper No. 33-06*, Paris, 1984.

[27] A. I. Ibrahim and H. W. Dommel, "A Knowledge Base for Switching Surge Transients," in *International Conference on Power Systems Transients (IPST 05-050)*, Montreal, Canada, 2005.

[28] IEEE Task Force on Fast Front Transients, "Modeling Guidelines for Fast Transients," *IEEE Transactions on Power Delivery*, vol. 11, no. 1, pp. 493-506, Jan. 1996.

[29] CIGRE Working Group 13.04, "Capacitive Current Switching - State of the Art," *Electra*, no. No.155, pp. 33-63, 1994.

[30] J. C. Das, *Power System Analysis: Short-circuit load flow and harmonics*, 1st ed. CRC Press, 2002.

[31] S. Ramo, J. R. Whinnery, and T. van Duzer, *Fields and Waves in Communication Electronics*, 3rd ed. New York: John Wiley & Sons, Inc., 1993.

[32] J. D. Glover, M. S. Sarma, and T. J. Overbye, *Power Systems. Analysis and Design*, 4th ed. Australia: Thomson, 2007.

[33] H. W. Dommel, *Electromagnetic Transients Program Manual (EMTP Theory Book)*. Portland, Oregon: Bonneville Power Administration, 1986.

[34] C. M. Wiggins and S. E. Wright, "Switching Transient Fields in Substations," *IEEE Transactions on Power Delivery*, vol. 6, no. 2, pp. 591-599, Apr. 1991.

[35] CIGRE Working Group 13.05, "The Calculation of Switching Surges. II. Network Representation for Energization and Re-Energization Studies on Lines Fed by an Inductive Source," *Electra*, no. 32, pp. 17-42, 1974.

[36] *Alternative Transient Program Rule Book*. Leuven EMTP Centre, 1987.

[37] A. I. Ibrahim, S. Henschel, A. C. Lima, and H. W. Dommel, "Application of a New EMTP Line Model for Short Overhead Lines and Cables," *International Journal of Electrical Power & Energy Systems*, vol. 24, no. 8, pp. 639-645, Oct. 2002.

[38] J. R. Marti, "Accurate Modeling of Frequency-dependent Transmission Lines in Electromagnetic Transients Simulations," *IEEE Transactions on Power Apparatus and Systems*, vol. PAS-101, no. 1, pp. 147-155, Jan. 1982.

[39] D. F. Peelo, R. P. P. Smeets, S. Kuivenhoven, and J. G. Krone, "Capacitive Current Interruption in Atmospheric Air," in *CIGRE SC A3 & B3 Joint Colloquium Paper No. 106*, Tokyo, 2005.

[40] H. K. Hoidalen, *New features in ATPDraw ver. 4.0 for Advanced Simulation of Electromagnetic Transients in Power Systems*. 2004.

[41] DigSILENT, "DigSILENT Technical Documentation: Overhead Line Models," TechRef LineModels V1, 2007.

# Papers

Three papers were submitted to conferences over the duration of this thesis.

- The paper entitled "*Load Disconnect Switches as affected by Switching Currents*" was presented at the South African Universities Power Engineers Conference in January 2005 (SAUPEC '05).

- The paper entitled "*Evaluation of Switching Capacitive Currents by Disconnect Switches Using DIgSILENT Software Tool*" was presented at the Australiasian Universities Power Engineering Conference in September 2005 (AUPEC '05).

- The paper entitled "*Comparison of No-Load Transmission Line Switching Using ATP/EMTP and DIgSILENT PowerFactory Simulation Tools*" was presented at the South African Universities Power Engineers Conference in January 2009 (SAUPEC '09).

Copies of the above mentioned papers are included in this section.

# LOAD DISCONNECT SWITCHES AS AFFECTED BY SWITCHING CURRENTS


## S. Arigye-Mushabe, K.A. Folly

*University of Cape Town*



**Abstract:** This paper discusses the various problems encountered during switching operations, with specific emphasis placed on the switching of capacitive currents as gathered from the relevant literature as well as the interruption of small inductive currents. It brings into focus induced transients associated with switching operations by considering the results of previous research studies that were performed on switching transients as well as mitigation techniques employed. The paper seeks to find evidence as to whether or not disconnect switches can be successfully used in current interruption of HV networks and to make recommendations or proposals for future research work.



**Keywords:** disconnect switch, current interruption, switching transients, capacitive currents, inductive currents.


### 1 INTRODUCTION

A disconnect switch is an air break switch, opened in air. It is a mechanical switching device which provides an insulating distance in the open position. It is not fitted with arcing horns. It is able to open and close a circuit if either a negligible current is switched or if no significant change occurs in the voltage between the terminals of its poles. Disconnect switches are motorised or hand operated devices. They have three separate switches, one per phase, but are mechanically linked to a single hand crank or a motor. They play a very important role in a substation, which is to isolate equipment. They are also found separating transformers or capacitor banks from the bus-bars for instance. Disconnect switches are not designed to break large currents. For that reason, before operating the switch, a substation must first be disconnected from its secondary or load side before the primary or high voltage side can be disconnected using the disconnect switch [1].

This paper analyses the various aspects involved in current interruption, the types of currents that would be switched, thereafter the problems often associated with switching – the induction of current transients into the network, as well as briefly mentioning some the mitigation techniques that have been employed in the past. Finally, the paper proposes some possible areas of research.

### 2 CURRENT INTERRUPTION FOR AC NETWORKS

When a switch is opened, the circuit will try to 'oppose' the operation, and current will continue to flow as the insulating medium (in the case of disconnect switches – air) breaks down and an arc is drawn so as to 'recover' the voltages. This voltage is known as the transient recovery voltage (TRV) [2]. The arc that is drawn is finally interrupted; a high-frequency oscillation is superimposed on the power frequency and appears across the contacts. There are two components to the recovery voltage: the high-frequency damped oscillation and the power frequency recovery voltage [2,3]. This high frequency component is given by the equation:

$$f_n = \frac{1}{2\pi\sqrt{LC}} \quad (1)$$

where L and C are the equivalent inductance and capacitance of the circuit [2].

In ac circuits, the current crosses the zero point twice in a period. If a current interrupting operation occurs at this time, current will be interrupted.

However, in a opening operation, the insulation gap ("break gap") of the switch is increased as the contacts move away from each other, and should the insulation gap not be wide enough, a current re-strike will occur because the dielectric strength of the break-gap is not strong enough to withstand the voltage stresses across the contacts. Moreover, if the natural frequency is high, the voltage across the switch contacts rises

very quickly. And should the rate of rise of the recovery voltage (RRRV) exceed the rate at which the dielectric strength of the air builds up, the switch will not be able to hold off the voltage and a 'reignition' will occur [4]. Another definition given for a reignition and a restrike is: A dielectric breakdown of the arc channel within a period of ¼ cycle of the initial arc extinction, the phenomena are called reignitions and if the breakdown occurs after the ¼ cycle, the phenomena are called restrikes [2].

If an adequate electrical strength could be obtained across the contacts after the current zero, and by so doing, eliminate the development of restrikes.

The configuration of the network as seen from the terminals of the switch as well as the elements in the network will determine the amplitude, frequency and shape of the current and voltage oscillations, especially elements like transformers or capacitor banks which introduce inrush currents into the network [4].

Consider switching a basic LC circuit, as shown in Fig 1; for simplicity, we analyse the case in which a DC source energises the network by closing an ideal switch [4].

Assuming at t=0 the switch is open, after closing the switch, an oscillation occurs due to the fact that energy is exchanged between the capacitor (electric energy) and the inductor (magnetic energy) with a certain frequency, $\omega_0$, defined by the circuit.

Using Kirchoff's voltage law,

$$E = L\frac{di}{dt} + \frac{1}{C}\int i dt \qquad (2)$$

where, E is the DC source, L is the inductance of the circuit and C is the capacitance.

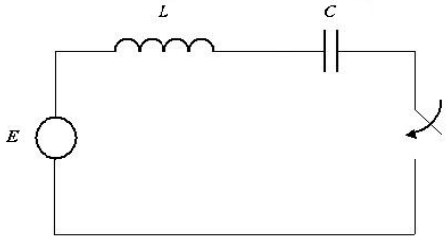


**Fig 1 A DC source switched on an LC series network**

Using Laplace transforms to solve, where *s* is the complex Laplace variable:

$$\frac{E}{s} = sLi(s) - Li(0) + \frac{i(s)}{sC} + \frac{V_C(0)}{s} \qquad (3)$$

Solving for *i*, we have

$$i(s)\left(s^2 + \frac{1}{LC}\right) = \frac{E - V_C(0)}{L} + si(0) \qquad (4)$$

The initial conditions, in this case $i(0) = 0$, the current in the network is zero before the switch closes. And because of the physical law of conservation of the flux., $i(0) = 0$ immediately after closing switch.

The capacitor however, may have initial voltage because of trapped charge on the capacitor. But for this case, we assume $V_C(0) = 0$ thus, no initial charge.

$$i(s) = E\sqrt{\frac{C}{L}}\frac{\omega_0}{s^2 + \omega_0^2} \qquad (5)$$

$$i(t) = E\sqrt{\frac{C}{L}}\sin(\omega_0 t) \qquad (6)$$

where, $\omega_0^2 = 1/LC$; from this, the natural frequency of the circuit at which the current starts to flow after closing the switch is [4], $\omega_0 = \frac{1}{\sqrt{LC}}$.

As can be seen from Eq. 6, the transient current $i(t)$ depends on the initial conditions in the circuit and the circuit parameters.

## 3 INTERRUPTING SMALL INDUCTIVE CURRENTS

Small inductive currents occur when unloaded transformers are taken in and out of service, motors are disconnected or electric furnaces are switched. From Fig 2, the inductivity L of the load is dominant, which means that the load current lags the voltage. When the small inductive current is interrupted, the load capacitance C is charged at

$$u_C = L\frac{di}{dt}, \qquad (7)$$

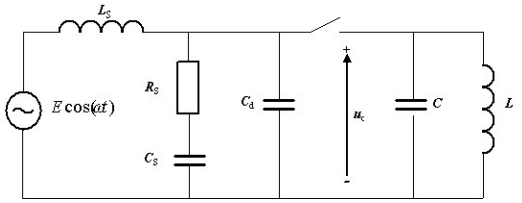


**Fig 2 Single-phase lumped element representation of a circuit for small inductive currents**

which is a value close to the supply voltage.

After current interruption, C discharges itself through L by means of an oscillating current with frequency

$$f_1 = \frac{1}{2\pi\sqrt{LC}}. \qquad (8)$$

This could cause a steep increase in the TRV at the load, if re-ignition occurs, the inductive load is connected with the supply again and the capacitance of the load is charged by a current with frequency

$$f_s = \frac{1}{2\pi\sqrt{L_s C}}. \qquad (9)$$

The capacitance C is charged to a higher value because the rise of the re-ignition current will be much higher than the power frequency current, which was interrupted earlier. But the capacitance will discharge itself again through the inductivity L. Depending on how far the arcing contacts have moved, the process will be repeated until the gap between the arcing contacts can withstand the dielectric breakdown of the contact gap [4].

## 3 CAPACITIVE SWITCHING

Unlike inductive switching, capacitive switching requires special attention because, after current interruption, the capacitive load contains an electrical charge that can cause a dielectric re-ignition of the switching device. When this process repeats, the interruption of capacitive currents causes high over-voltages.

These capacitive current are small though; a few Amperes to several hundreds of Amperes, compared with the rated short-circuit current for which a circuit breaker is designed.

At the instant of current interruption, the capacitor is fully charged and the voltage is approximately equal to the peak voltage of the supply. After half a cycle, the supply voltage has reversed its polarity and the voltage across the breaker terminals is twice the peak value of the supply voltage [4].

If one assumes the worst, when switching a capacitive current in a back-to-back situation (as shown in Fig 3), a re-ignition occurs when the initial voltage on the capacitor to be energised has a polarity opposite to that from the capacitor already connected to the same bus. The discharge current then flows from one capacitor to the other via the stray inductance (caused by the loop of the bus-bars and the connecting wires). This causes very high inrush currents, much higher than in the case of single capacitor bank switching [4].

Switching unloaded high-voltage transmission lines in and out of service is, in principle, the same as switching a capacitor bank because an unloaded transmission line has a dominantly capacitive behaviour. The Ferranti effect is more pronounced the longer the line is and the higher the applied voltage is. It causes a rise in voltage from the sending end towards the remote end. The voltage rise at the sending end is caused by the flow of the leading current drawn by the open line through the inductances of the system on the source side of the switching device [5,6].

Should a transmission line be energised after the closing of a switching device, the resulting voltage wave reflects and causes doubling of the voltage at the open end of the line. The Ferranti rise causes a transient voltage jump that results in a voltage wave travelling along the line. This could result in a steep voltage jump across the contacts of the interrupting device and can cause a re-ignition and prolong the arcing time [4,5].

When switching unloaded high-voltage cables within a substation (e.g. Busbar), only the capacitive load current is interrupted. This current is small in comparison with the current

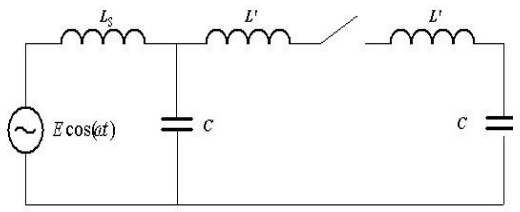


**Fig 3 Single-line representation of a back-to-back situation**

involved when switching capacitor banks, but large compared with the capacitive current when switching unloaded high-voltage overhead transmission lines.

When analysing the three-phase switching of unloaded high-voltage transmission lines, phase-to-phase and phase-to-ground capacitive coupling has to be considered.

According to Van der Sluis [4], the voltage transient is a source-side phenomenon, as there is no change in voltage at the load side. This is illustrated in Fig 4. The trapped charge at the load side terminals, causes a constant voltage, but when the supply voltage has the opposite polarity, then nearly twice the peak value of the supply voltage is present across the switch contacts. When the re-ignition occurs, the capacitance discharges itself via the re-ignited arc channel and the inductances $L_s$ and L'. The result is an oscillating current with the following frequency and peak value:

$$f = \frac{1}{2\pi\sqrt{L_s C}}, \qquad (10)$$

$$I = \frac{2E_s}{\sqrt{\frac{L_s}{C}}}; \qquad (11)$$

From Eqs. 10 and 11, it can be seen that the smaller the value of $L_s$, the higher the frequency and larger the amplitude of the transient current [4].

## 5 SWITCHING TRANSIENTS

A transient is described as a short-lived oscillation in a system caused by a sudden change of voltage or current or load, this most frequently occurs when a switching operation takes place.

High frequency currents like those associated with switching transients cause problems for sensitive equipment. They produce severe mechanical stresses and they induce undesirable transients in neighbouring circuits. Particularly susceptible to these transients, are low power relays and control circuits which are designed to minimize service interruption and to limit damage to equipment when failures occur [3,4].

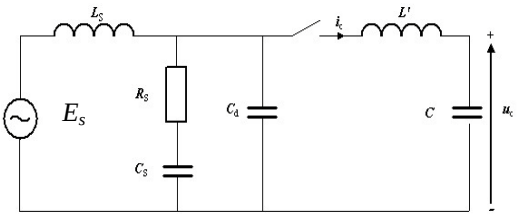


**Fig 4 Single-line representation of capacitive current**

where,

- $L_s$ represents the inductance of the supply and the synchronous inductance of the supplying generator as well as the leakage inductance of the power transformers.
- $R_s$ and $C_s$ together represent the damping and the capacitance of the voltage transformers, current transformers and bus-bars.
- C the lumped capacitor, represents the capacitive load.
- L' is the stray inductance present on line.
- $E_s$ is the magnitude of the power supply voltage.

The arcs drawn on opening a switch create current transients waves. These travel away from the switch in both directions. The current transients travelling on the bus excite electric and magnetic field transients in regions near the bus. However, all three phases of the switch do not operate coincidentally. Thus, the phase containing the switch which operated first will launch the initial current transient on the phase of the bus. The radiated electric and magnetic fields from the initial current transient can then couple energy to the nearby phases, inducing current transients on them [2].

According to Wiggins et al [1], the transients produced by the four types of basic switching operations of opening and closing circuit breakers and disconnect switches had significant similarities and differences.

Breakers operate much faster than the hand-operated disconnect switches, so transients are produced over only a few cycles (at 60Hz). The peak amplitude of the transients produced from the disconnect switches operations may be up to 10 times larger than those produced by circuit breaker close operations and up to 50 times larger than those produced by circuit breaker open operations. However, transient produced by circuit breaker operations contain frequency

components up to 10 times higher than those observed in disconnect transients [3].

In a study performed by Pretorius [6], the electric and magnetic field characteristics associated with high voltage and bus current transients that occur during normal operation of switchgear in substations were analysed. The results that were found in the study agreed with what the other authors had experienced:

- Radiated transients resulting from the switching activities in substation with peak levels of several tens of kV/m and A/m and frequency spectrum up to 100MHz have been reported for disconnect and breaker operations.
- Transient in air insulated substations (AIS) and gas insulated substations (GIS) differ due to difference in dimension and geometry, surge impedance, frequency dependent damping and breakdown characteristics of switching gap.
- The low frequency transients of AIS correspond with those of GIS disconnectors.

The study described a model used by Wiggins and Nilsson, from conference proceeding, CIGRE Session 36-202 in Aug/Sept1994, entitled: Comparison of Interference from Switching, Lightning and Fault Events in High Voltage Substations.

The model used a number of interrelated EMTP-type travelling wave models. These included very high frequency transient models for calculating: substation bus currents and voltages, electric and magnetic fields radiated from the bus and certain ground conductors, conducted and radiated coupling to current transformer and capacitively coupled voltage transformer circuits and other cable types of a number of different load impedances. Switching transients were calculated for disconnect operations assuming 2p.u. initial conditions across the switch gaps, nominally the worst case [6].

The agreement between the modelled and measured disconnect switching transient waveforms is well documented in the study.

## 6 MITIGATING FACTORS THAT HAVE BEEN RESEARCHED IN THIS AREA.

Different methods have been employed to try and lessen the effects of capacitor-bank switching transients. These include the use of circuit switchers with pre-insertion impedances; (either an inductor or resistor in series). This reduces the initial collapse in the bus voltage (referred to as the fast front) through voltage support by current flow through the impedances.

## 7 CONCLUSION

Unwanted results occur when switching small capacitive currents or small inductive currents; high overvoltages. The main difference between the two switching cases is that the capacitance C at the load side, in the case of small inductive current switching, does not remain charged but discharges itself through the load L.

As mentioned before, this paper sought to find evidence as to whether or not disconnect switches could be successfully used in the current interruption of HV networks. However, nothing conclusive could be found from the literature stating exactly what currents could be switched by disconnect switches. Moreover, severe transients are found to be associated with the switching operations of disconnect switches. Further research will be undertaken to comparatively determine the degree of improvement of the transient response made when different mitigation techniques are employed during switching operations of capacitive currents by disconnect switches.

## 8 REFERENCES

[1] C.M. Wiggins, F.S. Nickel, A.J. Haney, S.E. Wright, “Measurement of switching transients in a 115kV substation,” *IEEE Transaction on Power Delivery*, Vol. 4, No.1, January 1989.

[2] Das, J.C., “Power system analysis”, Marcel Dekker, New York, 2002.

[3] Allan Greenwood, “Electrical transients in Power Systems”, John Wiley, New York, 1991.

[4] Van der Sluis, L, “Transients in power systems”. Chichester; New York: Wiley, c2001.

[5] C.E. Sölver, S. de A. Morais, “Line-Charging Current Interruption by HV and EHV Circuit Breakers: Standard and Non-Standard Test Requirements as Determined by the Stresses Applied and by Breaker-Capability Considerations.” http://www.ipst.org/TechPapers/2001/IPST01Paper117.pdf

[6] Pretorius, P.H., “Radiated Fast Transients resulting from switching activities in substations: Detailed Literature Study”, *ESKOM –Technical Research Report*. Report No: TRR/E/94/EL073. 1994

# Evaluation of Switching Capacitive Currents by Disconnect Switches Using DIgSILENT Software Tool

Sharon Arigye-Mushabe
Department of Electrical Engineering
University of Cape Town
Cape Town, Western Province, South Africa
arigyes@powerelec.ee.uct.ac.za

Komla A. Folly
Department of Electrical Engineering
University of Cape Town
Cape Town, Western Province, South Africa
kfolly@ebe.uct.ac.za

## ABSTRACT

*This paper discusses the switching of capacitor currents by disconnect switches. It presents a brief background to the theory behind the switching of capacitive currents. It seeks to demonstrate the type of effect this switching operation has on a system by simulating a simple model using the DIgSILENT software tool. It also attempts to verify if the results from the DIgSILENT simulations are comparable to the results obtained by other researchers.*

## INTRODUCTION

Switching operations in substations or on transmission lines have always caused problems with the transient currents and overvoltages they generate. Even more so now, as utilities and industries tend towards automation and use of electronically controlled equipment, the problems are aggravated. Increasing numbers of capacitor banks are being located on 3-phase buses at almost all voltage levels to improve the power factor or in the case of transmission systems, to support voltage and improve the power handling capability of transmission lines [1, 2].

Switching of capacitive currents is a normal duty for many medium and high voltage circuit breakers and switches. As load conditions vary, these capacitive currents are switched quite frequently. Typical cases are the disconnecting of capacitor banks and the dropping of unloaded overhead lines or cables [1, 2].

If the switching operation is unsuccessful, that is, if the switch used for this purpose should restrike or reignite in the course of the operation, severe transient overvoltages may occur. These switching transients produce hazardous mechanical stresses and induce undesirable transients in neighbouring circuits [2]. During capacitive switching, the electrical stress experienced by the switching device is normally relatively close to the rated values of the device [2, 3, 4].

Disconnect switches are primarily intended for isolation of equipment, bus sections, lines from buses, etc. They are not specifically designed to interrupt current, but are expected to be capable of interrupting the low currents associated with normal no-load switching operations. This is limited, however, by the space available for the arc produced to get extinguished [5].

In this paper, a simple model is used to simulate switching operations using DIgSILENT. The model is adapted from a model used by Baptista *et al* [6]. The objective of the paper [6] was to study the effect that the switching of a capacitor bank in a 60kV substation had on a Portuguese electrical system, in particular the effects experienced by the generating units in the network.

This paper, however, attempts to verify if the results from the DIgSILENT simulations are comparable to the results obtained in paper [6], also it includes in the simulations with DIgSILENT, the effect de-energising a transmission line with a disconnect switch has on the network

This paper is structured as follows: section 2 gives a background on the interrupting currents with disconnect switches. Section 3 analyses the effect of the switching of a capacitive current on a system, by simulating a simple model using DIgSILENT. Section 4 presents the model that was adapted from the paper by Baptista *et al* [6]. Later on in section 4, the results obtained from the switching simulations are shown and discussed. Further, switching transient mitigating techniques are suggested as methods to limit the transients to within acceptable parameters. Finally, the conclusions are presented in section 5.

## INTERRUPTING CURRENTS WITH DISCONNECT SWITCHES

A fair amount of research has been performed concerning the current interrupting capability of disconnect switches [5, 7, 8]. This was done by determining the maximum line charging current that could safely be interrupted. In his paper, Peelo [5] presents the maximum lengths of line and busbar for various system voltages that can be switched by disconnect switches. Some of them are: 61km of line for a 15kV, 20km for 27.5KV or 3.6km for 72.5kV system voltage. Andrews *et al* [7] found that for a 132kV line charging current, a switch fitted with a horn-gap could interrupt about 7A of charging current. In [8], Foti demonstrated that on a 1.9mile section of line, charging currents of 2.4A at 400kV and 3.0A at 505kV could be interrupted by disconnect switches.

It should be mentioned that in all these studies, the disconnect switches had to be fitted with a range of fixtures to ensure their effectiveness and/or to reduce wear on the fixed contacts. For example, the use of arcing horns, high-speed whip type interrupting devices [5], fixed resistors or non-linear resistors [8].

Different methods have been employed to try and lessen the effects of capacitor-bank switching transients. These include the use of circuit switchers with pre-insertion impedances; (either an inductor or resistor in series), whose objective is to control inrush currents. [8, 9]

### CAPACITIVE CURRENT SWITCHING

To analyse capacitive current switching, let us consider a single-phase lumped element representation of a capacitive circuit, as shown in Figure 1.

In Figure 1, $V$ is the magnitude of the supply voltage, $C$ is the lumped capacitor that represents the capacitive load, $L_s$, $R_s$ and $C_s$ represent the impedances at the supply side of the switch ($S$) and $L$ is the stray inductance through which C is charged. It should be noted that $L_s \gg L$ [3].

Switch $S$ is opened and the current through $L$ and $C$ is interrupted. After current interruption, the capacitor $C$ is fully charged to maximum voltage because of the relative phase of current and voltage (current leads the voltage by approximately 90°). The capacitance, now isolated from the source, retains its charge. As the supply voltage reverses polarity, at half a cycle after the interruption, the voltage across the switch ($S$) terminals reaches twice the peak value of the supply voltage, as can be seen in Figure 2.

The 2 pu voltage that develops across the switch is potentially dangerous as there is an increased likelihood of the switch re-igniting. When the re-ignition occurs, the capacitance $C$ discharges itself via the re-ignited arc channel and the inductances $L_s$ and $L$. This re-ignition current is given by Equation 1 [2]:

$$i(t) = \frac{2V}{\sqrt{\frac{L_s}{C}}} \sin \omega_0 t\,, \qquad (1)$$

and it oscillates at a frequency, $f_0$:

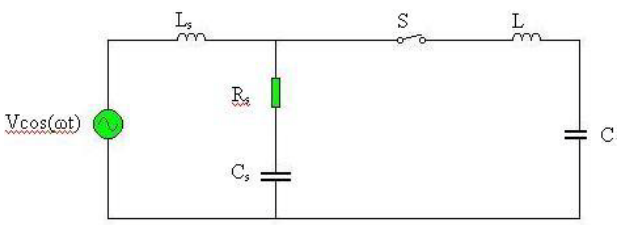


$$f_0 = \frac{1}{2\pi\sqrt{L_s C}}\,. \qquad (2)$$

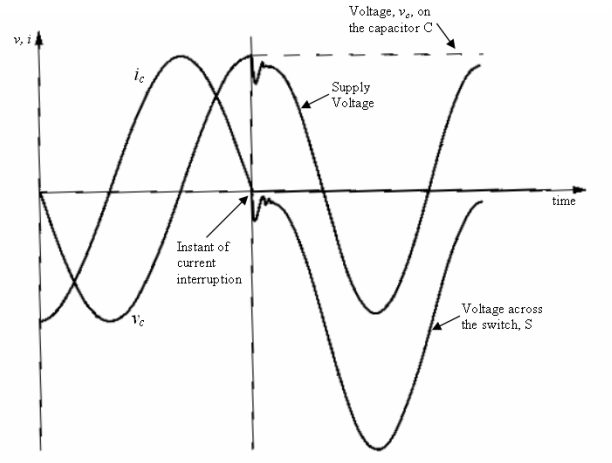


Figure 1: Single-Phase lumped element representation of a capacitive circuit.

Figure 2: Current and voltage traces during the interruption of a capacitive current. [3]

As previously mentioned, a single-phase representation was used to analyse the interruption of a capacitive current. For a three phase circuit, if the neutral of the three-phase capacitor banks and the source neutral are solidly interconnected, then the analysis used for a single-phase circuit would apply to the individual phases of the three-phase circuit without modification [2].

## CASE STUDY

The model investigated in this study is adapted from a previous paper by Baptista et al [6]. The model was chosen for its simplicity and it gives one the opportunity to test various aspects concerning capacitive switching, namely: the switching of capacitor banks, back-to-back switching, de-energising of transmission lines and monitoring the effect this type of switching has on the generators and the transformers shown in the model.

Because not all information required was made available to reproduce the network accurately, the parameters used to model the network in DIgSILENT differed from those provided in the paper [6]. .

A single line diagram of the model used is shown in Figure 3. The network consists of two 60kV substations: Valdigem and Telheira and a switching substation, Soutelo; 3 generators G1, G2 and G3; 20MVar capacitor bank at Valdigem and two 8MVar capacitor banks at Telheira. The network frequency is 50Hz.

The analysis tool used to simulate the model network is DIgSILENT PowerFactory Version 13.1.255.

### NETWORK ELEMENTS AND SIMULATION

### GENERATORS

The generators used in the simulation were salient pole rotor types and rated voltage of 6kV. Table 1 shows the data of the three generators

### TRANSFORMERS

All the transformers were 20MVA, 60kV/6kV transformers, with a phase orientation of YNyn0.

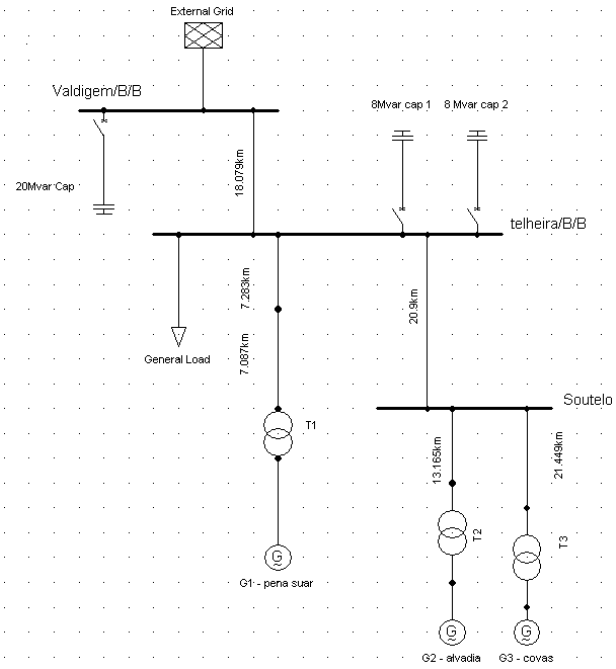


Figure 3: Network Model [6].

Table 1: Generator characteristics

| Generator: | G1 | G2 | G3 |
|---|---|---|---|
| Power: | 9MVA | 10MVA | 8MVA |
| Voltage set pt.: | 0.98 pu | 1.01 pu | 1.03 pu |
| pf (cos $\theta$ ) | 0.9 | 0.9 | 0.9 |

## CAPACITORS

The capacitor bank details are given in Table 2:

Table 2: Capacitor bank details

| *Substation* | *Power* | *Voltage* | *Connection* |
|---|---|---|---|
| Telheira | 2 x 8 MVar | 60kV | Star (YN) |
| Valdigem | 20 MVar | 60kV | Star (YN) |

## TRANSMISSION LINES

Transmission lines were modelled as lumped (pi) parameters. They are all single circuit overhead lines, with the exceptions of the 18.079km line between Valdigem and Telheira substation and the first 7.283km of line from Telheira substation to G1. These lines are double-circuit lines.

## LOAD

There is only one load in the system. This load is connected to the Telheira substation; with a rated power of 40MW and a power factor of 0.8 lagging.

## NETWORK EQUIVALENT

The model shown in Figure 3 forms part of a bigger network. This remaining network will therefore have some influence in the way the model responds to various operations. This external network, as shown in Fig. 3, is modelled using the port element available in DIgSILENT and is modelled as a slack bus with voltage set point of 1.0pu and an angle of 0.

## RESULTS

The study was conducted by analysing the switching of the capacitor banks for different topologies of the system and to inspect the overvoltage effects de-energising and energising of an unloaded transmission line has on the system.

## SWITCHING THE CAPACITOR BANKS

In the simulations, the capacitors are all initially switched out. During the simulation, the 8MVar capacitor bank at Telheira substation is switched in at the instant 20ms, and at 80ms, the 20MVar capacitor bank at Valdigem is switched. The different system topologies used in the DIgSILENT simulations are tabulated in Table 3. For instance, the switching operation (Sw. op 3) in Table 3 explains that before the capacitors are switched as an initial condition, the generator G2 and G3 are removed from or switched out of the system while G1 is generating: the G2 and G3 breakers are 'open', while G1 is closed.

Table 3: Simulated topologies of the system studied when cap banks were switched: 2X8MVar at 20ms and 20MVar at 80ms

| | Switch situation | | |
|---|---|---|---|
| Sw. op | G1 | G2 | G3 |
| 1 | open | closed | open |
| 2 | open | open | closed |
| 3 | closed | open | open |
| 4 | open | closed | closed |
| 5 | closed | open | closed |
| 6 | closed | closed | open |
| 7 | closed | closed | closed |

The results of the simulations on the 7 topologies shown in Table 3 are displayed in Table 4. The switches were simulated to open immediately and all phases were opened at the same time. Table 4 also compares these results of DigSilent (Dig.Sim columns) with those obtained from the paper [6].

From Table 4, one notes that the results obtained from the DIgSILENT simulations differ noticeably from those

documented in paper [6]. This can mainly be attributed to the fact that the parameters, especially the transmission line parameters, used to model the network in DIgSILENT differs from those in the paper [6].

Table 4: Table comparing the results obtained from Baptista paper [6] (Bap.) and results from DIgSILENT 13.1 simulations (Dig.Sim)

| Sw. op | Maximum overvoltages (p.u.) | | | | | |
|---|---|---|---|---|---|---|
| | Alvadia (G2) | | Covas (G3) | | Pena suar (G1) | |
| | Bap. | Dig.Sim | Bap. | Dig.Sim | Bap. | Dig.Sim |
| 1 | 2.0 | 2.01 | - | 2.25 | - | 1.52 |
| 2 | - | 1.94 | 1.78 | 1.88 | - | 1.52 |
| 3 | - | 2.19 | - | 2.03 | 2.12 | 1.47 |
| 4 | 1.67 | 1.79 | 1.58 | 1.83 | - | 1.43 |
| 5 | - | 1.95 | 1.62 | 1.93 | 1.89 | 1.61 |
| 6 | 1.73 | 1.88 | - | 2.11 | 1.95 | 1.49 |
| 7 | 1.59 | 1.70 | 1.53 | 1.86 | 1.91 | 1.64 |

In their paper Baptista *et al*, state that the worst transients experienced during the switching operations were experienced at generator G1 during switching operation three, where only generator G1 was in use. In contrast, from Table 4, the worst transients on average occurred at generator G3 (1.98 pu) and generator G2 (1.93 pu) during the simulations performed using DIgSILENT. Figures 4 and 5 show the phase voltages experienced at the generators during some of the simulations. Figure 4 shows the phase voltages at generator G1 during switching operation 3 (Sw. op3) as per Table 3. The highest peak overvoltage is 1.47pu. Figure 5 displays the phase voltages at generator 2, after the switching operation 7 (Sw. op 7) is performed, here the peak overvoltage is 1.70pu.

## SWITCHING AN UNLOADED TRANSMISSION LINE

An unloaded transmission line behaves the same as a capacitor. During the switching operation 3, the 20.9km line between Telheira substation and Soutelo was generating approximately 0.63MVar of reactive power, and carrying a capacitive current of 6.22A at 60kV. This is likened to what Andrews *et al* [7], had determined to be an interruptible charging current of 7A, however this current was at a system voltage of 132kV.

After switching operation 3 was performed, simulation to drop the 6.22A on the 20.9km line was performed in DIgSILENT. A disconnect switch at Telheira substation was switched open at 50ms to drop the line and at 80ms the switch was closed. The resultant voltage waveforms due to the line dropping at G2 are shown in Figure 6. No overvoltages are measured during the de-energising operation, but a maximum transient voltage of over 2pu is registered when the line is re-energised.

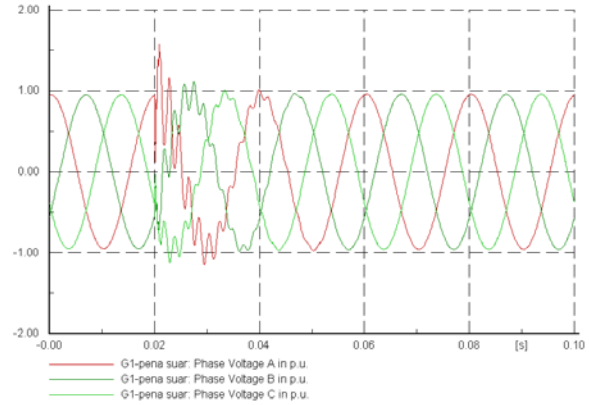


Attempts were made to simulate some of the mitigation techniques discussed earlier in the paper; but, using the

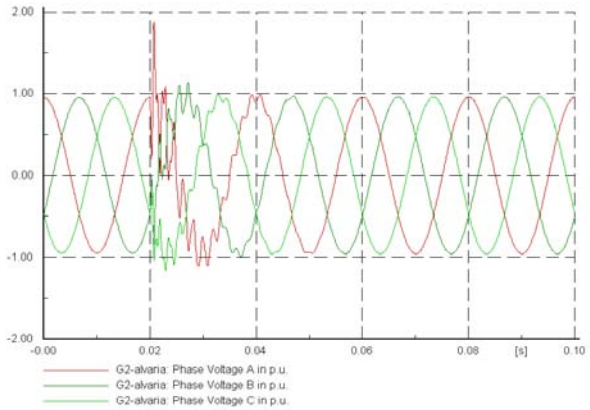


DIgSILENT software tool made it difficult to model these methods. What is expected are significantly

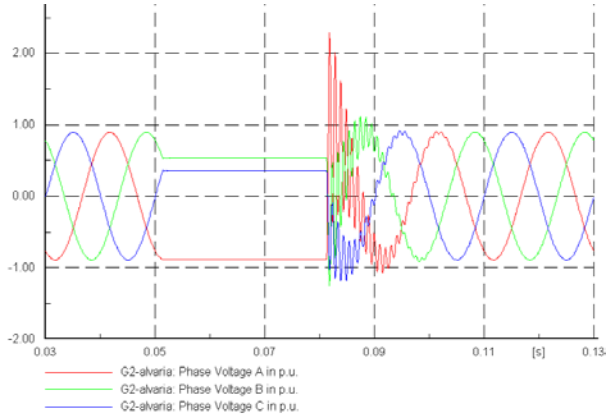


reduced transients when using these methods, as documented in various studies cited before [1,5,7,8].

Figure 4: Phase Voltages at generator G1, after switching operation 3 (Sw.op 3) is simulated.

Figure 5: Phase voltages at generator G2, after switching operation 7 (Sw.op 7) is simulated.

Figure 6: Phase Voltages at generator G2 during line dropping simulation at 50ms and energisation of the same line at 80ms.

Unfortunately, verification of the effectiveness of these methods using DIgSILENT was unattainable.

## CONCLUSIONS

The results shown in this paper indicate that disconnect switches can be used to switch small capacitive currents however, transients induced into the network can be extreme.

When a line dropping simulation was performed, see Figure 6, no transient overvoltages were experienced, but when the line was energised, overvoltages in excess of 2pu were recorded.

The future direction of this study is to simulate all the switching operations mentioned in this paper, using the same network model and element parameters, but with another power analysis software tool and compare those results to the results displayed in this paper. Furthermore, to ensure mitigation techniques can be modelled simply and adequately with this tool.

## APPENDIX

Line characteristics used: 60kV, rated current – 500A.

R=0.0529Ω/km; X=0.529Ω/km; $R_0$=0.1587Ω/km; $X_0$=1.587Ω/km; B=3.3081μS/km; $B_0$=0.1007μS/km;

Table 5: Synchronous machine constants used to model the generator in Figure 3

| | |
|---|---|
| $X_d$ | 1.8 |
| $X_q$ | 1.9 |
| $X'_d$ | 0.3 |
| $X'_q$ | 0.55 |
| $X''_d$ | 0.25 |
| $X''_q$ | 0.25 |
| $X_2$ | 0.2 |
| $X_0$ | 0.1 |
| R(ac) | 0.0025 |
| R2 | 0 |
| $T'_d$ | 8s |
| $T''_d=T''_q$ | 0.03 |
| H (inertia) | 6.5s |

## REFERENCES


[1] CIGRE WG 13.04, "Capacitive Current Switching-state of the art," Electra, vol.155, Part 5-6, pp 32-63, August 1994.

[2] A. Greenwood, *Electrical Transients in Power System*. 2nd Ed. Wiley & Sons, New York, 1991.

[3] L. van der Sluis, *Transients in Power Systems.* Wiley & Sons, Chichester, 2002.

[4] R. P. O'Leary and R. H. Harner, "Evaluation of Methods for Controlling the Overvoltages produced by the Energization of Shunt Capacitor Bank," International Conference on Large High Voltage Electric Systems (CIGRE), Paris, 28 August – 3 September 1988. Available online: [http://www.sandc.com/edocs_pdfs/edoc_024669.pdf]

[5] D. F. Peelo, "Current Interrupting Capability of Air Break Disconnect Switches," IEEE Transactions on Power Delivery, vol. PWRD-1, no. 1, pp 212-216, January 1986.

[6] J. M. R. Baptista, M. R. Cordeiro and A. Machado e Moura, "Overvoltages due to Capacitors Bank Switching in a 60kV System," International Conference on Power Systems Transients. (IPST '01). Rio de Janeiro, Brazil, June 24-28, 2001. Available Online: [http://www.ipst.org/TechPapers/2001/IPST01Paper038.pdf]

[7] F. E. Andrews, L. R. Janes and M. A. Andersson, "Interrupting Ability of Horn-Gap Switches," AIEE Transactions, vol.69, pp 1016-1027, 1950.

[8] A. Foti ad J. M. Lakas, "EHV Switch Tests and Switching Surges," IEEE Transactions on Power Apparatus and Systems, vol. PAS-83, no. 4, pp 266-271, 1964.

[9] S. Arigye-Mushabe and K. A. Folly, "Load Disconnect Switches as affected by switching currents," Proceedings of the South African University Power Engineers Conference (SAUPEC '05), University of the Witwatersrand, Johannesburg, 27-28 January 2005.

[10] DIgSILENT PowerFactory Version 13.1.255

# COMPARISON OF NO-LOAD TRANSMISSION LINE SWITCHING USING ATP/EMTP AND DIGSILENT POWERFACTORY SIMULATION TOOLS

**S Arigye-Mushabe, K.A. Folly**

*University of Cape Town, Dept. of Electrical Engineering, Cape Town, South Africa*

**Abstract.** This paper discusses simulation results of disconnector switching operations for the interruption of capacitive currents, typically associated with unloaded overhead transmission lines. The first part of the paper compares results obtained when using different transmission line models to simulate de-energizing and re-energizing of unloaded transmission lines. The second part of the paper compares the results using two different simulation tools: ATP/EMTP and DigSILENT PowerFactory. The network used for the simulations is modelled from an existing sub-transmission network in the Western Region of South Africa. The findings of the paper show that a constant parameter transmission line model and a frequency dependent transmission line model can be used to simulate the de-energising and re-energising of an unloaded transmission line. DigSILENT PowerFactory simulation results show higher currents and overvoltages than ATP/EMTP simulations do for the same model. Field tests are recommended to verify the results obtained from both simulations.

**Keywords.** Disconnectors, "no-load" transmission lines, Switching transients, ATP/EMTP, DigSILENT PowerFactory

## 1. INTRODUCTION

Disconnectors are known by various names across the world. In North America, they are known as disconnecting switches or disconnect switches [1]. In South Africa, they are interchangeably referred to as disconnectors, disconnect switches or isolators or colloquially as "links".

The primary function of disconnectors is to electrically isolate equipment from the power system for maintenance or repair. The IEC standard on high voltage switchgear defines a disconnector as a "mechanical switching device which provides, in the open position, an isolating distance in accordance with specific requirements" [2]. The standard further notes that a disconnector is capable of opening and closing a circuit when either negligible current is broken or made or when no significant change in the voltage across the terminals of each of the poles of the disconnector occurs [2]. Negligible currents include the capacitive charging currents of bushing, bus bars, connectors, very short lengths of cables and the current of voltage instrument transformers. Furthermore, disconnectors in some applications are used for load transfer from one bus system to another [3].

The current interrupting capability of disconnectors has been a subject of research from as early as 1950 [4][5][6] [7]. In these papers, the results were based on empirical studies that were performed on disconnectors in air insulated substations. The disconnectors were required to interrupt unloaded transformer magnetizing current, line charging currents and loop currents.

The ability of a disconnector to make or break current depends on the characteristic values of the circuit being operated on, the operation speed of the disconnector, the dielectric characteristic of the switch and current ratings of the disconnector [3]. A study was concluded in 2004 that was based on utility practices by BC Hydro in Canda and laboratory tests at Eindhoven University of Technology and KEMA in the Netherlands[8] [9][10]. It shows that the magnitudes of the overvoltages caused by interrupting a capacitive current with a disconnector were dependent on the current magnitude, source and load side capacitances, partial arc collapses and disconnector type. These findings were in agreement with the results of an earlier study [11] that found that "flashover lengths are influenced by the level of the supply-side capacitance" when switching capacitive currents with disconnectors. Higher values of overvoltages were measured when a supply-side capacitance was not part of the test than when one was included [11].

This paper presents results from a study that was initiated to explore the extent to which the limited current interrupting capability of a disconnector could be utilised during switching operations. The study focuses on the interruption of capacitive currents as associated with no-load overhead transmission lines. This study also compares simulation results of disconnector switching operations using different transmission line modelling techniques in the Alternative Transients Program (ATP/EMTP). Comparisons are also made between the results from ATP/EMTP and DigSILENT PowerFactory.

ATP is a royalty free version of the Electromagnetic Transients Program (EMTP). It is widely used for digital simulations of transient phenomena of electromagnetic as well as electromechanical nature [12].

PowerFactory is a power simulation software tool developed by DigSILENT GmbH. This software is capable of performing load flow studies in radial and meshed networks (balanced and unbalanced), short

circuit analysis and electromagnetic transient simulation studies, to name but a few [13].

Eskom Distribution, the power utility in South Africa, acquired a corporate licence for PowerFactory. The tool is used mainly for steady state simulations and rarely for transient studies. Literature on PowerFactory is limited and this makes understanding and manipulating simulation models more difficult in PowerFactory than in ATP. One of the aims of this paper is to model and simulate switching operations using electromagnetic transient simulations in PowerFactory and to determine how the results from these simulations compare to the results obtained when using ATP.

The following conditions of the disconnectors were assumed for this study: the disconnectors are air-insulated, they have enough phase to phase spacing to prevent flashovers with adjacent phases and they are not fitted with any auxiliary interrupting devices.

The structure of the paper will be as follows: section 2 will briefly discuss switching overvoltages; section 3 will focus on capacitive current switching, after which section 4 reviews transmission line modelling. In section 5, the network that is studied is introduced and the different transmission line models used in the simulations on ATP are discussed. Thereafter, the results from the ATP simulations are compared to PowerFactory simulation results. Finally, in section 6, some conclusions are drawn.

## 2. SWITCHING OVERVOLTAGES

When a switch is opened, an arc is drawn. As a result, current transient waves or travelling waves are generated on the lines, cables or bus-bar sections that are linked by the switch [14]. A transient can be described as a short-lived oscillation in a system caused by a sudden change of voltage or current or load. The primary cause of such a disturbance in a system is the closing or opening of a breaker or other switching equipment, short circuit, earth fault or a lightning strike.

When an arc is interrupted, a high-frequency oscillation is superimposed on the power frequency and appears across the contacts of the switch. The high frequency component is called the transient recovery voltage (TRV) [15].

The frequencies of the travelling waves due to transient phenomena in power systems range from DC to about 50MHz [16]. The CIGRE Brochure 39 [16], a guideline for representation of network elements due to transients, classifies the frequency range for switching overvoltages and line reclosing between 50/60Hz to 20kHz. The brochure also classifies disconnector switching (single restrike) and faults in GIS in the frequency range of 100kHz to 50MHz [16].

Field tests were conducted and documented by Wiggins and Wright, where electric and magnetic fields of switching transients were characterized according to type voltage level as well as type of switch [17]. These tests included switching of air-insulated disconnectors. It was found that disconnector switching produced transients inside a substation of significantly larger amplitude than those produced by circuit breakers. Furthermore, that the frequencies associated with air-insulated disconnect switches ranged from 120Hz to 40kHz [17].

The frequencies on the current and voltage waves produced by switching operations need to be noted as they influence how the transmission lines can be modelled in the simulations. Transmission line modelling will be discussed briefly later in this paper.

## 3. CAPACITIVE CURRENT SWITCHING

To analyse capacitive current switching, let us consider a single-phase lumped element representation of a capacitive circuit, as shown in Figure 1.

In Figure 1, $V$ is the magnitude of the supply voltage, $C$ is the lumped capacitor that represents the capacitive load. $L_s$, $R_s$ and $C_s$ represent the impedances at the supply side of the switch ($S$) and $L$ is the stray inductance through which C is charged. It should be noted that $L_s$ much greater $L$ [18].

Switch $S$ is opened and the current through $L$ and $C$ is interrupted. After current interruption, the capacitor $C$ is fully charged to maximum voltage because of the relative phase of current and voltage (current leads the voltage by approximately 90°). The capacitor $C$, now isolated from the source, retains its charge.

As the supply voltage reverses polarity, at half a cycle after the interruption, the voltage across the switch ($S$) terminals reaches twice the peak value of the supply voltage. The 2 p.u. voltage that develops across the switch is potentially dangerous as there is an increased likelihood of the switching arc re-igniting. When the re-ignition occurs, the capacitor $C$ discharges itself via the re-ignited arc channel and the inductances $L_s$ and $L$.

## 4. TRANSMISSION LINE MODELLING

Interrupting current on an unloaded transmission line is similar to interrupting a capacitive current. Consequently, how the transmission line is modelled becomes very important.

Two types of time domain models have been

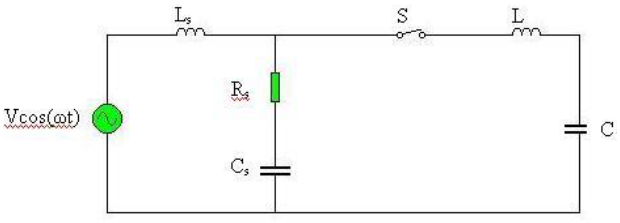


**Figure 1:** Single-phase lumped element representation of capacitive circuit

developed for overhead lines: lumped and distributed parameter models. Lumped parameter models are the simplest representation of a transmission line. The model represents transmission systems by lumped elements, in a T or π. The values of these lumped elements are calculated at a single frequency, usually the steady state frequency of 50Hz/60Hz. Each phase can be represented by a resistor equal to the line surge impedance, $Z_0$ [19]:

$$Z_0 = \sqrt{\frac{L'}{C'}} \tag{1}$$

And the propagation constant, γ:

$$\gamma = j\omega\sqrt{L'C'} \tag{2}$$

Where:

L′ - line inductance per unit length

C′ - line capacitance per unit length.

The appropriate selection of a model depends on the line length and the highest frequency to be simulated [19].

The error in modelling a transmission line with a T or π equivalent for the other frequencies is small provided the line length is short compared with the quarter wavelength of the highest frequency being considered. At 50Hz, a quarter wavelength is 1500km. At 20kHz and 40kHz, a quarter wavelength is 3.75km and 1.875km, respectively [14]. Based on frequency range given for switching overvoltages in [16], using a T or π equivalent representation for switching overvoltages would not produce accurate results.

Cascaded π-sections are often used to approximate transient behaviour in during transient studies [16] [20][21]. The number m of π-sections required for the correct representation can be determined by finding the maximum line section that can be represented by a single π-section. A rule of thumb is provided by [16]:

$$s_{\max} = \frac{v}{5.f_{\max}}. \tag{3}$$

In equation 3, $v=1/\sqrt{L'C'}$ is the propagation speed of the electromagnetic wave and $f_{\max}$ is the highest frequency that can be attained on the section.

The most accurate models for transient calculations are those that take the distributed nature of parameters into account. Distributed models provide a travelling wave solution that introduces a surge impedance (or admittance) matrix and the propagation characteristics of the lines. Mathematical transformations that allow application of the different modes of propagation are used, e.g. for transposed 3 phase lines the αβ0 transformation can be used [20][21]. The distributed parameter model can be divided into two categories: the constant parameter and the frequency dependent parameter model [19].

The constant parameter model is obtained with constant L′ and C′ distributed over the length of the line. In order to account for losses in the line model, R is lumped in three places [20]. R/2 is lumped in the middle and R/4 at both ends of the line.

If one considers a small line segment of a lossy transmission line, as shown in figure 2, R, L, G and C are the line parameters expressed in per-unit length. These parameters are frequency dependent, although for overhead lines C can be assumed constant and G can usually be neglected [19] [20].

The voltage drop along a transmission line is given by equation 4 [20]:

$$\left[\frac{dV}{dx}\right] = [Z'][I] \tag{4}$$

$$[Z'] = [R'(\omega)] + j\omega[L'(\omega)] \tag{5}$$

Where:

[*dV/dx*] - the vector of phasor voltages over a conductor segment *dx*.

[I] - the vector of phasor currents in the conductor.

[Z′] - the series impedance matrix.

[R′(ω)] – resistance of line as a function of frequency.

[L′(ω)] – inductance of line as a function of frequency.

At power frequencies of 50Hz or 60Hz, the ac resistance of a conductor is not appreciably higher than the conductor's dc resistance. However, for transient analysis, where frequencies can be higher than 1kHz, it is not appropriate to use the dc values of R′(ω) and L′(ω). Also, several transient frequencies can be carried in a particular model, making the task of choosing one frequency at which to calculate the transmission line parameters difficult [14]. For constant parameter models, various sources [14][16] [20] suggest that choosing the constant line parameters at the dominant resonance frequency or natural frequency of the line produced more accurate results. The equation for the natural frequency is given by:

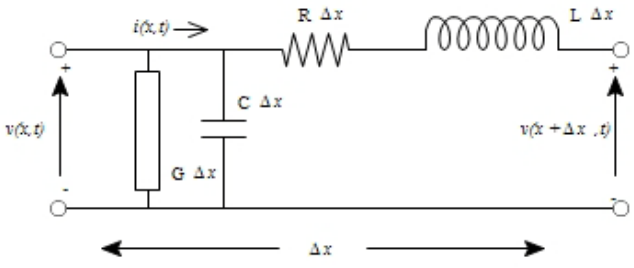


**Figure 2:** Small line segment of a lossy transmission line

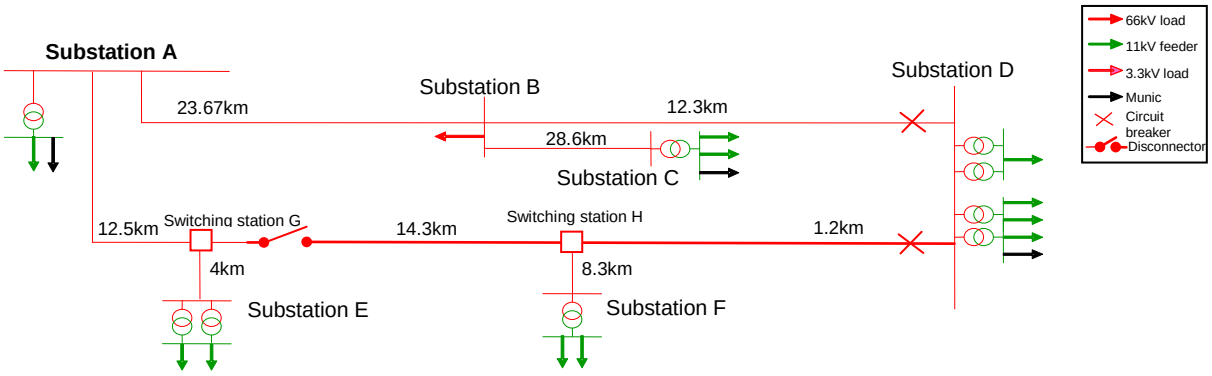


**Figure 3**: System configuration of a 66kV Network

$$f_n = \frac{1}{2\pi l\sqrt{L'C'}}, \qquad (6)$$

Where: $l$ is the length of the line.

Yet, it should be mentioned that, after transforming the phase quantities to modal quantities, the travel times, surge impedances are not the same for the different modal quantities. This compounds the decision as to which frequency to choose to calculate the constant line parameters.

Furthermore, in order to calculate the series impedance [Z′], the ground resistivity also needs to be taken into account. Carson's formula for homogeneous earth is discussed in various publications [14][19][20][22], and is often used as data for detailed multilayer earth return is seldom available. Carson's formula is, however, deemed accurate enough for power system studies [20].

A frequency dependent line model was developed [23] by approximating the line characteristic impedance by R-C combinations and a weighting function a(t). This is done by first calculating the characteristic impedance and propagation constant from DC to such a high frequency where both $A(\omega) = e^{-\gamma l}$ becomes negligibly small and $Z_c(\omega)$ becomes practically constant [20][23].

The frequency dependence of the line parameters needs to be accounted for in order to achieve accurate results with transient simulations. Previous studies by other researchers [20][23] [24] have shown that the constant-parameter representation produces magnification of the higher harmonics of the signals and, as a consequence, a general distortion of the wave shapes and exaggerated magnitude peaks.

However, it is noted that the frequency dependence of the resistance and inductance of a line is most pronounced in the zero-sequence mode [23]. In cases were the types of transients that are simulated contain appreciable zero sequence voltages and currents, e.g. single line-to-ground faults, frequency dependent models are important. However, for the accurate simulation of the characteristic impedance for open-ended lines, similar to those in this study, is not as essential to model the transmission line as a frequency dependent line [20] [23] .

## 5. MODELLING OF THE TEST CIRCUIT

### 5.1 Simulated test circuit

Figure 3 shows a system configuration of the network that was modelled for this study. The network forms part of the Eskom Distribution 66kV Western Grid. The customer base that is supplied by this network includes a few district municipalities as well as rural farmer schemes.

Substation *A* is a 132/66kV substation. Two 66kV single circuit lines are interconnected between this substation, *A*, and substation *D*. On the one 66kV line, switching stations *G* and *H* can be found. While on the other 66kV line, substations *B* and *C* are supplied.

It is desired that maintenance work to be performed on the section of line between substation *D* and the switching station *H* with limited supply interruption to customers at substation *F*. The network configuration is such that several switching operations are performed in order to isolate the desired portion of line. One of these operations requires that a disconnector is used to interrupt the current associated with the unloaded transmission line between the switching station *G* and substation *D*.

The first switching operation is to open the 66kV breaker at substation *D*, followed by the 66kV transformer breaker at substation *F*. This is done to ensure that the disconnector at the switching station *G* is not operated under load conditions. As discussed earlier, disconnectors are only capable of opening and closing a circuit when either negligible current is broken or made.

After removing the loads at supplied by substations *F* and *D*, the line disconnector at switching station *G* is opened. Once the line between the switching stations *G* and *H* is unloaded, the portion of line between switching station *H* and substation *D* can be isolated and maintained. Later in order to re-energize the line, the disconnector at switching station *G* can be closed, followed by the breakers at substations *F* and *D*.

### 5.2 Simulated characteristics of the 66kV network

The 66kV lines between substation *A* and *D* were built with an ASCR conductor, Hare. The two 66kV lines are untransposed.

The tower configurations on which the lines were built are of a single circuit flat configuration for most part of the lines. The lines were modelled as flat for the entirety of the lines. It was not anticipated that the few changes that were made to the tower configuration in some places during design, construction or maintenance would greatly affect the results.

Modelling of the transmission line was done for only the three phase conductors. No earth wire was modelled.

The line parameters R′ and L′ are not constant but functions of frequency. Where possible the line models were simulated to take skin effect of the conductor into account.

There is no available data for ground resistivity for the circuit under consideration. It was assumed, for the purposes of the study that ground resistivity was uniform. The value of 100Ωm was used.

Details of various aspects of the simulated model are shown in the appendix. Load flow studies show that the capacitive current of 2.47A is interrupted by the disconnector at switching station *G*.

The only characteristics in the simulations that were changed with each simulation were the transmission line models, i.e. lumped or frequency dependent models. These transmission line models are discussed in the next section.

### 5.3 Simulated Transmission Line Models

How a transmission line is modelled in a transient simulation influences the accuracy of the results. Different transmission line models of the test circuit were simulated in ATP. The results of these simulations were compared.

It should be noted that the time step $\Delta t$ for the simulations needs to be less than the travel time of shortest line in the simulation [24]. The shortest line simulated in the model was the 1.2km line between switching station *H* and substation *D*. The time step used for this simulation was 3μs.

The list that follows shows the simulated transmission line models performed in ATP.

1. Lumped π model (figure 4)
2. Cascaded 2π – section model (figure 5)
3. Constant Parameter model at 3280Hz (figure 6)
4. Frequency Dependent model with a frequency range from dc to 5kHz (figure 7)

A lumped π model was modelled first, followed by two π-sections for the cascaded π model. Because of the short lengths of line involved in the circuit, the maximum line section calculated (using equation 3) follows that two cascaded π-sections would be sufficient in the simulation.

Using equation 6 to find the natural frequency of the 14.3km line between the switching station *G* and *H;* a constant parameter line model was simulated at 3280Hz.

Lastly, the circuit was simulated with frequency dependent line models. The frequency range modelled was from 0.001Hz (DC) to 5000Hz which is the default ATP settings for a frequency dependent line model.

## 6. RESULTS FROM SIMULATED TRANSMISSION LINE MODELS

The results shown in this section are for the different transmission line models discussed in section 5.3. The simulated results shown in the figures 4 - 7 are phase voltages (only phase A) at switching station *G* for each simulation. Table 1 shows the maximum and minimum voltage peaks that appear on the phase voltage when the line between switching station *G* and *H* is re-energized. The time when the line is re-energised is at t=0.13s (see Table 5 in the appendix for switching operation times). It is observed that no overvoltages are generated when the transmission line is de-energised.

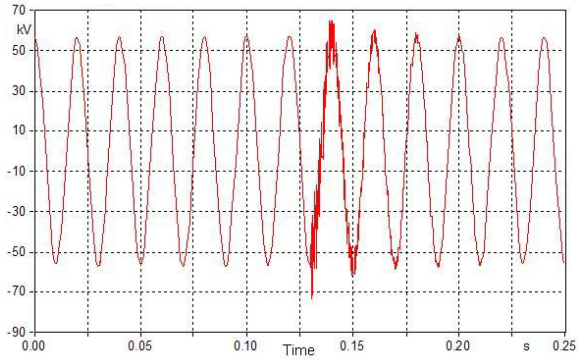


**Figure 4:** Phase Voltage at Switching Station *G* [ATP simulation: lumped π-model]

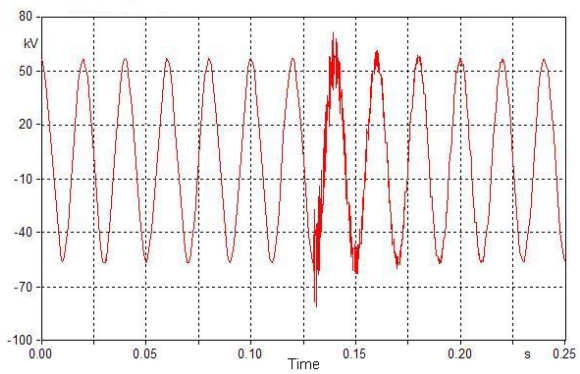


**Figure 5:** Phase Voltage at Switching Station *G* [ATP simulation: cascaded 2π-section model] * note different scale used

The phase currents of the simulated transmission line models are shown in the figures 8 - 11 that follow. The phase current in these figures are simulated to

measure the current through the transmission line between switching stations *G* and *H*. Only phase A is shown. Table 2 shows the maximum and minimum peaks present on the phase current when the line between switching station *G* and *H* is re-energized.

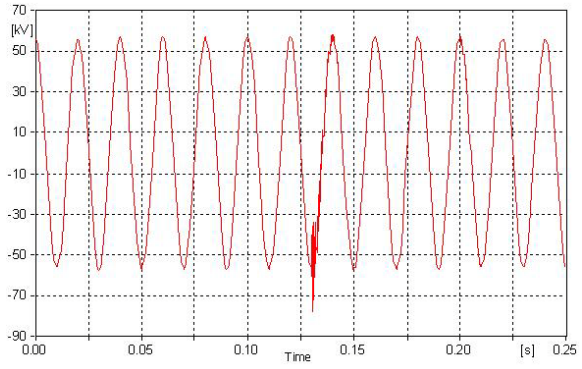


**Figure 6:** Phase Voltage at Switching Station *G* [ATP simulation: constant parameter model at 3280Hz]

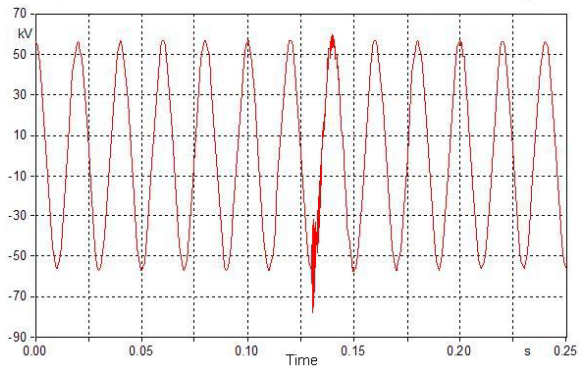


**Figure 7:** Phase Voltage at Switching Station *G* [ATP simulation: frequency dependent model]

**Table 1:** Maximum and minimum phase voltages (phase A) at Switching Station *G* for the simulated transmission line models in ATP

| Simulated Transmission line model | Min. Phase Voltage in p.u. | Max. Phase Voltage in p.u. |
|---|---|---|
| Lumped | -1.29 | 1.14 |
| Cascaded 2 π | -1.43 | 1.24 |
| Constant Parameter (3280Hz) | -1.37 | 1.02 |
| Frequency dependent | -1.37 | 1.05 |

The phase voltages of the constant parameter model at a frequency of 3280Hz as well as the frequency dependent model of the transmission line produce similar results. The minimum peak overvoltage is -1.37pu. The lumped model produces a minimum peak of -1.29 p.u. while the cascaded 2π model had a peak of -1.43.

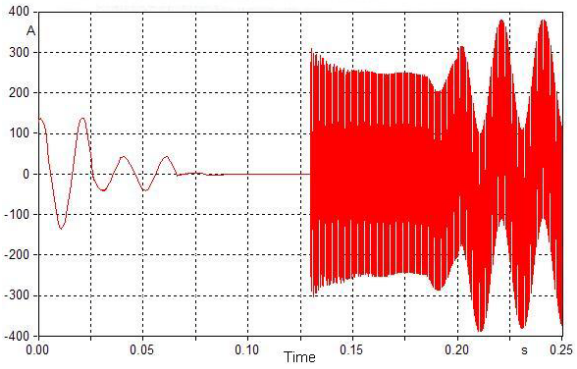


**Figure 8:** Phase current between switching station *G* and *H* [ATP simulation: Lumped model]

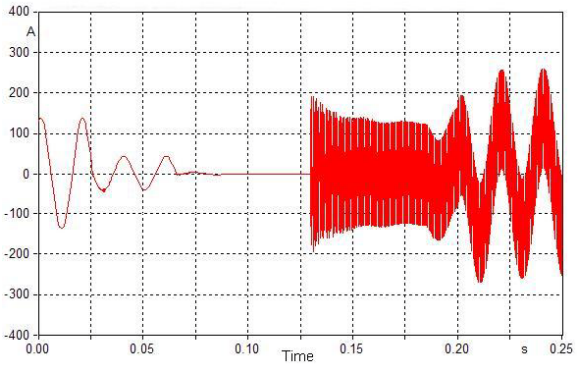


**Figure 9:** Phase current between switching station *G* and *H* [ATP simulation: cascaded 2 π model]

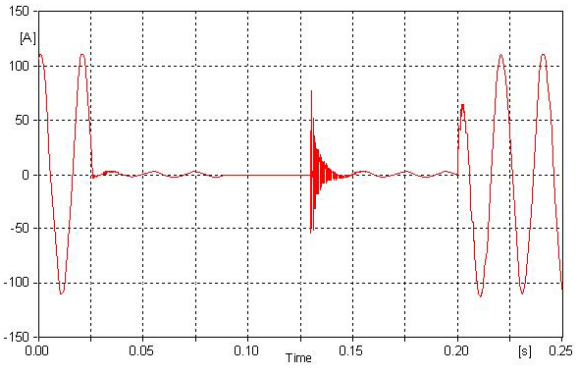


**Figure 10:** Phase current between switching station *G* and *H* [ATP simulation: constant parameter model – 3280Hz]

Analysis of the current waveforms shows that the lumped model and cascaded 2π model produces undamped oscillations when the transmission line is re-energised. The peak currents are 307A and 191A for the respective models (see Table 2). The constant parameter model and frequency dependent model have maximum peak current at 72A and 73A, respectively.

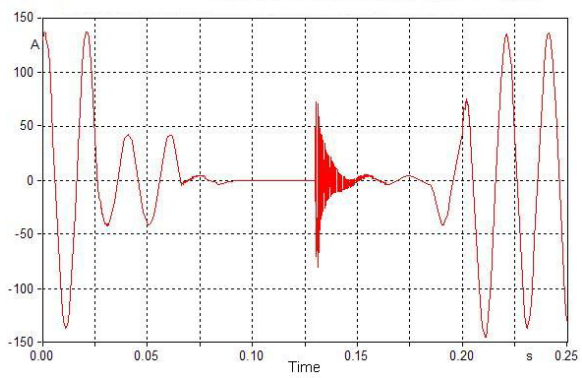


**Figure 11:** Phase current between switching station *G* and *H* [ATP simulation: frequency dependent model]

**Table 2:** Maximum and minimum phase current (phase A) through the transmission line between switching stations *G* and *H* for the simulated transmission line models in ATP

| Simulated Transmission line model | Min. Phase Current in A | Max. Phase Current in A |
|---|---|---|
| Lumped | -301.8 | 307.3 |
| Cascaded 2 π | -192.1 | 190.9 |
| Constant Parameter (3280Hz) | -52.1 | 71.9 |
| Frequency dependent | -81.1 | 72.7 |

Based on the voltage and current waveforms, the lumped and cascaded 2π line models would not be adequate to study the electromagnetic transients associated with this switching operations. The undamped current waveforms show phase currents in excess of the nominal load current even after all the switching operations have been executed.

The constant parameter model and the frequency dependent model are comparable for both voltage and current waveforms. As expected, for circuits with very little zero sequence voltages and currents, the difference between the constant parameter and frequency dependent line models is small. This difference is small depending on the frequency at which the constant parameter model elements are calculated.

## 7. POWERFACTORY SIMULATIONS

In the previous section, the transmission line models that are best suited for simulations involving switching transients and unloaded lines, namely: constant parameter line model (at a specific frequency, e.g. natural line frequency) or frequency dependent line model. This section presents the results of the test circuit when modelled in PowerFactory.

The characteristics and inputs that were simulated in PowerFactory were the same as those used in ATP. Testing of the same circuit allows for direct comparisons between the two simulation tools.

Only the results of the constant parameter line model calculated at 3280Hz and the frequency dependent line model are presented in the paper. Figure 12 and 13 show the phase voltage at the switching station *G* for both line models. Figure 14 and Figure 15 show the phase current through the transmission line between switching station *G* and *H*. Table 3 highlights the minimum and maximum peak overvoltages experienced at switching station *G* when the transmission line is re-energized. Table 4 outlines the peak phase currents from figures 14 and 15.

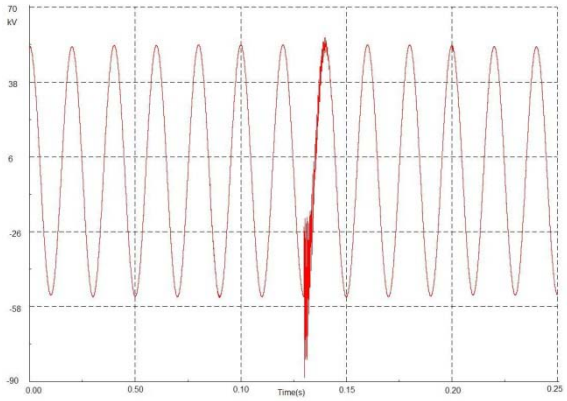


**Figure 12:** Phase Voltage at Switching Station *G* [PowerFactory simulation: constant parameter model at 3280Hz]

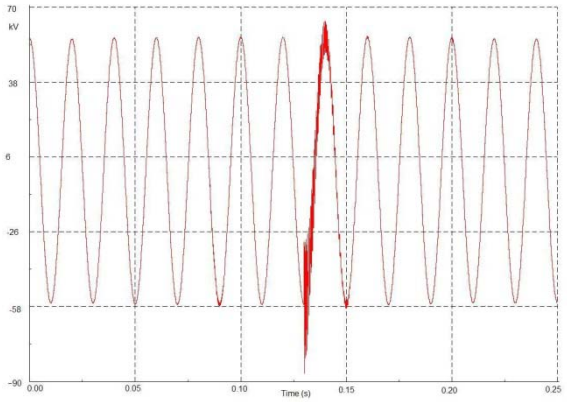


**Figure 13:** Phase Voltage at Switching Station *G* [PowerFactory simulation: frequency dependent model]

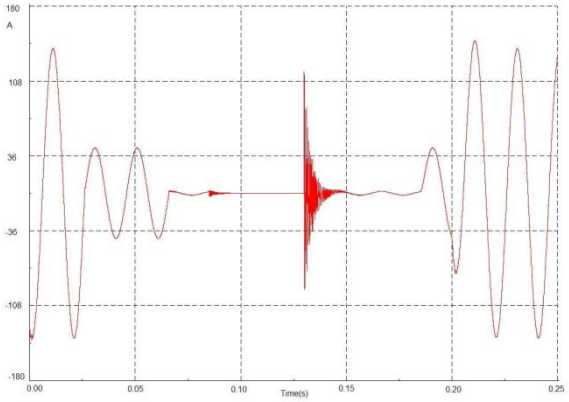


**Figure 14:** Phase current between switching station *G* and *H* [PowerFactory simulation: constant parameter model – 3280Hz]

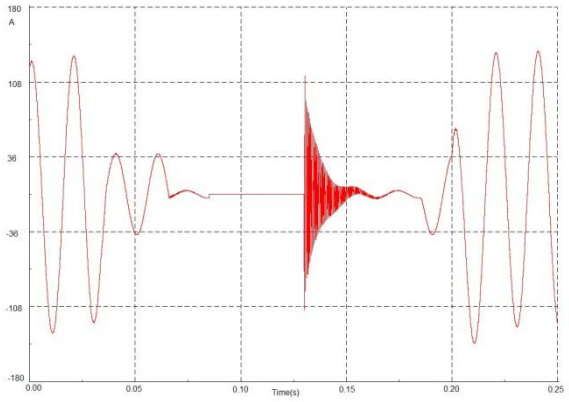


**Figure 15**: Phase current between switching station *G* and *H* [PowerFactory simulation: frequency dependent model]

**Table 3**: PowerFactory simulation: Maximum and minimum phase voltages (phase A) at Switching Station *G*

| Simulated Transmission line model | Min. Phase Voltage in p.u. | Max. Phase Voltage in p.u. |
|---|---|---|
| Constant Parameter (3280Hz) | -1.64 | 1.06 |
| Frequency dependent | -1.61 | 1.17 |

**Table 4:** PowerFactory Simulation: Maximum and minimum phase current (phase A) through the transmission line between switching stations *G* and *H*

| Simulated Transmission line model | Min. Phase Current in A | Max. Phase Current in A |
|---|---|---|
| Constant Parameter (3280Hz) | -92.9 | 117.1 |
| Frequency dependent | -110.5 | 112.3 |

The overvoltages generated at switching station *G* in the PowerFactory simulations are higher than those generated in the ATP simulations. For a constant parameter line model simulated for a frequency of 3280Hz, the PowerFactory simulation gives a minimum peak overvoltage of -1.64 p.u. In comparison, the ATP simulation produces a minimum peak of -1.37. The frequency dependent line model yields similar results: -1.61 p.u. for the PowerFactory simulation and -1.37 p.u. for the ATP simulation. Again, it is observed that no overvoltages are generated when the transmission line is de-energised.

The current waveforms also exhibit higher amplitudes for the PowerFactory simulations than the ATP simulation when the unloaded transmission line is re-energized, see Table 4.

Unfortunately, due limited literature for PowerFactory, there is inadequate information as to explain the theories and assumptions that PowerFactory uses in its simulations. Having said this, without field tests to verify the simulations presented one cannot say which simulation package or tool gives the more accurate result.

## 8. CONCLUSIONS

Theory states that when switching capacitive currents overvoltages of up to 2pu can be expected. In the simulations presented here, overvoltages of up to1.37 p.u. are reached using ATP and 1.6 p.u. using PowerFactory.

Frequency dependent transmission line models as well as the constant parameter transmission line models produce results that can be used for switching transient studies that involved unloaded transmission lines. However, the constant parameter model requires further analysis to determine at which frequency the calculation of the transformation matrix will give the best results. Lumped transmission line models are not suited for these tests.

PowerFactory simulation results show higher overvoltages than those produced with ATP run simulations. Field tests are necessary for validation and verification of results presented in this paper.

## REFERENCES

[1] IEEE Standard C37.30. IEEE Standards for High Voltage Switches. 1997.

[2] IEC 60050-441. Amendment 1 - International Electrotechnical Vocabulary. Switchgear, Controlgear and fuses. 2.0 2000.

[3] IEC 62271-102. High-voltage switchgear and controlgear - Part 102: Alternating current disconnectors and earthing switches. First Edition 2001-12.

[4] Andrews, F.E., Janes, L.R. and Andersson, M.A. Interrupting Ability of Horn-Gap Switches. *AIEE Transactions.* 1950, Vol. 69, pp. 1016-1027.

[5] IEEE Committee Report. Results of survey on interrupting Ability of Air Break Switches. *IEEE Transactions on Power*

*Apparatus and Systems.* September 1966, Vols. PAS-85, No. 9, pp. 1008-1019.

[6] Rankin, E.C. Experience with methods of extending the capability of High-Voltage Air Break Switches. *AIEE Transactions.* February 1960, Vol. 79, pp. 1634-1637.

[7] Peelo, D. F. and Hydro, B. C. Current Interrupting Capability of Air-Break Disconnect Switches. *IEEE Transactions on Power Apparatus and Systems.* January 1986, Vols. PWRD-1, No. 1.

[8] Peelo, D.F. *Current interruption using high voltage air-break disconnectors.* Eindhoven University of Technology. 2004. PhD Thesis.

[9] Peelo, D. F., et al. *Current Interruption with High Voltage Air-Break Disconnectors.* Paris : CIGRE, 2004. Paper No. A3-301.

[10] Peelo, D.F., et al. *Capacitive Current Interruption in Atmospheric Air.* Tokyo : CIGRE SC A3 & B3 Joint Colloquium, 2005. Paper No. 106.

[11] Knobloch, H. Switching of Capacitive Currents by Outdoor Disconnectors. *Fifth Symposium on High Voltage Engineering.* Braunschweig : s.n., August 24-29, 1987.

[12] Kizilcay, M. *Alternative Transients Program.* [Online] August 23, 2008. [Cited: December 10, 2008.] www.emtp.org.

[13] DigSILENT GmbH. [Online] 2008. [Cited: December 10, 2008.] http://digsilent.de/Software/PowerFactory_Features/.

[14] Greenwood, A. *Electrical Transients in Power Systems.* 2nd ed. New York : John Wiley & Sons, Inc., 1991.

[15] Das, J.C. *Power System Analysis: Short-circuit load flow and harmonics.* s.l. : CRC Press, 2002.

[16] CIGRE Working Group 33.02. Guidelines for Representation Network Elements when Calculating Transients. *CIGRE Brochure 39.* 1990.

[17] Wiggins, C. M. and Wright, S. E. Switching Transient Fields in Substations. *IEEE Transactions on Power Delivery.* April 1991, Vol. 6, No. 2, pp. 591-599.

[18] van der Sluis, L. *Transients in Power Systems.* Chichester : John Wiley & Sons Ltd., 2001.

[19] Martinez, J. A, Gustavsen, B. and Durbak, D. Parameter Determination for Modeling System Transients - Part I: Overhead Lines. *IEEE Transactions on Power Delivery.* July 2005, Vol. 20, 3, pp. 2038-2044.

[20] Dommel, H. W. *Elecctromagnetic Transients Program Manual (EMTP Theory Book).* Portland, Oregon : Bonneville Power Administration, 1986.

[21] CIGRE Working Group 13.05. The Calculation of Switching Surges. II. Network Representation for Energization and Re-Energization Studies on Lines Fed by an Inductive Source. *Electra.* 1974, No. 32, pp. 17-42.

[22] Carson, J. R. Wave Propagation in Overhead Wires with Ground Return. *Bell Systems Techical Journal.* 1926, Vol. 5, pp. 539-554.

[23] Marti, J. R. Accurate Modeling of Frequency-dependent Transmission Lines in Electromagnetic Transients Simulations. *IEEE Transactions on Power Apparatus and Systems.* January 1982, Vols. PAS-101, No. 1, pp. 147-155.

[24] Ibrahim, A. I., et al. Application of a New EMTP Line Model for Short Overhead Lines and Cables. *Electrical Power and Energy Systems 24.* 2002, pp. 639-645.

## APPENDIX

*Simulated Tower configuration:*
Flat configuration:

| | | |
|---|---|---|
| Phase 1: | x=-3.8m | y=9.6m |
| Phase 2: | x= 0m | y=9.6m |
| Phase 3: | x= 3.8m | y=9.6m |

Sag of phase conductors is 1.455m for an average span length of 200m of Hare conductor.
*Hare Conductor specification:*
$X_a$=0.327641 Ω/km (reactance for one unit spacing)
$R_{out}$ = 0.708 cm(outer radius of conductor)
$R_{in}$ = 0.236 cm(inner radius of conductor)
Resis= 0.2733 Ω/km (conductor resistance at DC)

*Source:* Ideal source is used for the simulations presented in this paper. Voltage setting is at 1.056 p.u. System voltage is 66kV. Power frequency is 50Hz.

**Table 5:** Simulated switching in ATP and PowerFactory

| Item to operate | Time of operation | Type of operation |
|---|---|---|
| 66kV breaker at substation *D* | 0.026 | Open |
| Breaker at substation *F* | 0.064 | Open |
| Disconnector at switching station *G* | 0.085 | Open |
| Disconnector at switching station *G* | 0.13 | Close |
| Breaker at substation *F* | 0.185 | Close |
| 66kV breaker at substation *D* | 0.2 | Close |

# Appendix A: Modal quantities and Transformation Matrices

In general, transmission line equations are given by:

$$-\left[\frac{dV_\varphi}{dx}\right]=\left[Z'_\varphi\right]\left[I_\varphi\right] \tag{A.1}$$

$$-\left[\frac{dI_\varphi}{dx}\right]=\left[Y'_\varphi\right]\left[V_\varphi\right] \tag{A.2}$$

where

$\left[V_\varphi\right]$ and $\left[I_\varphi\right]$ are the vectors of the phase voltages and phase currents respectively.

$\left[Z'_\varphi\right]=\left[R'_\varphi\right]+j\omega\left[L'_\varphi\right]$. is the line impedance

$\left[Y'_\varphi\right]=\left[G'_\varphi\right]+j\omega\left[C'_\varphi\right]$ is the line admittance.

Line parameters need to be computed. This can be done at the design stage or after the line has been built. Line parameters are calculated for individual conductor of a transmission line. For example, if a double circuit, three phase line is built with twin conductors and one ground wire, there will be 13 conductors and 6 phases [33]. This illustrated in the figure, Figure A.1 below.

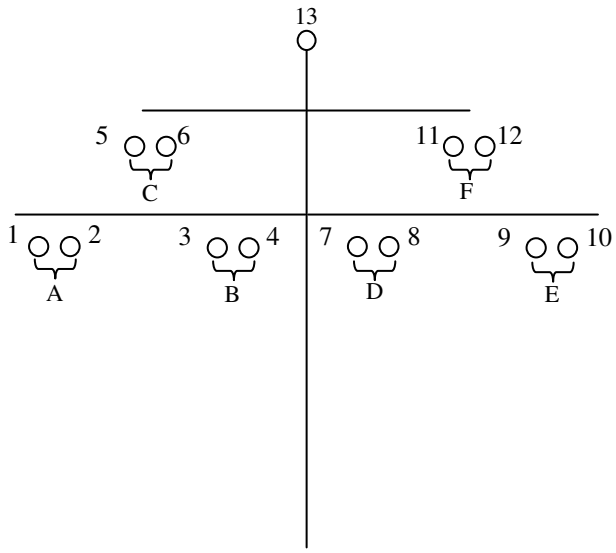


Figure A.1 Transmission line tower configuration: Line parameters - individual conductors and phases

If the tower in question has *n* number of conductors, then to get to equation (A.1), we start off with the individual conductors where:

$$\begin{bmatrix} \frac{dV_1}{dx} \\ \frac{dV_2}{dx} \\ \vdots \\ \frac{dV_n}{dx} \end{bmatrix} = \begin{bmatrix} Z'_{1,1} & Z'_{1,2} & \cdots & Z'_{1,n} \\ Z'_{2,1} & \ddots & & Z'_{2,n} \\ \vdots & & \ddots & \vdots \\ Z'_{n,1} & \cdots & \cdots & Z'_{nn} \end{bmatrix} \begin{bmatrix} I_1 \\ I_2 \\ \vdots \\ I_n \end{bmatrix} \tag{A.3}$$

where:

$[Z'] = [R'] + j\omega[L']$ is the series impedance of the conductor.

Furthermore,

$[Y'] = [G'] + j\omega[C']$ is the shunt admittance of the conductor.

However, for overhead lines, the shunt conductance is generally ignored except when frequencies involved are low (approaching dc) [33]. Thus, in this case, $G' = 0$ and so

$[Y'] = j\omega[C']$.

The shunt capacitance matrix, $[C']$, is found as a function of the line charges and the voltage from *n* conductors. That is:

$$[q] = [C'][V] \tag{A.4}$$

where:

$[q']$ is the charge per unit length on conductor *i*.

For ac steady state conditions, the vector of charges $[Q]$ is related to the vector of leakage currents: $-\left[\frac{dI}{dx}\right]$, by [33]:

$$[Q] = -\frac{1}{j\omega}\left[\frac{dI}{dx}\right] \tag{A.5}$$

$$-\left[\frac{dI}{dx}\right] = j\omega[C'][V] \tag{A.6}$$

The equations shown above in (A.3) and (A.6) are still based on the individual conductors. The user is usually interested in the phase quantities for the voltage and current. In order to achieve this, bundling of conductors into the various phases is required. Methods of circuit reduction are discussed in more detail in [33]. One method uses the reality that in a bundle, the sub-conductors have equal voltage. Hence, in the case of Figure A.1, for phase A: $I_1 + I_2 = I_A$ and $\frac{dV_1}{dx} = \frac{dV_2}{dx} = \frac{dV_A}{dx}$ and $q_1 + q_2 = q_A$ and $v_1 = v_2 = v_3$. This is analogous for the other phases. The result of the bundling is then:

$$-\left[\frac{dV_{\text{phase}}}{dx}\right]=\left[Z'_{\text{phase}}\right]\left[I_{\text{phase}}\right] \tag{A.7}$$

$$-\left[\frac{dI_{\text{phase}}}{dx}\right]=\left[Y'_{\text{phase}}\right]\left[V_{\text{phase}}\right] \tag{A.8}$$

Accordingly, for a three phase single circuit overhead line, the reduction from individual conductors to phase quantities for equation (A.7) will have the form:

$$\begin{bmatrix}\frac{dV_{\text{A}}}{dx}\\ \frac{dV_{\text{B}}}{dx}\\ \frac{dV_{\text{C}}}{dx}\end{bmatrix}=\begin{bmatrix}Z'_{\text{AA}} & Z'_{\text{AB}} & Z'_{\text{AC}}\\ Z'_{\text{BA}} & Z'_{\text{BB}} & Z'_{\text{BC}}\\ Z'_{\text{CA}} & Z'_{\text{CB}} & Z'_{\text{CC}}\end{bmatrix}\begin{bmatrix}I_{\text{A}}\\ I_{\text{B}}\\ I_{\text{C}}\end{bmatrix} \tag{A.9}$$

Unfortunately in the case of (A.7) and (A.8), the values obtained are coupled together in the phase domain. Thus transformations to decouple the *n* conductor system are necessary.

If the overhead transmission line is a balanced, single circuit, three phase line, the transformation used to decouple the equations above is to use α, β, 0-components due to Edith Clarke [33]. This is shown below:

$$\begin{aligned}\left[v_{\text{phase}}\right]&=\left[T\right]\left[v_{0\alpha\beta}\right]\\ \left[v_{0\alpha\beta}\right]&=\left[T\right]^{-1}\left[v_{\text{phase}}\right]\end{aligned} \tag{A.10}$$

where

$$\left[v_{0\alpha\beta}\right]=\begin{bmatrix}v_0\\ v_\alpha\\ v_\beta\end{bmatrix}, \tag{A.11}$$

$$[T]=\frac{1}{\sqrt{3}}\begin{bmatrix}1 & \sqrt{2} & 0\\ 1 & -\frac{1}{\sqrt{2}} & \frac{\sqrt{3}}{\sqrt{2}}\\ 1 & -\frac{1}{\sqrt{2}} & -\frac{\sqrt{3}}{2}\end{bmatrix}, \tag{A.12}$$

and

$$[T]^{-1}=\frac{1}{\sqrt{3}}\begin{bmatrix}1 & 1 & 1\\ \sqrt{2} & -\frac{1}{\sqrt{2}} & -\frac{1}{\sqrt{2}}\\ 0 & \frac{\sqrt{3}}{\sqrt{2}} & -\frac{\sqrt{3}}{2}\end{bmatrix}. \tag{A.13}$$

Similarly,

$$\begin{aligned}\left[i_{\text{phase}}\right]&=[T]\left[i_{0\alpha\beta}\right]\\ \left[i_{0\alpha\beta}\right]&=[T]^{-1}\left[i_{\text{phase}}\right]\end{aligned} \tag{A.14}$$

The transformation matrix above is known as the Clarke Transform and is used for balanced three phase lines [33]. Dommel [33] defines 'balanced' as a line where all the diagonal elements of $\left[Z'_{\text{phase}}\right]$ and $\left[Y'_{\text{phase}}\right]$ are equal among themselves, and all the off diagonal elements are equal. Having said this, singe circuit three phase lines are not 'truly' balanced, but come close when transposed and the length of line is much less than wavelengths of the frequencies involved. In which case, $\left[Z'_{\text{phase}}\right]$ can be approximated with:

$$\left[Z'_{\text{phase}}\right]=\begin{bmatrix}Z'_{\text{s}} & Z'_{\text{m}} & Z'_{\text{m}}\\ Z'_{\text{m}} & Z'_{\text{s}} & Z'_{\text{m}}\\ Z'_{\text{m}} & Z'_{\text{m}} & Z'_{\text{s}}\end{bmatrix}$$

where:

$Z'_{\mathrm{s}} = \frac{1}{3}\left(Z'_{\mathrm{AA}} + Z'_{\mathrm{BB}} + Z'_{\mathrm{CC}}\right)$, and

$Z'_{\mathrm{m}} = \frac{1}{3}\left(Z'_{\mathrm{AB}} + Z'_{\mathrm{BC}} + Z'_{\mathrm{AC}}\right)$.

Applying the transformation to the equation (A.7) results in:

$$-\begin{bmatrix} \frac{dV_0}{dx} \\ \frac{dV_\alpha}{dx} \\ \frac{dV_\beta}{dx} \end{bmatrix} = \begin{bmatrix} Z'_{\mathrm{s}} + 2Z'_{\mathrm{m}} & 0 & 0 \\ 0 & Z'_{\mathrm{s}} - Z'_{\mathrm{m}} & 0 \\ 0 & 0 & Z'_{\mathrm{s}} - Z'_{\mathrm{m}} \end{bmatrix} \begin{bmatrix} I_0 \\ I_\alpha \\ I_\beta \end{bmatrix} \tag{A.15}$$

Some lines however have more than 3 phases. For lines with M phases, the α, β, 0-transformation is generalised so that balanced M phase lines can be decoupled, Dommel provides more information in this respect in [33].

What's more, they are untransposed, and as a result unbalanced. Matrices of untransposed lines can be diagonalised using modal parameters derived from eigenvalue/eigenvector theory. How this is done is explained in detail in [33]. However, for the purpose of introduction and understanding, a few key equations are explored below.

For the reason that an overhead head transmission line is not transposed, transformation matrix used to decouple the line in question is not known a priori. That is to say, one cannot use the Clarke transform or an *n*-phase α, β, 0-transformation matrix to decouple the phase matrices in (A.7) and (A.8).

For the equations in (A.7) and (A.8), a transformation matrix must be calculated for each pair of parameter matrices $\left[Z'_{\mathrm{phase}}\right]$ and $\left[Y'_{\mathrm{phase}}\right]$.With eigenvalue theory, it is possible to transform two coupled equations, equations (A.7) and (A.8), from phase to "modal" quantities in such a way that the equation becomes decoupled and the associated matrices, in algebraic terms, become diagonal [33].

If equation (A.7) is differentiated with respect to x, and the current derivative is replaced with equation (A.8), a second order differential equation is obtained for voltages only.

$$\begin{aligned}\left[\frac{d^2V_{\text{phase}}}{dx^2}\right] &= -\left[Z'_{\text{phase}}\right]\left[\frac{dI_{\text{phase}}}{dx}\right] \\ &= \left[Z'_{\text{phase}}\right]\left[Y'_{\text{phase}}\right]\left[V_{\text{phase}}\right]\end{aligned} \tag{A.16}$$

Similarly, a second order differential equation for currents can also be obtained.

$$\left[\frac{d^2I_{\text{phase}}}{dx^2}\right] = \left[Y'_{\text{phase}}\right]\left[Z'_{\text{phase}}\right]\left[I_{\text{phase}}\right] \tag{A.17}$$

It should be noted that in equations (A.16) and (A.17), the matrix products of $[Z'_{\text{phase}}]$ and $[Y'_{\text{phase}}]$ are reversed and therefore different.

To decouple the equation for the phase voltages, the eigenvalues ($\lambda_k$) of the matrix product of $[Z'_{\text{phase}}][Y'_{\text{phase}}]$ together with the eigenvector ($[T_V]$) of the same matrix product of $[Z'_{\text{phase}}][Y'_{\text{phase}}]$ is obtained. $[T_V]$ is the transformation matrix, where the phase voltages are transformed to mode voltages $[V_{\text{mode}}]$.

$$\left[V_{\text{phase}}\right] = \left[T_V\right]\left[V_{\text{mode}}\right] \tag{A.18}$$

$$\left[V_{\text{mode}}\right] = \left[T_V\right]^{-1}\left[V_{\text{phase}}\right] \tag{A.19}$$

Using the equation (A.19) for $[V_{\text{mode}}]$ in the modal domain, the first-order and second-order differential equations of $[V_{\text{mode}}]$ are found.

$$\begin{aligned}\left[\frac{dV_{\text{mode}}}{dx}\right] &= \left[T_V\right]^{-1}\left[\frac{dV_{\text{phase}}}{dx}\right] \\ \left[\frac{d^2V_{\text{mode}}}{dx^2}\right] &= \left[T_V\right]^{-1}\left[\frac{d^2V_{\text{phase}}}{dx^2}\right]\end{aligned} \tag{A.20}$$

Substituting equation (A.16) into (A.20) gives:

$$\left[\frac{d^2V_{\text{mode}}}{dx^2}\right] = [T_V]^{-1}\left[Z'_{\text{phase}}\right]\left[Y'_{\text{phase}}\right]\left[V_{\text{phase}}\right] \tag{A.21}$$

Thereafter, $\left[V'_{\text{phase}}\right]$ is replaced with equation (A.18) to give:

$$\left[\frac{d^2V_{\text{mode}}}{dx^2}\right] = [T_V]^{-1}\left[Z'_{\text{phase}}\right]\left[Y'_{\text{phase}}\right][T_V][V_{\text{mode}}] \tag{A.22}$$

Equation (A.22) is then a decoupled voltage equation that can be analysed as if it were a single phase line. If

$$[\Lambda] = [T_V]^{-1}\left[Z'_{\text{phase}}\right]\left[Y'_{\text{phase}}\right][T_V] \tag{A.23}$$

where [Λ]is a diagonal matrix, then:

$$\left[\frac{d^2V_{\text{mode}}}{dx^2}\right] = [\Lambda][V_{\text{mode}}] \tag{A.24}$$

For the phase current, the transformation matrix $[T_I]$ is a matrix product of $\left[Y'_{\text{phase}}\right]\left[Z'_{\text{phase}}\right]$. The eigenvalues, however, are the same for phase currents and phase voltages.

$$\left[I_{\text{phase}}\right] = [T_{\text{I}}][I_{\text{mode}}] \tag{A.25}$$

$$[I_{\text{mode}}] = [T_I]^{-1}\left[I_{\text{phase}}\right] \tag{A.26}$$

Therefore, equation (A.17) is transformed to:

$$\left[\frac{d^2I_{\text{mode}}}{dx^2}\right] = [\Lambda][I_{\text{mode}}] \tag{A.27}$$

The $[Z'_{\text{phase}}]$ and $[Y'_{\text{phase}}]$ matrices are complex and frequency dependent. Correspondingly, the transformation matrices $[T_V]$ and $[T_I]$ are theoretically complex and frequency dependent. However, $[T_V]$ and $[T_I]$ are only defined at the frequency at which the matrix is calculated. In other words, if one wanted to transform a transmission line from phase quantities to modal quantities over a frequency range, one would end up with different transformation matrices for different frequencies. Thus, the conversion of a transmission line with *n* phases into decoupled single phase line equations cannot be done over a frequency range.

Dommel [33] states that it is simpler to work with decoupling phase quantities for transient solutions if the transformation matrix is constant over all frequencies. To achieve a real and constant transformation matrix is an approximation. This produces errors in the transformation matrix. The errors may be small in one particular frequency region, and larger in other regions. For switching studies, it is suggested in [33] that $[T_V]$ and $[T_I]$ are calculated for a particular frequency, thereafter the imaginary part is ignored. However, there are recommended manners in which the errors can be minimised. These recommendations are made by Dommel in [33]. It should be noted, though, an *n* phase line that is assumed to be balanced will have a transformation matrix that is real and constant.